ABSTRACT

CHEMISTRY

MIGDALIA ALVARADO B. S. UNIVERSITY OF PUERTO RICO, CAYEY 1993

SYNTHESIS AND CHARACTERIZATION OF HIGH PERFORMANCE POLYIMIDES CONTAINING THE BICYCLO[2.2.2]OCT-7-ENE RING SYSTEM

Advisor: Dr. Issifu I. Harruna

Thesis dated December, 1996

Processable polyimides containing the bicyclo[2.2.2]oct-7-ene ring system were prepared. The polyimides were synthesized by the polycondensation of bicyclo[2.2.2]oct-7-ene-2,3,5,6-tetracarboxylic dianhydride with 1,4-phenylenediamine, 1,3-phenylenediamine, 3,3'-dimethyl-4,4'-diaminobiphenyl diamine (*o*-tolidine), and 2,2'-bis(trifluoromethyl)benzidine in 1-methyl-2-pyrrolidinone (NMP). The respective polyamic acids were also isolated. All the polyamic acids and polyimides were characterized by infrared, proton and carbon-13 nuclear magnetic resonance (NMR) spectroscopy, viscosity, solubility, and X-ray scattering. The polymers exhibited enhanced solubility in organic solvents such as dimethylsulfoxide (DMSO), N,N-dimethylacetamide (DMAc) and N,N-dimethylformamide (DMF). Thermal stability of the polyamic acids and polyimides were determined by thermogravimetric analysis (TGA), differential scanning calorimetry (DSC), and optical polarizing microscopy. Thermogravimetric analysis indicates that the corresponding polyamic acids and polyimides are stable up to ca. 450 °C under argon and air atmospheres.

SYNTHESIS AND CHARACTERIZATION OF HIGH PERFORMANCE POLYIMIDES CONTAINING THE BICYCLO[2.2.2]OCT-7-ENE RING SYSTEM

A THESIS

SUBMITTED TO THE FACULTY OF CLARK ATLANTA UNIVERSITY

IN PARTIAL FULFILLMENT OF THE REQUIREMENTS

FOR THE DEGREE OF MASTER OF SCIENCE

BY

MIGDALIA ALVARADO

DEPARTMENT OF CHEMISTRY

ATLANTA, GEORGIA

DECEMBER 1996

ACKNOWLEDGMENT

I wish to thank God because he gave me the strength, the health and the knowledge to reach another important goal in my life. Special thanks to my husband, Onofre, because he inspired me during this two years of hard work.

Thanks to my advisor, Dr. Issifu I. Harruna for his guidance, and assistance through the course of this research program on polyimides. Also, thanks to my research group members: Delynn Hayes, Melody Bray and Odessa Petzold for their unconditional friendship, advice, and cooperation.

Finally, I would like to thank NASA through the High Performance Polymers and Ceramic Center (HIPPAC), Grant # NAGW2939, at Clark Atlanta University for financial support of this project.

TABLE OF CONTENTS

LIST OF FIGURES

Figure **Page**

LIST OF TABLES

Table **Page**

LIST OF SCHEMES

Scheme **Page**

INTRODUCTION

Ladder polymers are made up of regularly recurring fused-ring structures.[1] Two major ladder polymers are known: double-stranded polymers and single-stranded polymers, Figure 1. Aromatic ladder polymers are an example of macromolecules with no single-stranded linkages. Such materials are likely to have very high thermal stability. Typical aromatic ladder polymers are polybenzimidazoles, polyimidazopyrrolones, or polyquinoxalines, Figure 2. Single-stranded polymers, also known as semi-ladder polymers are polymers of cyclic moieties linked with open-chain units, Figure 3. Even though some ladder-type structure may be present, at least one skeletal bond per repeating unit is not a ladder structure.[2] Examples are polyquinoxyanilines, polybenzimidazoles, and polyimides.

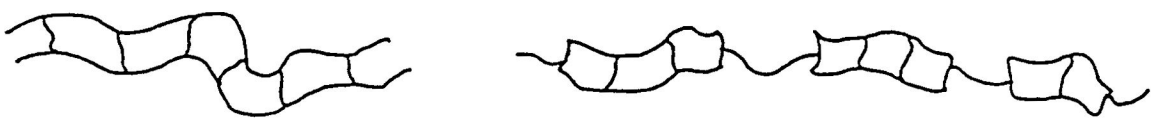

(a) (b)

Figure 1. Schematic representation of (a) double stranded and (b) single stranded polymers

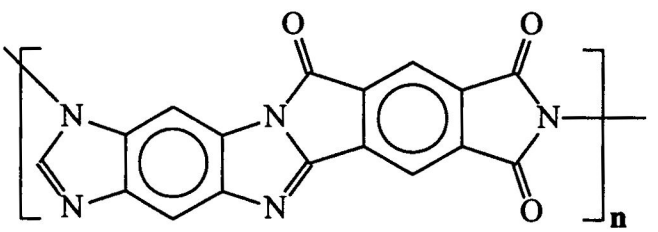

Figure 2. Structure of an aromatic ladder polymer

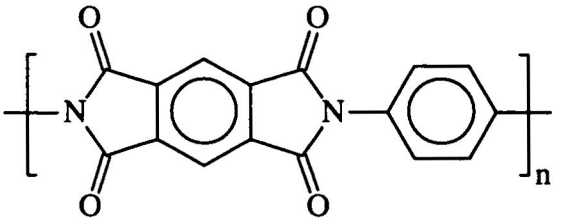

Figure 3. Structure of a semi-ladder polymer

Polyimides are high performance condensation polymers derived from bifunctional carboxylic acid anhydrides and primary diamines. They contain the imide structure -CO-NR-CO- as a linear unit along the main chain of the polymer backbone, Figure 4.

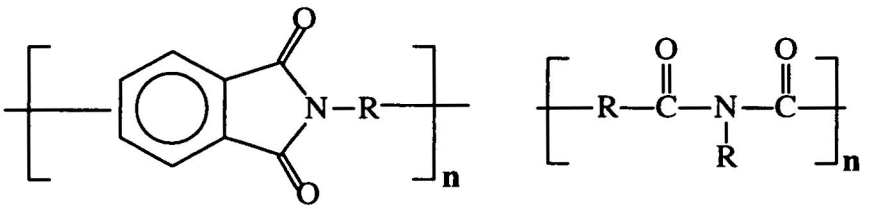

Figure 4. Representation of characteristic imide polymer backbone

Although the first synthesis of an aromatic polyimide was carried out in 1908, it was not until the late 1950's that high molecular weights polymers were prepared.[3,4] This interest has developed largely as a result of the increased need for advanced materials in the electronic and aerospace industries. Thermally stable polyimides are used in systems include resins for structural adhesives, coatings, selectively permeable membranes and composites matrices.

In the electronic industry, the most recent application is the use of polyimides as semiconductors. The two main applications for polyimides in the semiconductor industry are: as shielding and as an interlayer dielectric. A thin film of polyimide on the surface of a computer chip can prevent errors in memory devices such as DRAM (dynamic random

access memory), caused by alpha-ray particles. Polyimides have the ability to absorb alpha-ray particles from materials.[5]

As an interlayer dielectric, polyimides are used between wires as insulators. Polyimides can be used as coating materials in the electronic industry. The polyamic acid system can be coated on to the wire and thermally converted to the polyimide.

Other electronic applications include the use of polyimide foams as light weight materials in wall and ceiling panels, sections of bulkhead, as acoustical, thermal and vibrational insulation on aircrafts. As composites, polyimides can be used on wing skins, engines, and interior furniture of military and commercial aircrafts.[6]

Polyimides can be synthesized by the following methods: the imide functional group or its precursor is formed during the polymerization reaction, Type 1; a low molecular weight bisimide or an oligomeric bisimide serve as monomer in a polymerization reaction, Type 2; and an imide containing oligomer bearing polymerizable end groups is converted to a network polymer, usually by heating, Type 3.

Type 1 polyimides are prepared by initially forming a polyamic acid followed by ring closure to form the polyimide, Scheme 1.[7-9] Among the important polyimides prepared by the dianhydride-diamine routes is du Pont Company's Kapton®, Figure 5. Kapton® has an extremely high melting temperature (Tm) and a high glass transition temperatures (Tg) above 400 °C.[10]

Scheme 1. Synthetic route to a Type 1 polyimide

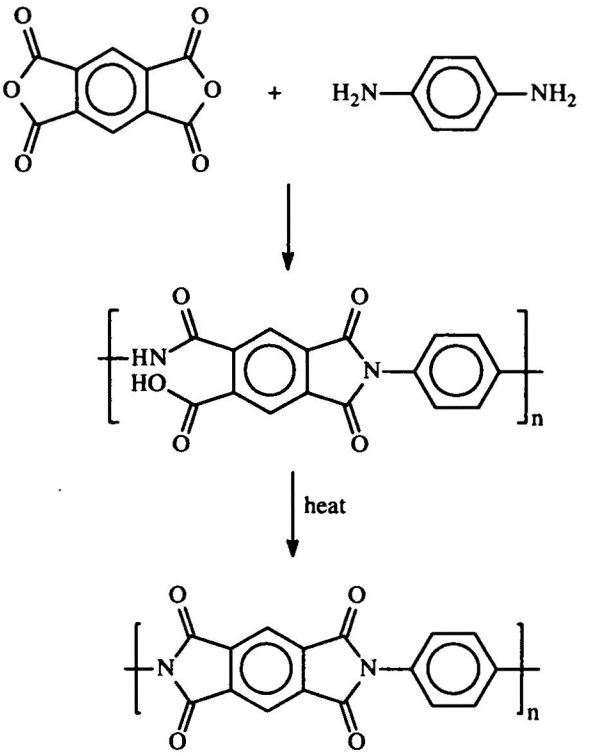

Type 2 polymers are synthesized by curing of oligomeric units in a range of 200 to 400 °C to yield highly crosslinked polymers. Two varieties of Type 2 polyimides have achieved commercial acceptance, one based on bismaleimides and the other on bisnadeimides, Figure 6.[11] An example of a bismaleimide type polyimide is Kerimid 601® which is synthesized by the reaction of 4,4'-diaminodiphenylmethane and bismaleimide, Scheme 2.

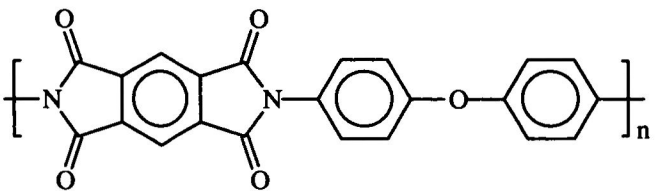

Figure 5. Schematic representation of high performance polyimide, Kapton®

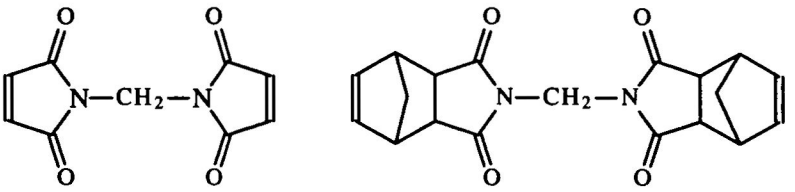

(a) (b)

Figure 6. Structure of (a) bismaleimide and (b) bisnadeimide

Scheme 2. Synthetic route to bismaleimide type polyimide, Kerimid 601®

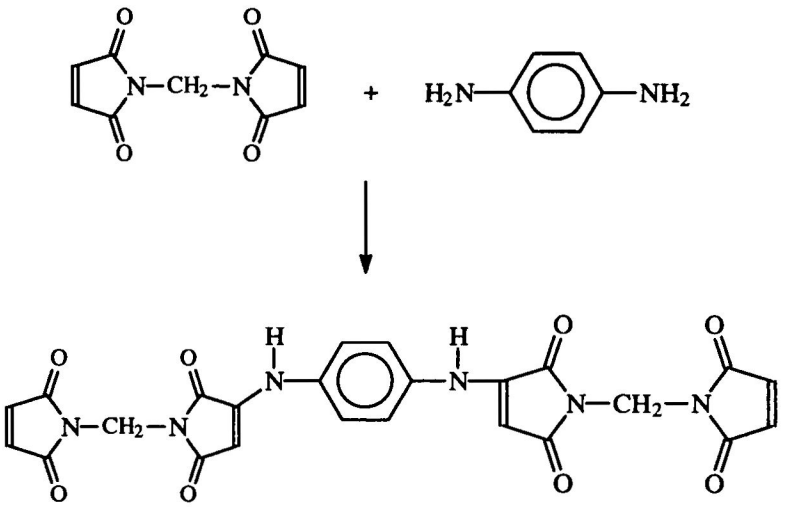

Bisnadimides type polyimides are synthesized using the polymerization of monomeric reactants (PMR) approach. These type of polyimides undergo a condensation reaction to form the imide prepolymer, Scheme 3, and undergo further polymerization to a temperature resistant three-dimensional network.[12] Examples of bisnadimide type polyimides are bis(allylnadimidodiphenylmethane) and bis(allylnadicimidohexane), Figure 7.

Scheme 3. Polymerization of a PMR-type nadimide end-capped prepolymer

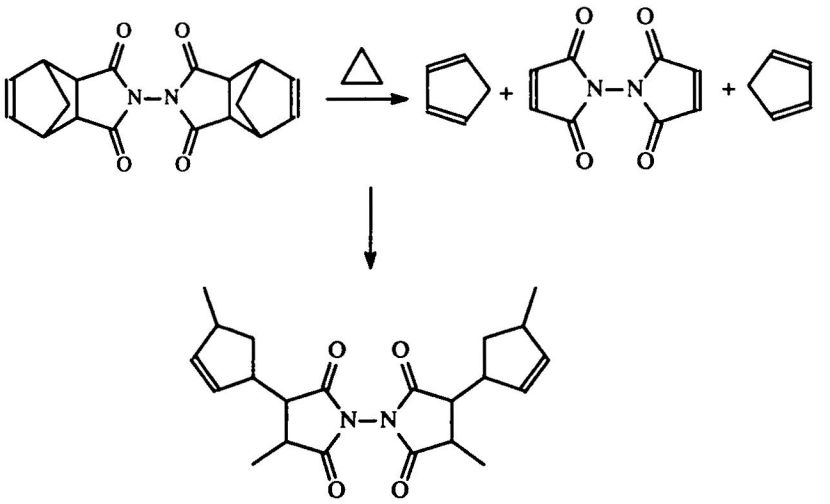

In order to improve processability of thermally stable polymers, polyimides are also synthesized by means of a oligomer containing polymerizable end groups upon heating, Type 3.[13] Ethynyl-capped polyimide oligomer is an example of this type of polyimides, Figure 8.

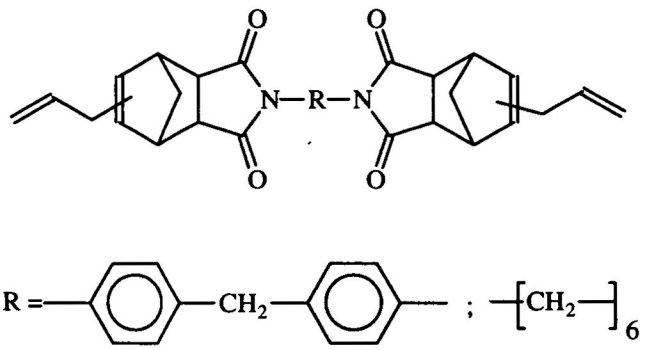

Figure 7. Structures of bis(allylnadimides)

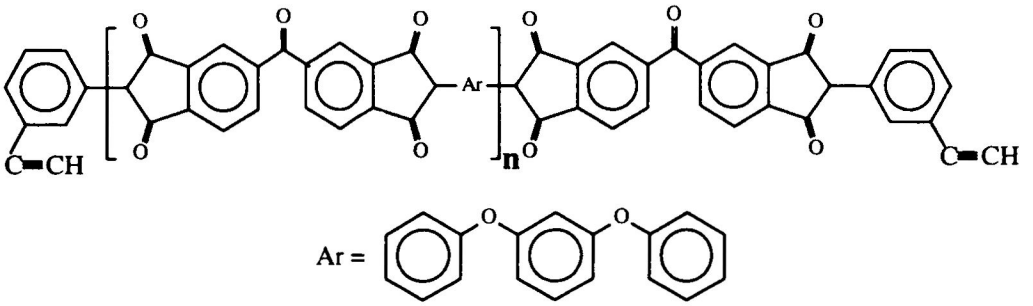

Figure 8. Structure of ethynyl-capped polyimide oligomer

The versatility in their synthesis, together with their high performance properties make polyimides a very interesting field of study. Polyimides have been recognized from the earliest days of their invention for their outstanding thermal stability both in air and inert atmospheres. These polymers are found to have excellent physical properties such as low density, remarkable thermal stability, solvent resistance and excellent mechanical and electrical performance over a wide temperature range. Polyimides have a number of advantages over inorganic molecules, such as, improved processability, improved stress relief (elasticity), ease of purification and a low dielectric constant.

Inspite of these excellent properties, they are very difficult to process (fabrication of films and fibers) due to their poor solubility in common solvents, the high processing temperature and the evolution of volatiles during imidization. The low solubility of these polymers in organic and inorganic solvents and their high melting transitions are due essentially to the rigidity of the aromatic ring system which result in large van der Waals forces between individuals polymer molecular chains.

Different approaches have been used to improve solubility and reduce melting transitions of polyimides without destroying the high performance properties of the polymers, especially, thermal and thermal oxidative stability. Efforts to increase the solubility of rodlike polymers include some structural modifications, such as, the use of bulky substituents, kinks, the introduction of a randomly spaced semi-flexible chain fragments, the replacement of the phenyl ring in the polymer system and the use of non-coplanar biphenyl moieties.

In 1972, Serafini *et al.* developed the 'polymerization of monomeric reactants approach' (PMR) in the synthesis of PMR-15.[14] PMR-15 is a high temperature polyimide used as a composite matrix resin, formed by the reaction of 4,4'-methylene diamine (MDA), 5-norbornene-2,3-dicarboxylic acid monomethyl ester (NE) and benzophenone tetracarboxylic acid dimethyl ester (BTDE) in low boiling alkyl alcohol, Figure 9.[15] PMR-15 is characterized by excellent mechanical properties but also have several disadvantages. For example, the quality control of PMR-15 methanol solutions is difficult due to varying triester levels found and the shelf life is limited by room temperature reactions that can occur between the monomers. Furthermore, PMR-15 contains the carcinogenic diamine (MDA) and the resin system is brittle due to its high degree of crosslinking. Aromatic polyamines have been used to eliminate the use of methylene dianiline in PMR-15 formulation. The monomer, 2,2'-bis[4-(4-aminophenoxy)phenyl] hexafluoropropane known as 4-BDAF was used in the PMR process to improve toughness and processability of polyimides due to the presence of hexafluoro groups.[16] PMR-II polyimide synthesized by the reaction of 5-norbornene-2,3-dicarboxylic acid monomethyl ester (NE), *para-*

phenylenediamine and the dimethyl ester of 4,4'-(hexafluoroisopropylidene)bis(phtalic acid), HFDE, results in improved processability and thermal stability, Figure 10.[17]

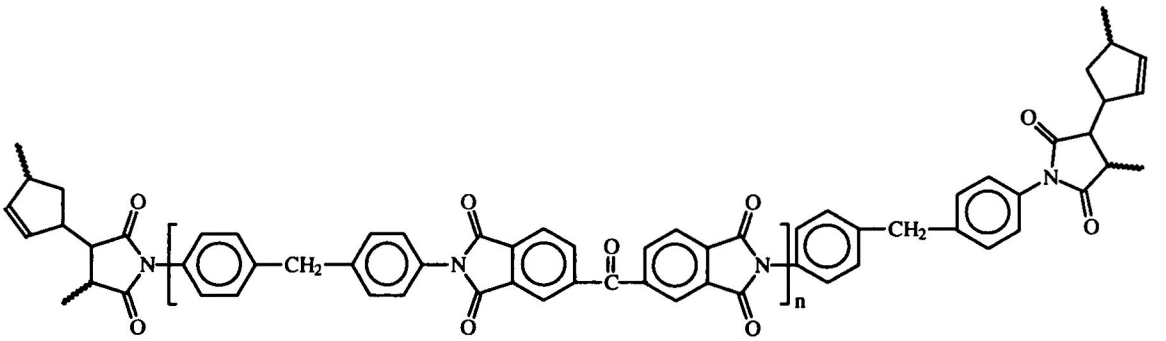

Figure 9. Structure of PMR-15 polyimide

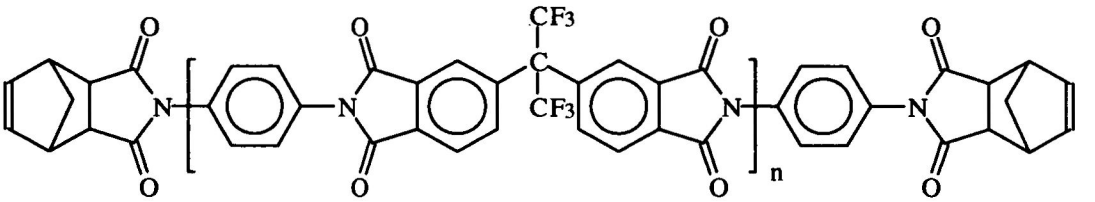

Figure 10. Structure of PMR-II polyimide

More recently, the use of processable precursor polymers which subsequently can be converted into the intractable rodlike polymers has been developed. Aromatic polyimides are generally prepared via a two-step process involving the synthesis of a processable poly(amic acid) precursor and an intramolecular ring closure to the polyimide. *para*-Linked aromatic poly(amic ethyl) esters showed solubility in high concentrations in solvents such as dimethylformamide (DMF) or N-methyl-2-pyrrolidinone (NMP) without inorganic salts as additives.[18]

The synthesis of highly phenylated dianhydride and diamine monomers give soluble and high glass transition temperature (Tg) polyimides.[19,20] The polyimides dissolve readily in N-methyl-2-pyrrolidinone (NMP) and *m*-cresol while maintaining high thermal stability.

Another effective approach to improving processability of high temperature aromatic polymers is the incorporation of a crank and twisted non-coplanar structure into the polymer main chain, by the use of novel diamines and dicarboxylic acids, Figure 11.[21] Polyimides derived from these diamines show improved solubility and high glass transition temperatures.

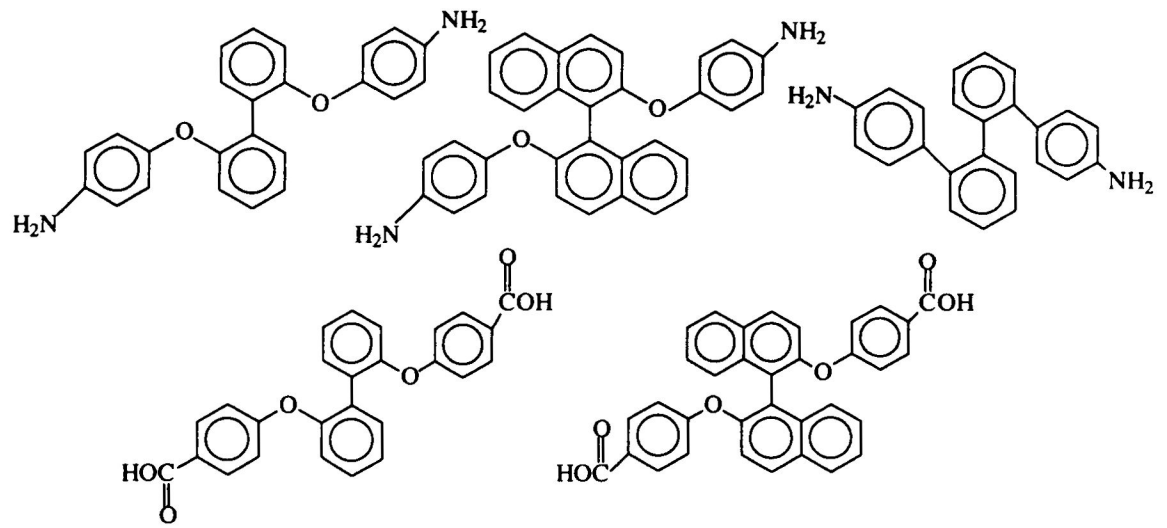

Figure 11. Aromatic diamines and diacids having crank and twisted non-coplanar structure

Aromatic polyimides containing the non-coplanar disubstituted biphenyl moieties (CF_3, CH_3) have been prepared to improve solubility of polyimides, Scheme 4.[22]

Scheme 4. Synthetic route to 2,2'-disubstituted biphenyl-4,4'-diamine type polyimide

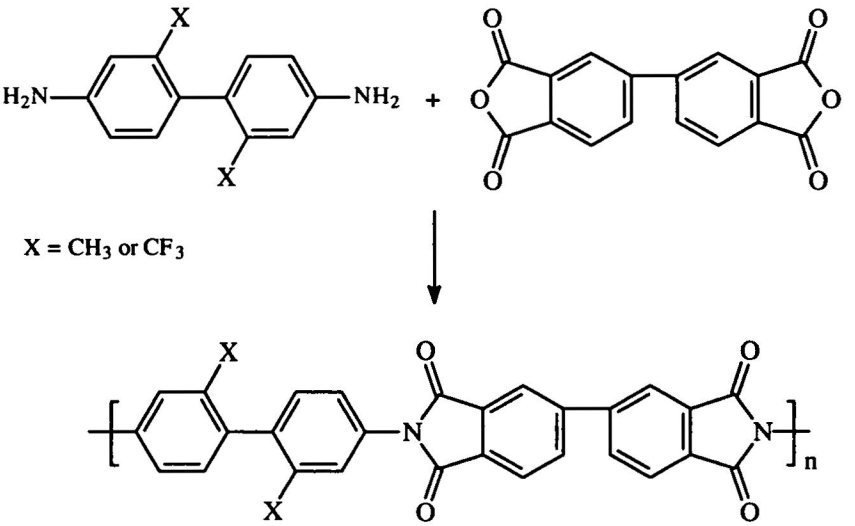

Wholly aromatic polyimides exhibit high thermal and thermooxidative stability but also exhibit a high degree of intractability due to high π-electron density. In order to improve upon the processability of these polymers, a six member ring, such as, bicyclo[2.2.2]oct-7-ene which is a precursor to the aromatic ring system has been used. The aromatic ring system and bicyclo[2.2.2]oct-7-ene ring system are similar in linearity, geometry, and polarizability.[23,24] Polymers derived from bicyclo[2.2.2]oct-7-ene ring system are expected to be easy to process due to a reduction in the symmetry of the polymer backbone and a reduction in the π-electron density of the system. For example, Polk *et al.* used the bicyclic ring system in the synthesis of homopolyesters which exhibited liquid crystalline properties.[25] Harruna *et al.* used a disubstituted bicyclic ring system as a precursor to the aromatic ring system in the synthesis of high performance

polyamides.[26] These polymers were converted to the desired aromatic system by pyrolysis in the presence of a Lewis acid, such as, $ZnCl_2$.

The objective of this work is to synthesize and characterize high performance polyimides containing the bicyclo[2.2.2]oct-7-ene ring system. This is accomplished by the substitution of an aromatic anhydride with a bicyclic type anhydride in combination with $-CF_3$ or $-CH_3$ disubstituted diamines. Our goal is to study the effects of the bicyclo[2.2.2]oct-7-ene ring system, and the methyl (CH_3) and trifluoromethyl (CF_3) substituents on thermal stability, liquid crystallinity and solubility of the polymers.

EXPERIMENTAL

Instrumentation and measurements

The structures of all synthesized polymers were confirmed by proton and carbon-13 nuclear magnetic resonance spectroscopy and infrared spectroscopy. Proton and carbon-13 nuclear magnetic resonance spectra were obtained in deuterated dimethylsulfoxide (DMSO)-d_6, deuterated dimethylformamide (DMF)-d_7 or deuterated sulfuric acid (D_2SO_4) using a Bruker WM-250 spectrometer. Solid state carbon-13 nuclear magnetic resonance (NMR) spectra were obtained with a Bruker ARX-400 and a Bruker AM-400 spectrometer equipped with a silicon graphics INDY computer. Solutions were prepared using tetramethylsilane (TMS) as an internal standard. Infrared spectra were performed on a Nicolet Omnicon FTIR spectrometer, using KBr pellets. Elemental analyses results were obtained from Atlantic Microlab Inc., Atlanta, GA and Galbraith Laboratories Inc., Knoxville, TN. X-ray scattering patterns were obtained using a Philips X' Pert-MPD X-ray difractometer.

Thermogravimetric analyses (TGA) was performed on a Seiko Scientific Instruments (SSI) TGA/DTA 220 thermogravimetric analyzer. Open platinum pans were used as reference and sample holders. Scans were run at 10 °C/min under argon and air atmospheres. Differential scanning calorimetry (DSC) were obtained with a Seiko Scientific Instruments (SSI) DSC 220 differential scanning calorimeter, under argon and in air. DSC curves were obtained at a heating rate of 10 °C/min using sealed aluminum reference and sample pans. Transitions were taken as peak minima (endotherm) and peak maxima (exotherm). Visual

observations of thermal transitions under cross polarized light were made using the Laborlux Pol 12 polarizing optical microscope equipped with a heating stage.

Inherent viscosity measurements were obtained at 30 °C with concentrations of 0.5g/100mL of polymer in dimethylsulfoxide (DMSO) or concentrated sulfuric acid (H_2SO_4). Solubility tests were determined at room temperature.

Materials and Solutions

The monomers, 1,4-phenylenediamine and 1,3-phenylenediamine, were commercial products obtained from Aldrich Chemical Company and were purified by sublimation. Bicyclo[2.2.2]oct-7-ene-tetracarboxylic dianhydride was obtained from Chiskev Company and was purified by recrystalization from acetonitrile. 1,2,4,5-Benzene tetracarboxylic dianhydride, *o*-tolidine and 2,2'-bis(trifluoromethyl)benzidine monomers were obtained from Chiskev Company, Aldrich Chemical Company and Frinton Chemical Company, respectively, and were used as recieved. All monomers were dried and characterized by FTIR, proton and carbon-13 nuclear magnetic resonance spectroscopy.

Polymer Synthesis

Glassware for the polycondensations were dried with a heat gun and flushed with nitrogen. Polymerization procedure were performed under inert atmosphere and with anhydrous solvents.

Synthesis of bicyclo[2.2.2]oct-7-ene-2,3,5,6-tetracarboxylic dianhydride and 1,4-phenylenediamine containing polyamic acid AI and polyimide AII. In a three-necked round bottom flask (250 mL) equipped with a mechanical stirrer, thermometer, septum, condenser, calcium chloride drying tube, nitrogen inlet and bubbler was added 1.09 g (0.0101 mol) of 1,4-phenylenediamine, 1.56 g of dry LiCl and 60 mL of anhydrous NMP. The mixture was stirred until all the solids dissolved. The solution was cooled to 0 °C. A mixture of anhydrous NMP (40 mL) and bicyclo[2.2.2]oct-7-ene-2,3,5,6-tetracarboxylic dianhydride (2.50 g, 0.0101 mol) were injected into the stirred solution through the septum. The reaction mixture was stirred for 1 h at 0 °C, and then slowly heated to 30 °C overnight. By means of a pasteur pipette, half of the reaction mixture was removed. The solution collected was precipitated in 200 mL of distilled water and the solids collected by suction filtration. The solids were washed two times with 60 mL of ethanol and dried under vacuum for 1 h at 50 °C to give the crude 1,4-phenylenediamine containing polyamic acid (2.46 g). The solids were extracted with acetone using a Soxhlet extraction apparatus for 48 h. The polyamic acid was dried under vacuum at 100 °C for 12 h to give 1,4-phenylenediamine containing polyamic acid AI (2.30 g).

The septum was replaced with a glass stopper and the remaining reaction mixture was stirred and heated at 180 °C for 22 h. The reaction mixture was precipitated in 300 mL of distilled water. The precipitate was collected by suction filtration. The solids were washed two times with ethanol and dried under vacuum at 50 °C for 1 h. Crude 1,4-phenylenediamine containing polyimide (3.11 g) was obtained. The solids were extracted with acetone using a Soxhlet extraction apparatus for 48 h. The polymer was dried under vacuum at 100 °C for 12 h to give 1,4-phenylenediamine containing polyimide AII (2.95 g).

Synthesis of bicyclo[2.2.2]oct-7-ene-2,3,5,6-tetracarboxylic dianhydride and 1,3-phenylenediamine containing polyamic acid BI and polyimide BII. In a three-necked round bottom flask (250 mL) equipped with a mechanical stirrer, thermometer, septum, condenser, calcium chloride drying tube, nitrogen inlet and bubbler was added 1.30 g (0.0120 mol) of 1,3-phenylenediamine, 1.86 g of dry LiCl and 60 mL of anhydrous NMP. The mixture was stirred until all the solids dissolved. The solution was cooled to 0 °C. A mixture of anhydrous NMP (40 mL) and bicyclo[2.2.2]oct-7-ene-2,3,5,6-tetracarboxylic dianhydride (2.98 g, 0.0120 mol) were injected into the stirred solution through the septum. The reaction mixture was stirred for 1 h at 0 °C, and then slowly heated to 30 °C overnight. By means of a pasteur pipette, half of the reaction mixture was removed. The solution collected was precipitated in 200 mL of distilled water and the solids collected by suction filtration. The solids were washed two times with 60 mL of ethanol and dried under vacuum for 1 h at 50 °C to give the crude 1,3-phenylenediamine containing polyamic acid (1.90 g). The solids were extracted with acetone using a Soxhlet extraction apparatus for 48 h. The polyamic acid was dried under vacuum at 100 °C for 12 h to give the 1,3-phenylenediamine containing polyamic acid BI (1.30 g).

The septum was replaced with a glass stopper and the remaining reaction mixture was stirred and heated at 180 °C for 22 h. The reaction mixture was precipitated in 300 mL of distilled water. The precipitate was collected by suction filtration. The solids were washed two times with ethanol and dried under vacuum at 50 °C for 1 h. Crude 1,3-phenylenediamine containing polyimide (3.10 g) was obtained. The solids were extracted with acetone using a Soxhlet extraction apparatus for 48 h. The polymer was dried under vacuum at 100 °C for 12 h to give 1,3-phenylenediamine containing polyimide BII (2.72 g).

Synthesis of bicyclo[2.2.2]oct-7-ene-2,3,5,6-tetracarboxylic dianhydride and *o*-tolidine containing polyamic acid CI and polyimide CII. In a three-necked round bottom flask (250 mL) equipped with a mechanical stirrer, thermometer, septum, condenser, calcium chloride drying tube, nitrogen inlet and bubbler was added 2.57 g (0.0121 mol) of *o*-tolidine, 1.87 g of dry LiCl and 60 mL of anhydrous NMP. The mixture was stirred until all the solids dissolved. The solution was cooled to 0 °C. A mixture of anhydrous NMP (40 mL) and bicyclo[2.2.2]oct-7-ene-2,3,5,6-tetracarboxylic dianhydride (3.00 g, 0.0121 mol) were injected into the stirred solution through the septum. The reaction mixture was stirred for 1 h at 0 °C, and then slowly heated to 30 °C overnight. By means of a pasteur pipette, half of the reaction mixture was removed. The solution collected was precipitated in 200 mL of distilled water and the solids collected by suction filtration. The solids were washed two times with 60 mL of ethanol and dried under vacuum for 1 h at 50 °C to give the crude *o*-tolidine containing polyamic acid (1.80 g). The solids were extracted with acetone using a Soxhlet extraction apparatus for 48 h. The polyamic acid was dried under vacuum at 100 °C for 12 h to give the *o*-tolidine containing polyamic acid CI (1.50 g).

The septum was replaced with a glass stopper and the remaining reaction mixture was stirred and heated at 180 °C for 22 h. The reaction mixture was precipitated in 300 mL of distilled water. The precipitate was collected by suction filtration. The solids were washed two times with ethanol and dried under vacuum at 50 °C for 1 h. Crude *o*-tolidine containing polyimide (4.51 g) was obtained. The solids were extracted with acetone using a Soxhlet extraction apparatus for 48 h. The polymer was dried under vacuum at 100 °C for 12 h to give *o*-tolidine containing polyimide CII (3.50 g).

Synthesis of bicyclo[2.2.2]oct-7-ene-2,3,5,6-tetracarboxylic dianhydride and 2,2'-bis(trifluoromethyl)benzidine containing polyamic acid DI and polyimide DII. In a three-necked round bottom flask (250 mL) equipped with a mechanical stirrer, thermometer, septum, condenser, calcium chloride drying tube, nitrogen inlet and bubbler was added 2.58 g (0.00806 mol) of 2,2'-bis(trifluoromethyl)benzidine, 1.25 g of dry LiCl and 40 mL of anhydrous NMP. The mixture was stirred until all the solids dissolved. The solution was cooled to 0 °C. A mixture of anhydrous NMP (35 mL) and bicyclo[2.2.2]oct-7-ene-2,3,5,6-tetracarboxylic dianhydride (2.00 g, 0.00806 mol) were injected into the stirred solution through the septum. The reaction mixture was stirred for 1 h at 0 °C, and then slowly heated to 30 °C overnight. By means of a pasteur pipette, half of the reaction mixture was removed. The solution collected was precipitated in 200 mL of distilled water and the solids collected by suction filtration. The solids were washed two times with 60 mL of ethanol and dried under vacuum for 1 h at 50 °C to give the crude 2,2'-bis(trifluoromethyl)benzidine containing polyamic acid (2.10 g). The solids were extracted with acetone using a Soxhlet extraction apparatus for 48 h. The polyamic acid was dried under vacuum at 100 °C for 12 h to give the 2,2'-bis(trifluoromethyl)benzidine containing polyamic acid DI (1.70 g).

The septum was replaced with a glass stopper and the remaining reaction mixture was stirred and heated at 180 °C for 22 h. The viscous reaction mixture was precipitated in 300 mL of distilled water. The precipitate was collected by suction filtration. The solids were washed two times with ethanol and dried under vacuum at 50 °C for 1 h. Crude 2,2'-bis(trifluoromethyl)benzidine containing polyimide (3.01 g) was obtained. The solids were extracted with acetone using a Soxhlet extraction apparatus for 48 h. The polymer was dried

under vacuum at 100 °C for 12 h to give 2,2'-bis(trifluoromethyl)benzidine containing polyimide DII (2.70 g).

Synthesis of 1,2,4,5-benzene tetracarboxylic dianhydride and 2,2'-bis(trifluoromethyl)benzidine containing polyamic acid EI and polyimide EII. In a three-necked round bottom flask (250 mL) equipped with a mechanical stirrer, thermometer, septum, condenser, calcium chloride drying tube, nitrogen inlet and bubbler was added 2.20 g (0.00688 mol) of 2,2'-bis(trifluoromethyl)benzidine, 1.10 g of dry LiCl and 40 mL of anhydrous NMP. The mixture was stirred until all the solids dissolved. The solution was cooled to 0 °C. A mixture of anhydrous NMP (35 mL) and bicyclo[2.2.2]oct-7-ene-2,3,5,6-tetracarboxylic dianhydride (1.50 g, 0.00688 mol) were injected into the stirred solution through the septum. The reaction mixture was stirred for 1 h at 0 °C, and then slowly heated to 30 °C overnight. By means of a pasteur pipette, half of the reaction mixture was removed. The solution collected was precipitated in 200 mL of distilled water and the solids collected by suction filtration. The solids were washed two times with 60 mL of ethanol and dried under vacuum for 1 h at 50 °C to give the crude 2,2'-bis(trifluoromethyl)benzidine containing polyamic acid (1.92 g). The solids were extracted with acetone using a Soxhlet extraction apparatus for 48 h. The polyamic acid was dried under vacuum at 100 °C for 12 h to give the 2,2'-bis(trifluoromethyl)benzidine containing polyamic acid EI (1.20 g).

The septum was replaced with a glass stopper and the remaining reaction mixture was stirred and heated at 180 °C for 22 h. The viscous reaction mixture was precipitated in 300 mL of distilled water. The precipitate was collected by suction filtration. The solids were washed

two times with ethanol and dried under vacuum at 50 °C for 1 h. Crude 2,2'-bis(trifluoromethyl)benzidine containing polyimide (2.95 g) was obtained. The solids were extracted with acetone using a Soxhlet extraction apparatus for 48 h. The polymer was dried under vacuum at 100 °C for 12 h to give 2,2'-bis(trifluoromethyl)benzidine containing polyimide EII (2.30 g).

RESULTS AND DISCUSSION

Polymers

1,4-Phenylenediamine containing polyamic acid AI and the corresponding polyimide AII; and 1,3-phenylenediamine containing polyamic acid BI and the corresponding polyimide BII were prepared by the approach outlined in Scheme 5. The synthetic route leading to *o*-tolidine containing polyamic acid CI and the corresponding polyimide CII; and 2,2'-bis(trifluoromethyl)benzidine containing polyamic acid DI and the corresponding polyimide DII are presented in Scheme 6. The synthetic route leading to 1,2,4,5-benzene tetracarboxylic dianhydride and 2,2'-bis(trifluoromethyl)benzidine containing polyamic acid EI and the corresponding polyimide EII are presented in Scheme 7.

Polymer Characterization

The polymers were characterized by elemental analysis, Fourier transform infrared (FTIR), proton and carbon-13 nuclear magnetic resonance (NMR) spectroscopy, solubility, solution viscosities, and X-ray scattering measurements. Thermal analysis data were obtained by differential scanning calorimetry (DSC), thermogravimetric analysis (TGA), and optical polarizing microscopy.

Scheme 5. Synthetic route to polymers AI, AII, BI, and BII

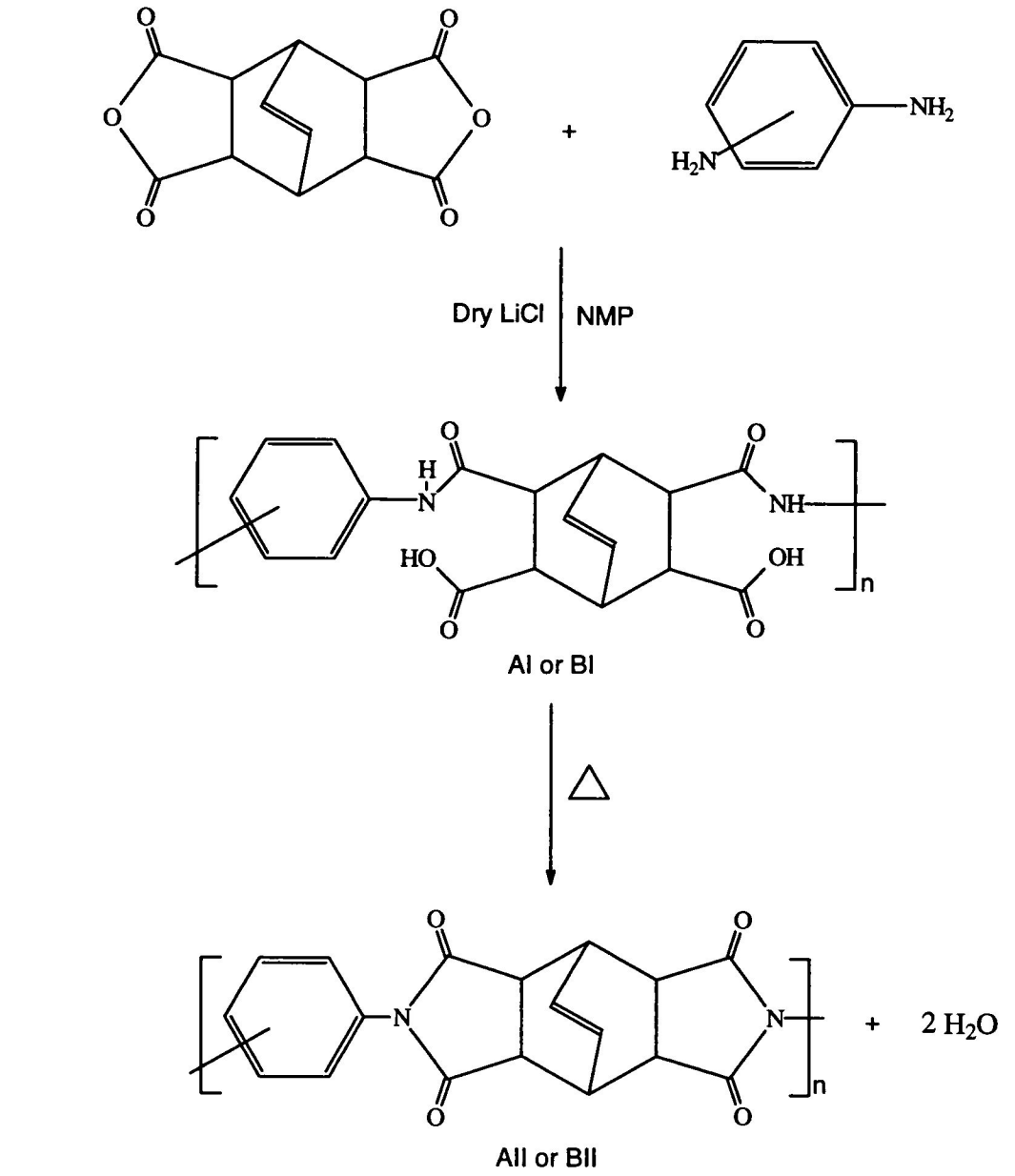

Scheme 6. Synthetic route to polymers CI, CII, DI, and DII

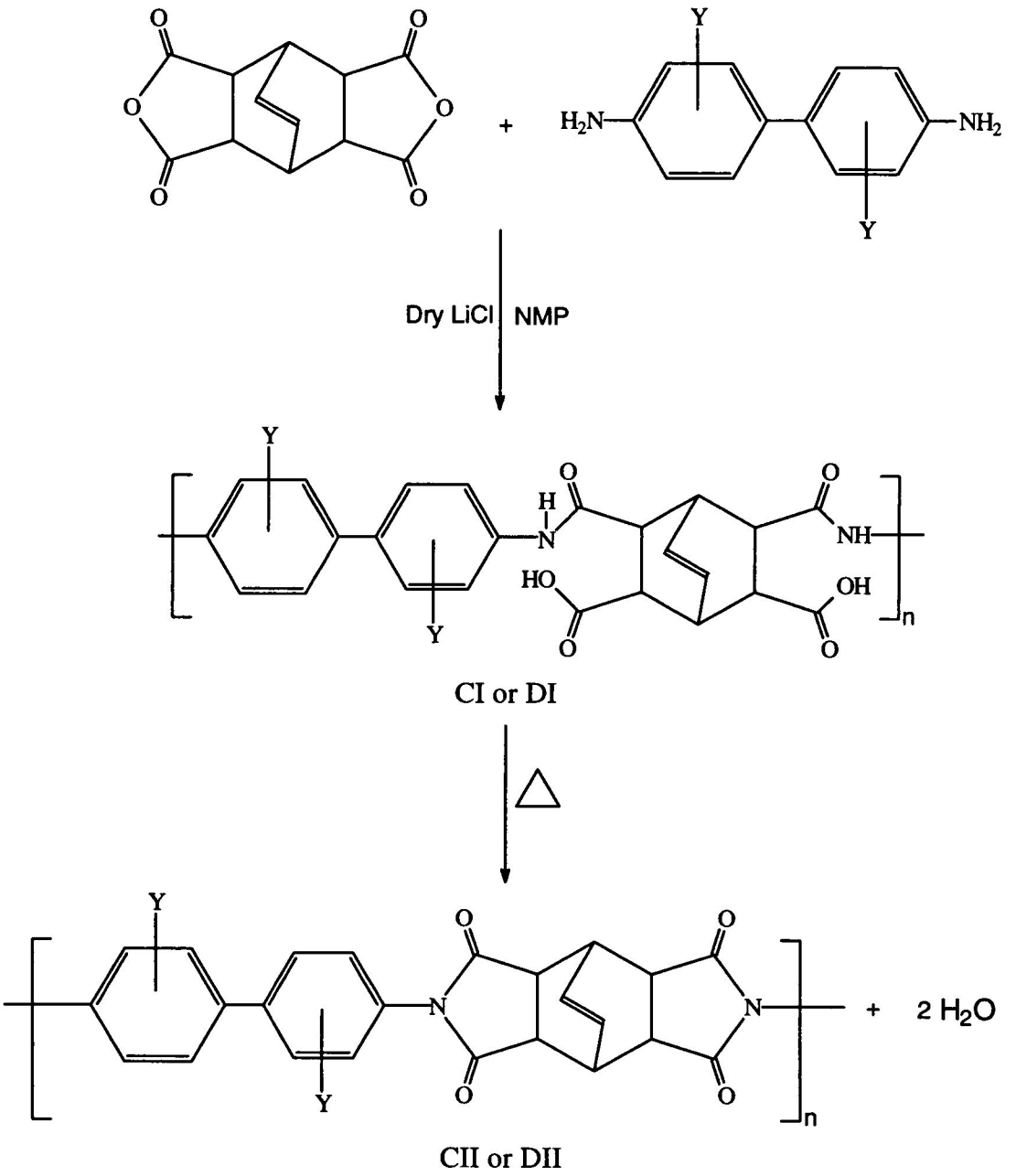

Y = 3,3'- CH_3 for CI and CII

Y = 2,2'- CF_3 for DI and DII

Scheme 7. Synthetic route to polymers EI and EII

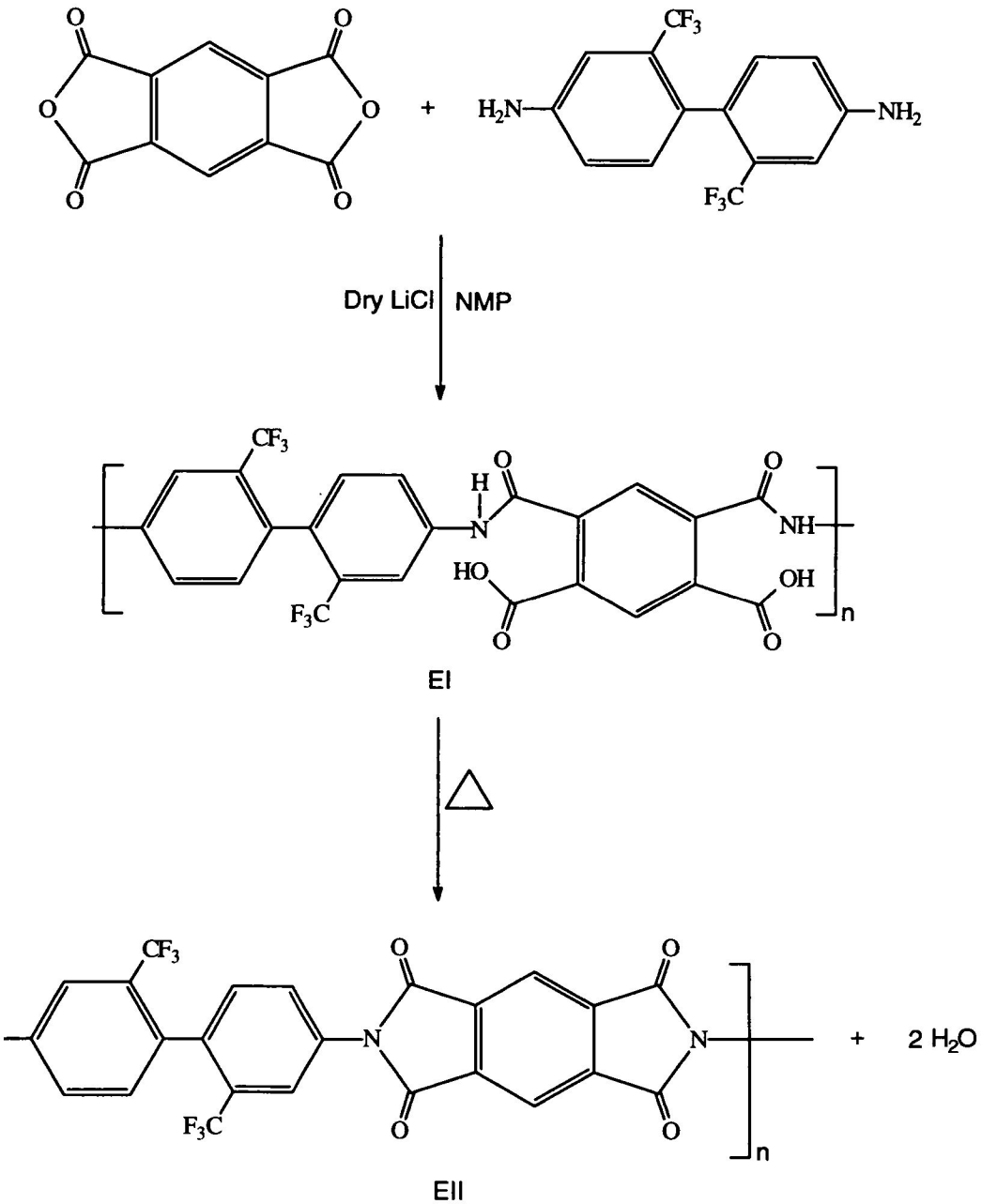

Structural Characterization

Elemental analyses of polyamic acids and polyimides are presented in Table 1.

Table 1. Elemental Analysis data of the polyamic acids and polyimides

	Theoretical %				Found %			
Polymers	C	H	N	F	C	H	N	F
AI	63.9	4.17	8.28	--	63.1	4.48	8.04	--
AII	67.5	3.78	8.74	--	66.3	3.99	8.77	--
BI	63.9	4.17	8.28	--	63.1	4.69	9.02	--
BII	67.5	3.78	8.74	--	66.7	3.95	8.69	--
CI	70.6	5.01	6.33	--	70.4	5.07	6.07	--
CII	73.6	4.75	6.61	--	72.9	4.99	6.72	--
DI	56.7	2.93	5.09	--	57.3	3.39	4.75	--
DII	58.6	2.65	5.26	21.4	57.2	2.31	5.36	20.1
EI	55.4	1.94	5.38	21.9	53.3	2.43	5.35	20.7
EII	57.4	1.61	5.58	22.7	56.2	2.47	5.12	22.5

Infrared spectrum of 1,4-phenylenediamine containing polyamic acid AI shows characteristic amide and carboxylic absorptions at approximately 3552 to 3000 cm^{-1} for the N-H and O-H stretching. A weak stretching absorption peak at 1872 cm^{-1} corresponds to the anhydride carbonyl (C=O) which indicates that the polyimide extension was incomplete after heating at 30 °C overnight. The symmetrical imide carbonyl (C=O) stretch appears at 1782 cm^{-1}. An unsymmetrical imide carbonyl (C=O) stretch, as well as the carboxylic acid and amide carbonyl stretches, overlapp in the region of 1710 to 1730 cm^{-1}. The C=C bridge stretching appears as a weak band at 1620 cm^{-1}. The relatively strong peak at 1512 corresponds to the amide N-C=O stretch and a medium stretching

absorption band at 1374 cm^{-1} corresponds to the imide carbon-nitrogen (C-N) stretching, Figure 12. The infrared absorption peak assignments for 1,4-phenylenediamine containing polyamic acid AI are summarized in Table 2.

Table 2. Infrared absorption peak assignments of the polyamic acids

Functionality	Energy / cm^{-1}	Assignments
N-H, O-H	3499-2637	amide, carboxylic
C=O	1872-1878	anhydride
C=O	1788-1782	imide
C=O	1726-1729	imide
C=O	1710-1716	carboxylic
C=O	1690-1700	amide
C=C	1604-1620	bridge
N-C=O	1499-1512	imide
C-N	1374-1378	imide
C-F	1100-1200[a]	trifluoromethyl

[a]infrared C-F absorption of polyamic acid DI and EI

The proton NMR of 1,4-phenylenediamine containing polyamic acid AI shows a chemical shift at δ 3.3 corresponding to the protons of the tertiary carbons on the bicyclic ring system (H-5, 6); a chemical shift at δ 3.5 indicates the bridge head protons (H-1, 4); the chemical shift at δ 5.3 corresponds to the amide N-H proton (H-9); a chemical shift at δ 6.3 corresponds to the bicyclic bridge protons (H-7, 8); the chemical shift at δ 7.3 ppm corresponds to the aromatic protons of the unsubstituted carbon atoms (H-1', 2'). Due to isomerism (exo, endo) on the bicyclic ring system, the proton NMR shows pairs of chemical shifts: a chemical shift from δ 6.5 to δ 6.7, and the chemical shift from δ 7.4 to δ 7.6 ppm corresponding to the protons on the tertiary carbons of the bicyclic ring system

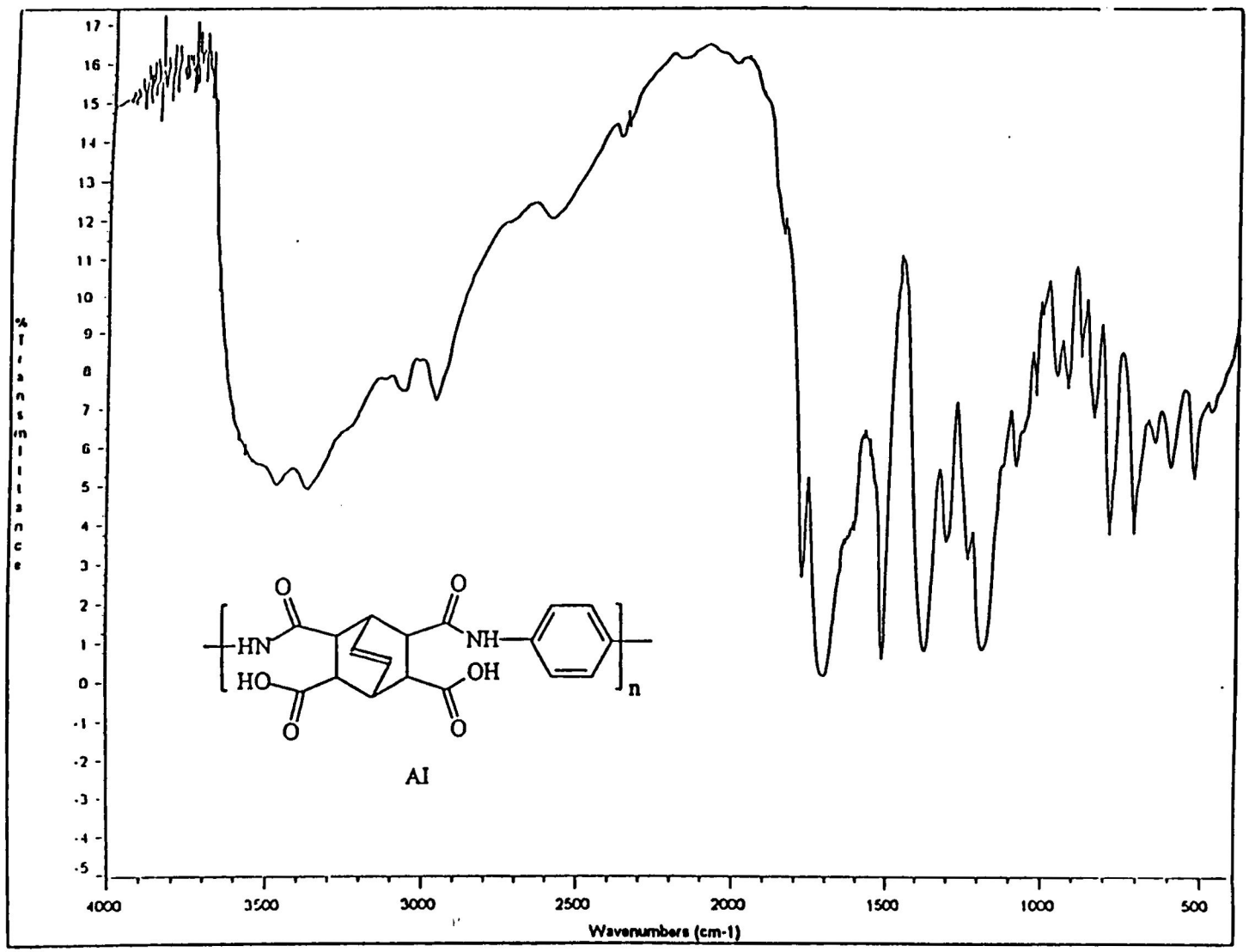

AI

Figure 12. Infrared spectrum of 1,4-phenylenediamine containing polyamic acid AI

(H-2, 3). The chemical shift at δ 10.1 ppm corresponds to the O-H carboxylic proton (H-10), Figure 13.

The carbon-13 NMR spectrum of 1,4-phenylenediamine containing polyamic acid AI exhibits chemical shifts at δ 28.2 corresponding to the bridge head carbons; and the chemical shifts from δ 37.8 to δ 41.0 ppm correspond to the tertiary carbons of the bicyclic ring system. The peaks from δ 129.1 to δ 131.7 ppm correspond to the bridge carbon and to the unsubstituted aromatic carbon atoms. The chemical shift at δ 134.7 ppm indicates the equivalent substituted aromatic carbon atoms. The chemical shifts from δ 151.0 to δ 168.3 ppm correspond to the carbons of the carbonyls of the imide, amide and carboxylic, Figure 14.

The infrared spectrum of 1,4-phenylenediamine containing polyimide AII shows a medium band at 3631-3200 cm^{-1} which corresponds to the N-H and O-H stretches. These results show incomplete ring closure of the polyimide. The weak absorption bands at 3100 to 2960 cm^{-1} correspond to the C-H stretching of the bicyclic and aromatic ring systems, respectively. The weak absorption band at 1872 cm^{-1} disappears as the imidization proceeds. The symmetrical and unsymmetrical imide carbonyl (C=O) stretches are observed at 1782 and 1729 cm^{-1}, respectively. The absorption at 1710 and 1700 cm^{-1} correspond to the carboxylic and amide carbonyl (C=O) stretch, respectively, indicating incomplete ring closure. The absorption of the carbon-carbon double bond (C=C) of the bridge in the bicyclic ring system is overlapped in the carbonyl stretching region. The sharp band at 1512 correspond to the amide N-C=O stretch and the medium absorption at 1374 cm^{-1} corresponds to the imide carbon-nitrogen (C-N) bond, Figure 15. The infrared

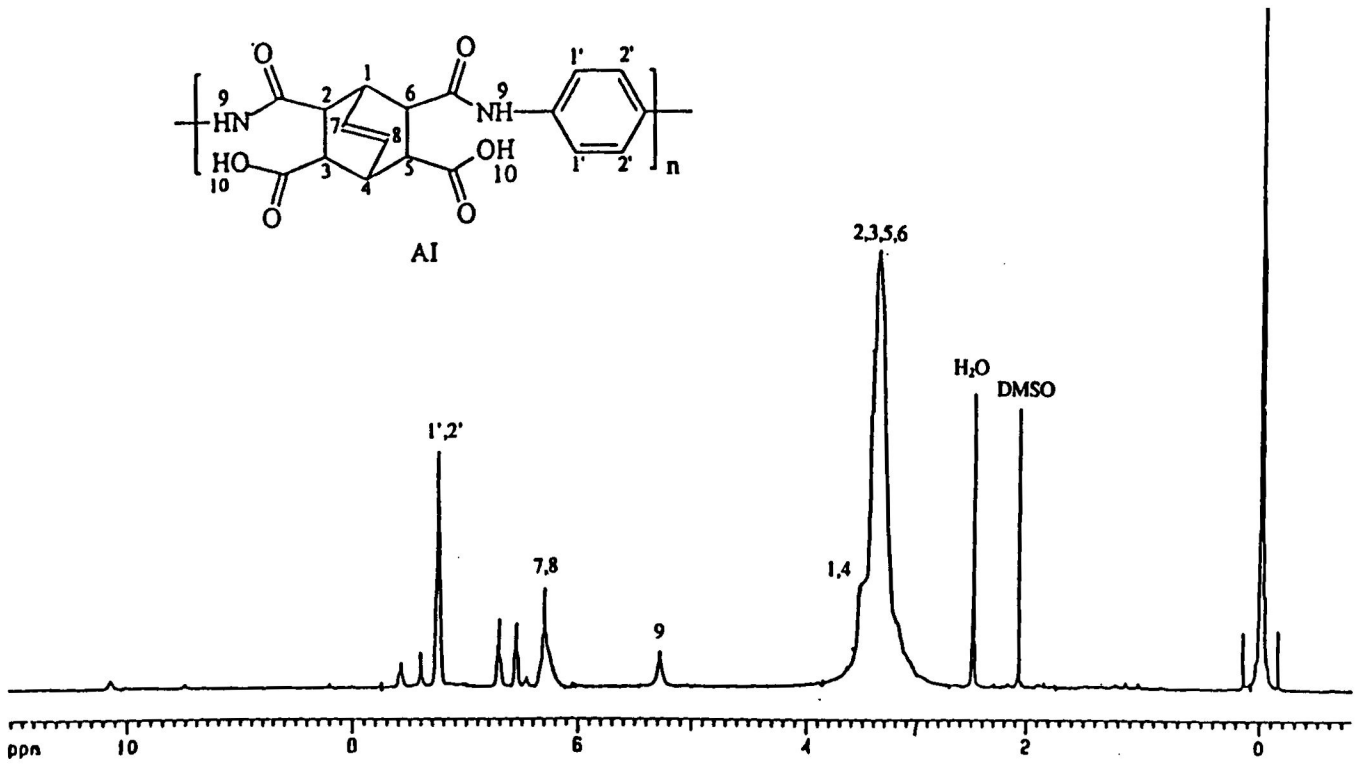

Figure 13. ^{1}H NMR spectrum of 1,4-phenylenediamine containing polyamic acid AI in dimethylsulfoxide-d_6

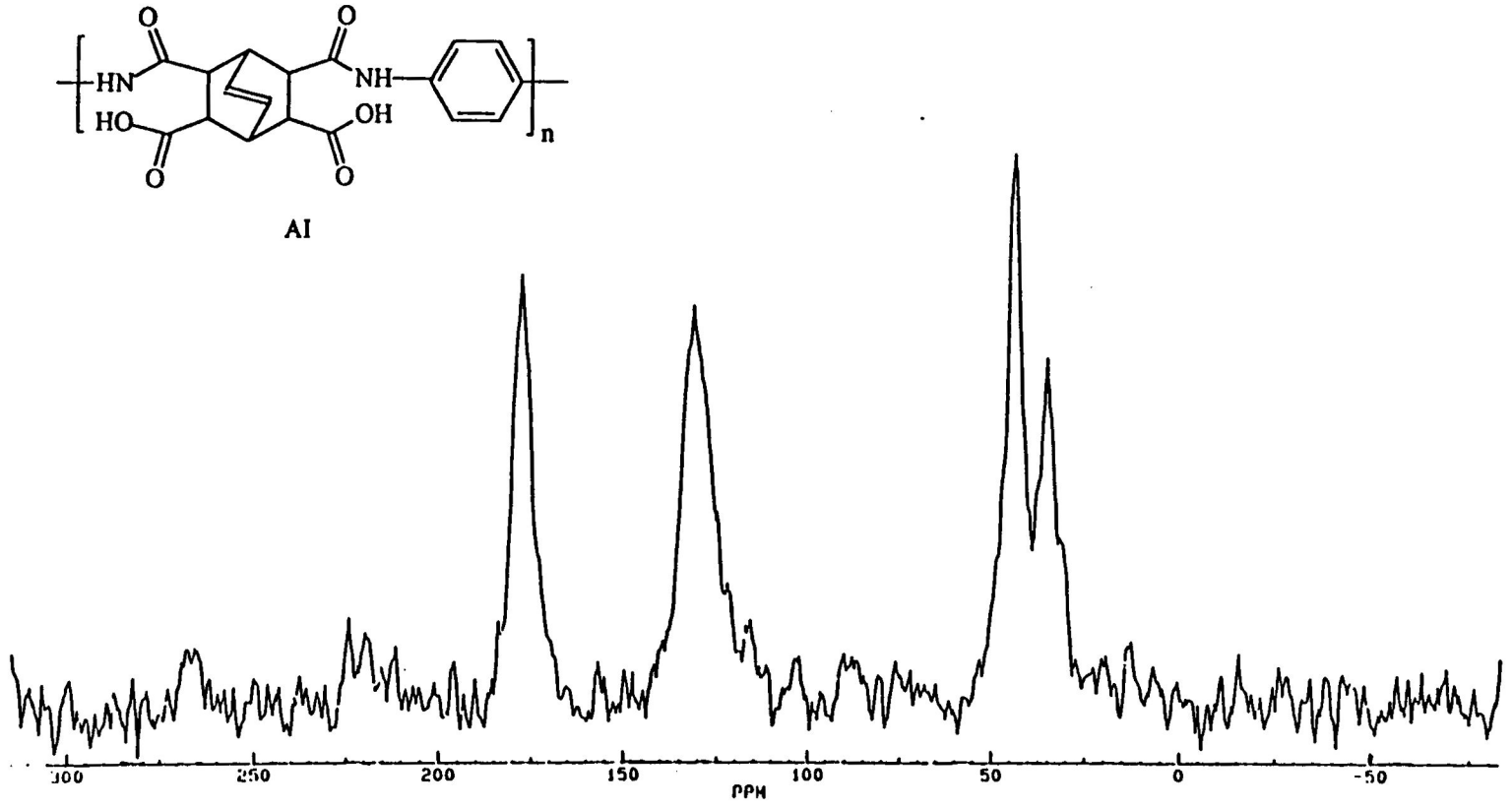

Figure 14. Solid state ^{13}C NMR spectrum of 1,4-phenylenediamine containing polyamic acid AI

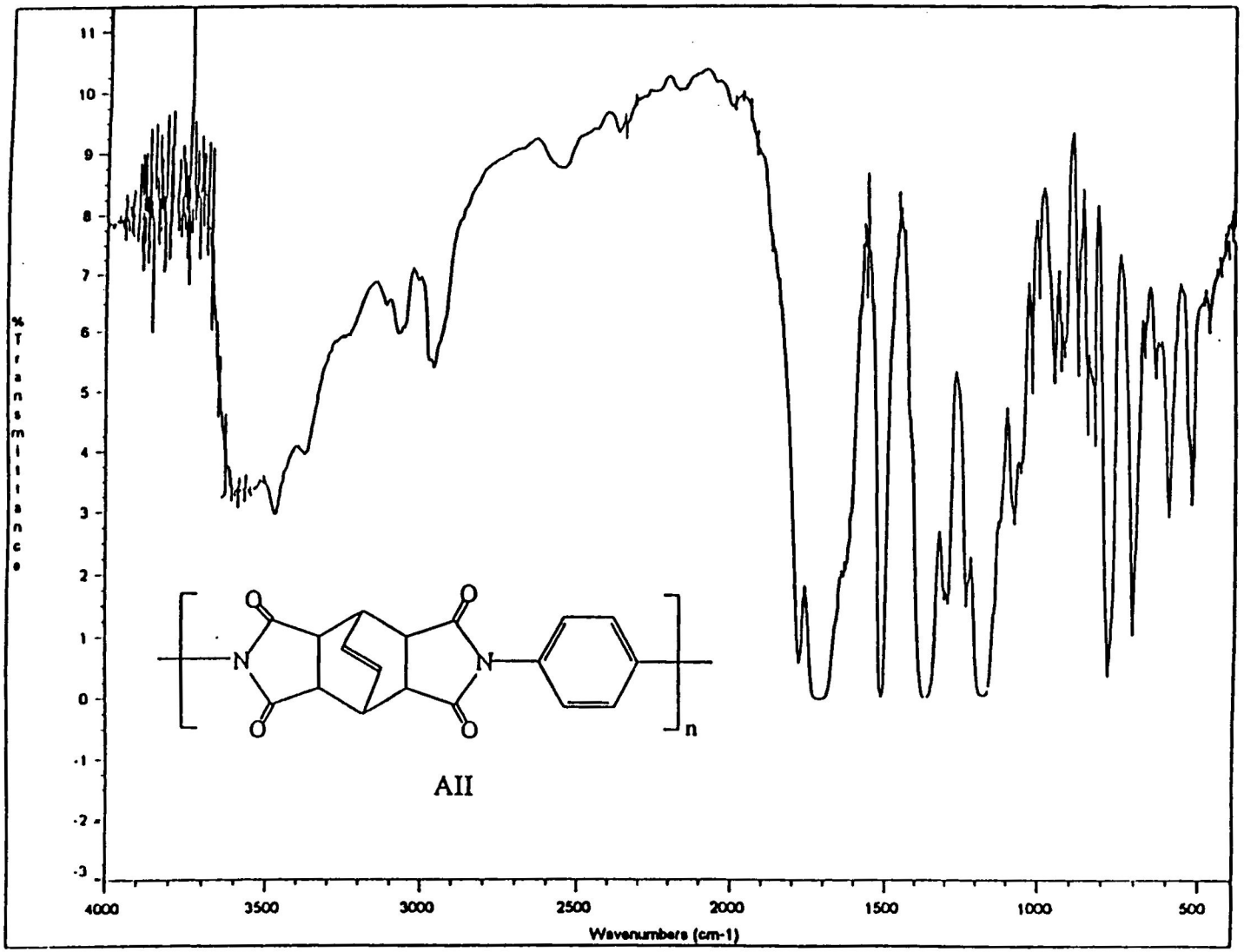

AII

Figure 15. Infrared spectrum of 1,4-phenylenediamine containing polyimide AII

absorption peak assignments of 1,4-phenylenediamine containing polyimide AII are summarized in Table 3.

Table 3. Infrared absorption peak assignments of the polyimides

Functionality	Energy / cm^{-1}	Assignments
N-H, O-H	3592-3200	amide, carboxylic
C-H	3100-2631	methyl
C=O	1788-1782	imide
C=O	1722-1729	imide
C=O	1710-1716	carboxylic
C=O	1690-1700	amide
C=C	1600-1617	bridge
N-C=O	1492-1512	imide
C-N	1374-1378	imide
C-F	1100-1200[a]	trifluoromethyl

[a]infrared C-F absorption of polyimide DII and EI

The proton NMR spectrum of 1,4-phenylenediamine containing polyimide AII is presented in Figure 16. The spectrum shows a chemical shift at δ 1.5 corresponding to the protons of the bicyclic ring system (H-2, 3, 5, 6); the chemical shift at δ 4.0 corresponds to the bridge head protons (H-7, 8); and the chemical shift at δ 8.7 ppm corresponds to the protons of the unsubstituted carbon in the aromatic ring system (H-1', 2').

The carbon-13 NMR spectrum of 1,4-phenylenediamine containing polyimide AII is presented in Figure 17. The spectrum shows a chemical shift at δ 34.8 corresponding to the bridge head carbon atoms; the chemical shift at δ 43.0 ppm corresponds to the tertiary carbons of the bicyclic ring system. The chemical shifts from δ 128.6 to δ 130.0 correspond to the aromatic ring unsubstituted carbon atoms; the chemical shift at δ 132.2

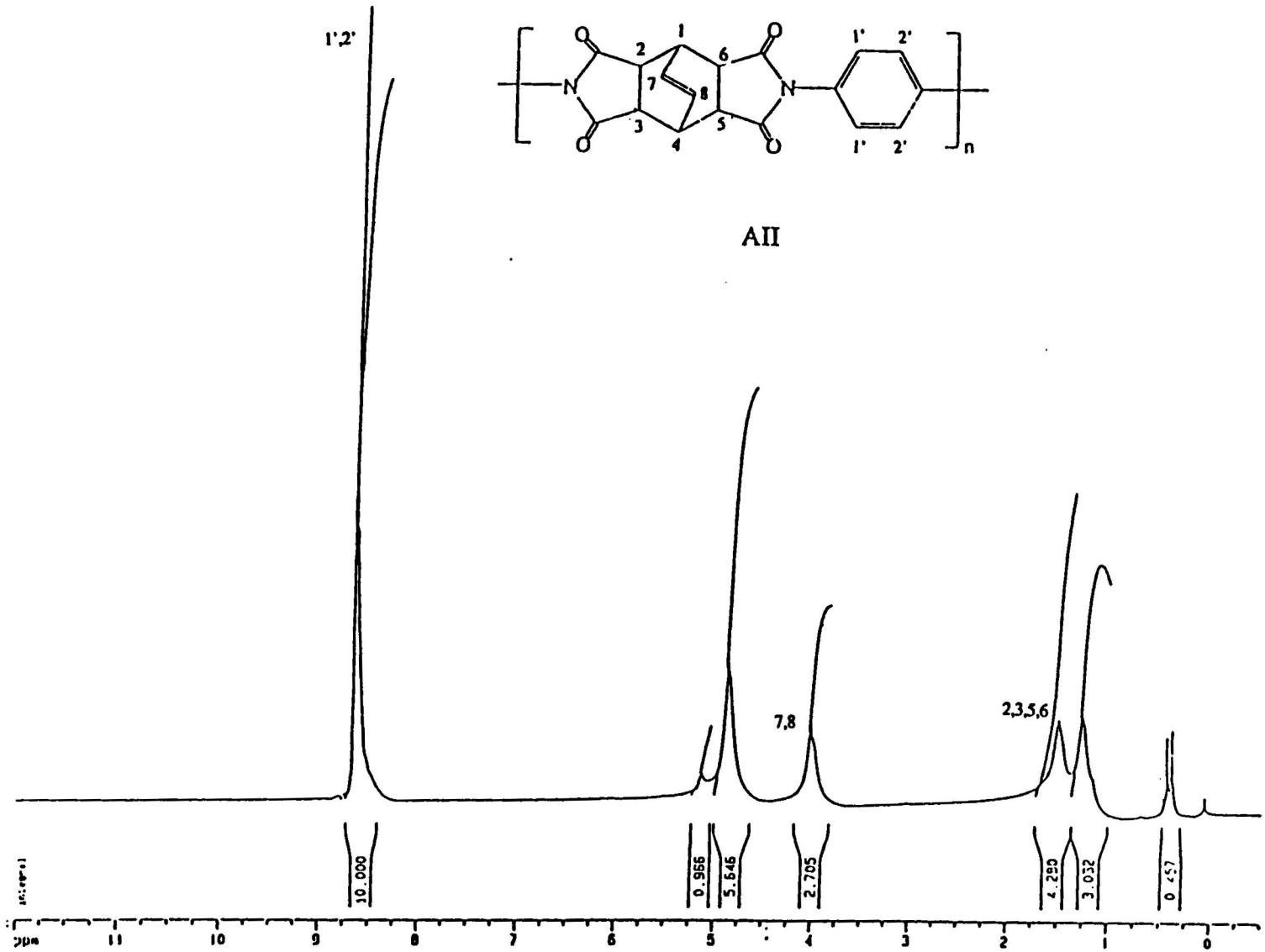

Figure 16. ^{1}H NMR spectrum of 1,4-phenylenediamine containing polyimide AII in sulfuric acid-d_2

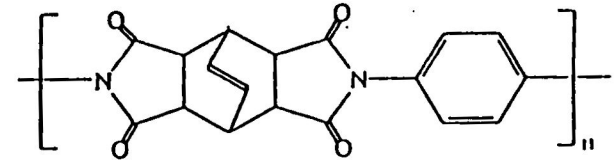

AII

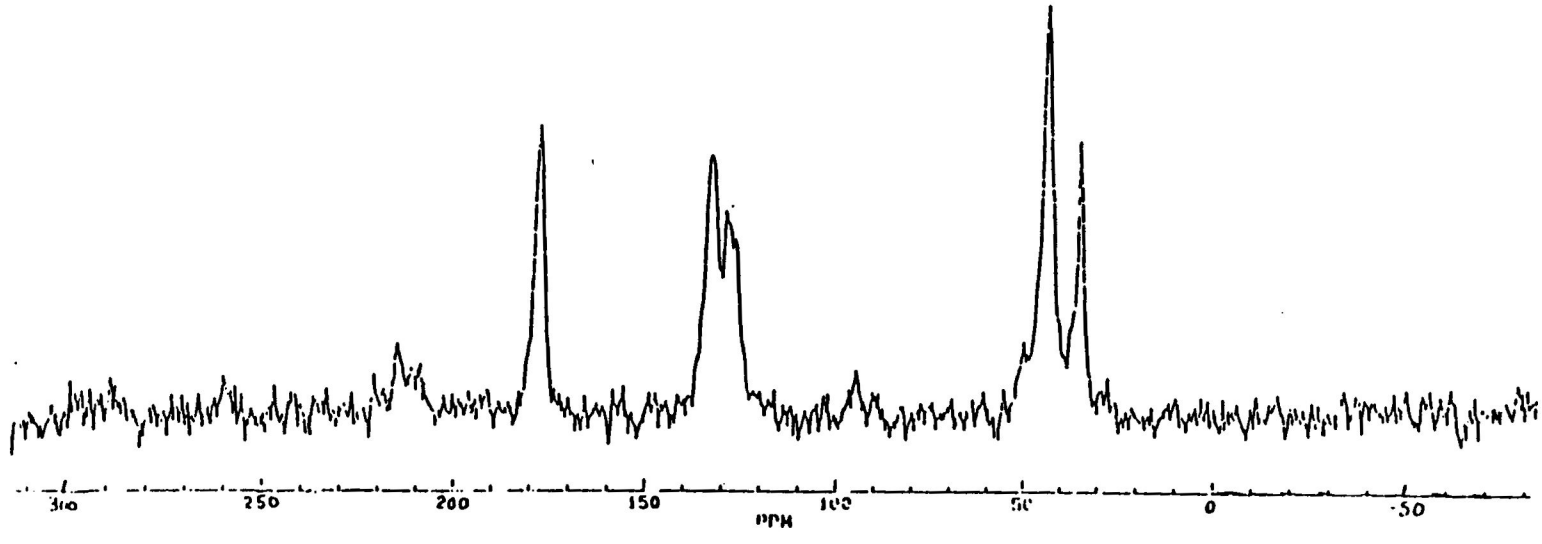

Figure 17. Solid state ^{13}C NMR spectrum of 1,4-phenylenediamine containing polyimide AII

corresponds to the carbon-carbon double bond carbon atoms, and the chemical shift at δ 176.9 ppm corresponds to the carbon atom of the imide carbonyl (C=O).

Infrared spectrum of 1,3-phenylenediamine containing polyamic acid BI is presented in Figure 18. The spectrum shows a broad band from 3605 to 2960 cm^{-1} corresponding to the N-H, O-H, and C-H overlapped stretching. A weak stretching absorption peak at 1872 cm^{-1} corresponds to the anhydride carbonyl (C=O) which indicates that the imidization process was incomplete after heating at 30 °C, overnight. Characteristic symmetrical and unsymmetrical imide carbonyl (C=O) stretches are observed at 1782 and 1729 cm^{-1}, respectively. The carboxylic and amide carbonyl (C=O) functional groups are observed at 1716 and 1700 cm^{-1}, respectively. The carbon-carbon double bond (C=C) bridge head stretch of the bicyclic ring system appears at 1611 cm^{-1} in the infrared spectrum. The absorptions at 1492 and 1374 cm^{-1} correspond to the amide N-C=O and imide carbon-nitrogen (C-N) stretching, respectively. The infrared absorption peak assignments for 1,3-phenylenediamine containing polyamic acid BI are summarized in Table 2.

The proton NMR spectrum of 1,3-phenylenediamine containing polyamic acid BI show a chemical shift at δ 3.5 corresponding to the protons of the bicyclic ring system (H-2, 3, 5, 6); the chemical shift at δ 3.7 corresponds to the bridge head protons of the bicyclic ring system (H-1, 4); a chemical shift at δ 5.3 ppm corresponds to the N-H protons. The NMR spectrum show a chemical shift at δ 6.3 ppm corresponding to the protons of the carbon-carbon double bond of the bicyclic ring system (H-7, 8). The

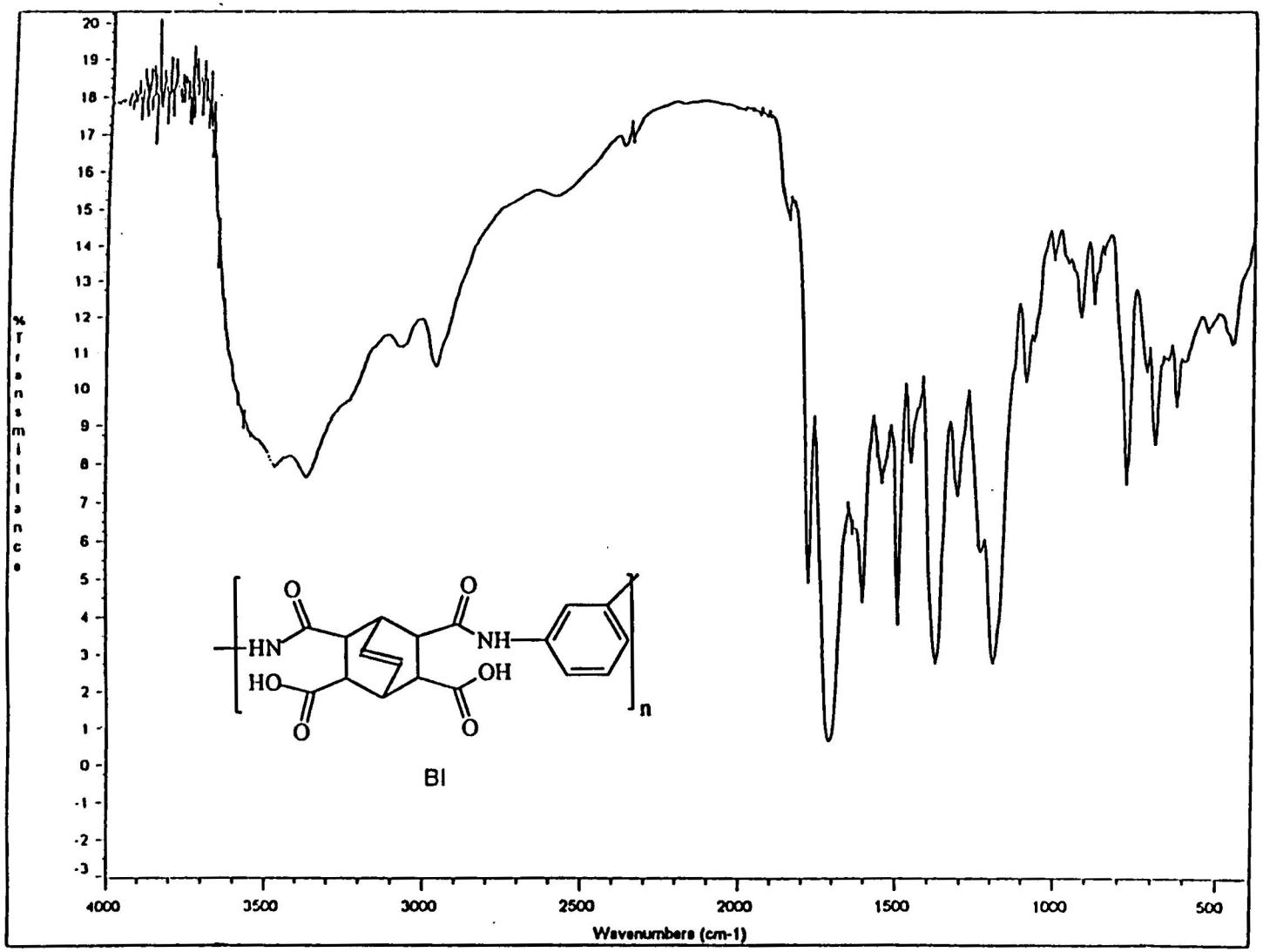

Figure 18. Infrared spectrum of 1,3-phenylenediamine containing polyamic acid BI

aromatic protons show a chemical shift at δ 6.1, δ 6.9, and δ 7.2 ppm (H-1', 2', 3'), respectively, Figure 19.

The carbon-13 NMR spectrum of 1,3-phenylenediamine containing polyamic acid BI is presented in Figure 20. The spectrum exhibits a chemical shift at δ 28.7 corresponding to the bridge head carbons of the bicyclic ring system; chemical shifts at δ 37.8, δ 34.8, and δ 43.77 ppm correspond to the tertiary carbons of the bicyclic ring system. The peaks at δ 126.2, δ 128.3, and δ 129.9 ppm correspond to the bridge carbons and to the unsubstituted aromatic carbon atoms, respectively. The chemical shift of the substituted carbon of the aromatic ring is observed at δ 131.8 ppm of the carbon-13 spectrum. The chemical shifts from δ 168.0 to δ 177.0 ppm correspond to the carbonyl carbons of the imide, amide, and carboxylic, respectively.

The infrared spectrum of model 1,3-phenylenediamine containing polyimide BII shows a broad band from 3638 to 3200 cm^{-1} which correspond to the N-H and O-H stretching. This indicates an incomplete ring closure of the polyimide. (The absorption at 1872 cm^{-1} disappears as the imidization process goes to completion.) The symmetrical and unsymmetrical imide carbonyl functional group show absorptions at 1782 and 1729 cm^{-1}, respectively. The absorption at 1710 and 1700 cm^{-1} correspond to the carboxylic and amide carbonyl (C=O) stretch, respectively. The peak at 1604 cm^{-1} corresponds to the carbon-carbon double bond (C=C) of the bridge in the bicyclic ring system. The absorption at 1492 cm^{-1} corresponds to the amide N-C=O stretch. Evidence of imide structure is the absorption at 1374 cm^{-1} corresponding to the imide carbon-nitrogen (C-N)

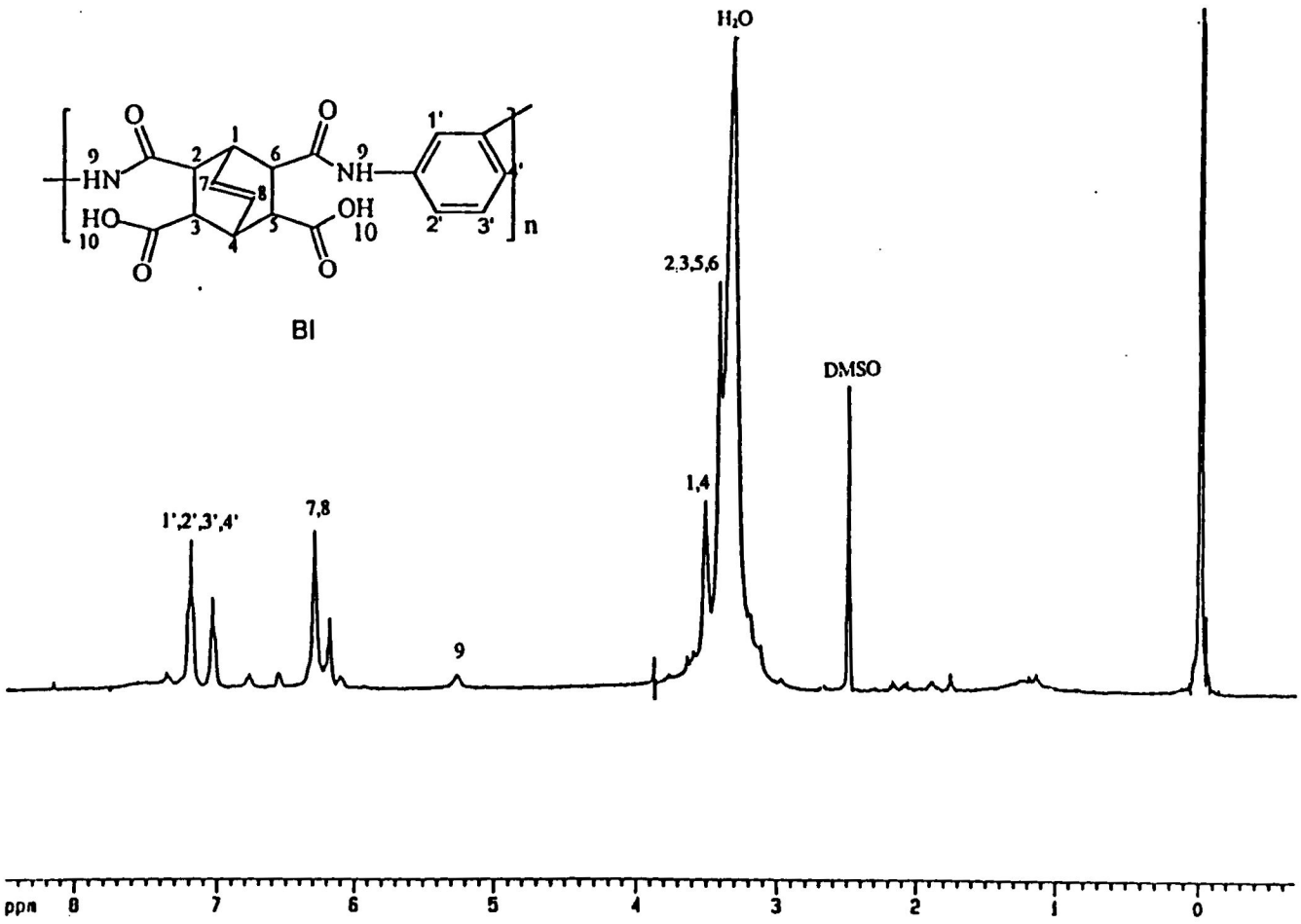

Figure 19. ^{1}H NMR spectrum of 1,3-phenylenediamine containing polyamic acid BI in dimethylsulfoxide-d_6

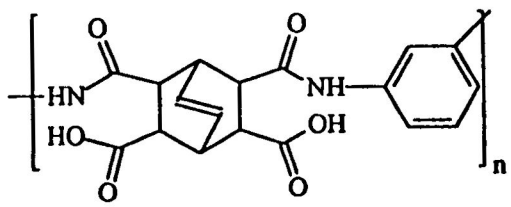

BI

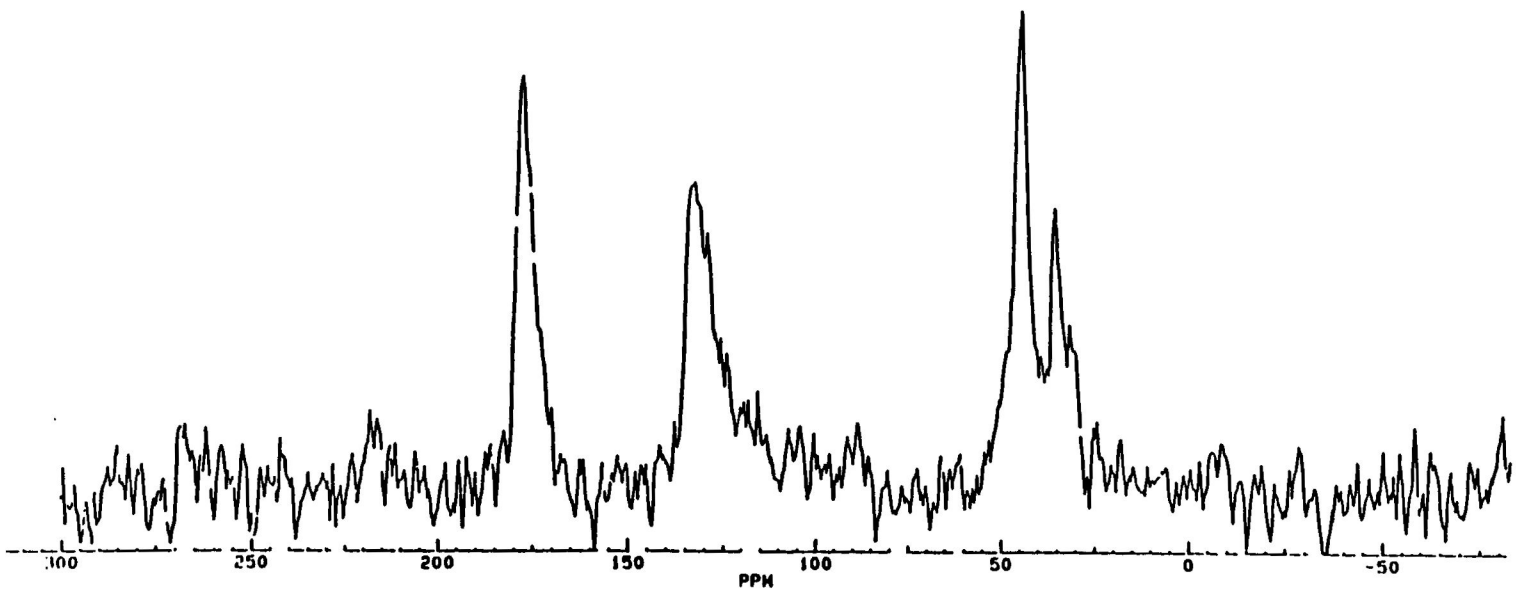

Figure 20. Solid state ^{13}C NMR spectrum of 1,3-phenylenediamine containing polyamic acid BI

stretch, Figure 21. Infrared absorption peaks of 1,3-phenylenediamine containing polyimide BII are summarized in Table 3.

The proton NMR spectrum of 1,3-phenylenediamine containing polyimide BII is presented in Figure 22. The spectrum shows a chemical shift at δ 3.6 that corresponds to the protons of the tertiary carbons in the bicyclic ring system (H-2, 3, 5, 6); a chemical shift at δ 3.7 corresponds to the bridge head protons of the bicyclic ring system (H-1, 4); the peaks at δ 7.5 correspond to the bridge protons of the bicyclic ring system (H-7, 8); and the chemical shift around δ 8.7 ppm corresponds to the aromatic protons (H-1', 2', 3', 4').

The carbon-13 NMR spectrum of 1,3-phenylenediamine containing polyimide BII is presented in Figure 23. The spectrum shows a peak at δ 34.3 corresponding to the bridge head carbon atoms of the bicyclic ring system; the peak with a chemical shift at δ 43.6 ppm corresponds to the tertiary carbons of the bicyclic ring system. The chemical shifts at δ 126.0 and δ 130.0 ppm correspond to the unsubstituted carbon atoms of the aromatic ring system. The chemical shift at δ 134.4 corresponds to the bridge carbons, and the chemical shift from δ 170.1 to δ 177.4 ppm corresponds to the imide, carboxylic and amide carbonyl carbon atoms.

The infrared spectrum of *o*-tolidine containing polyamic acid CI is presented in Figure 24. The infrared spectrum of polyamic acid CI shows a broad band from 3625 to 2940 cm^{-1} corresponding to the N-H, O-H and C-H overlapped stretching. Characteristic symmetrical and unsymmetrical imide carbonyl (C=O) stretches are observed at 1782 and 1729 cm^{-1}, respectively. The carboxylic and amide carbonyl (C=O) stretching are

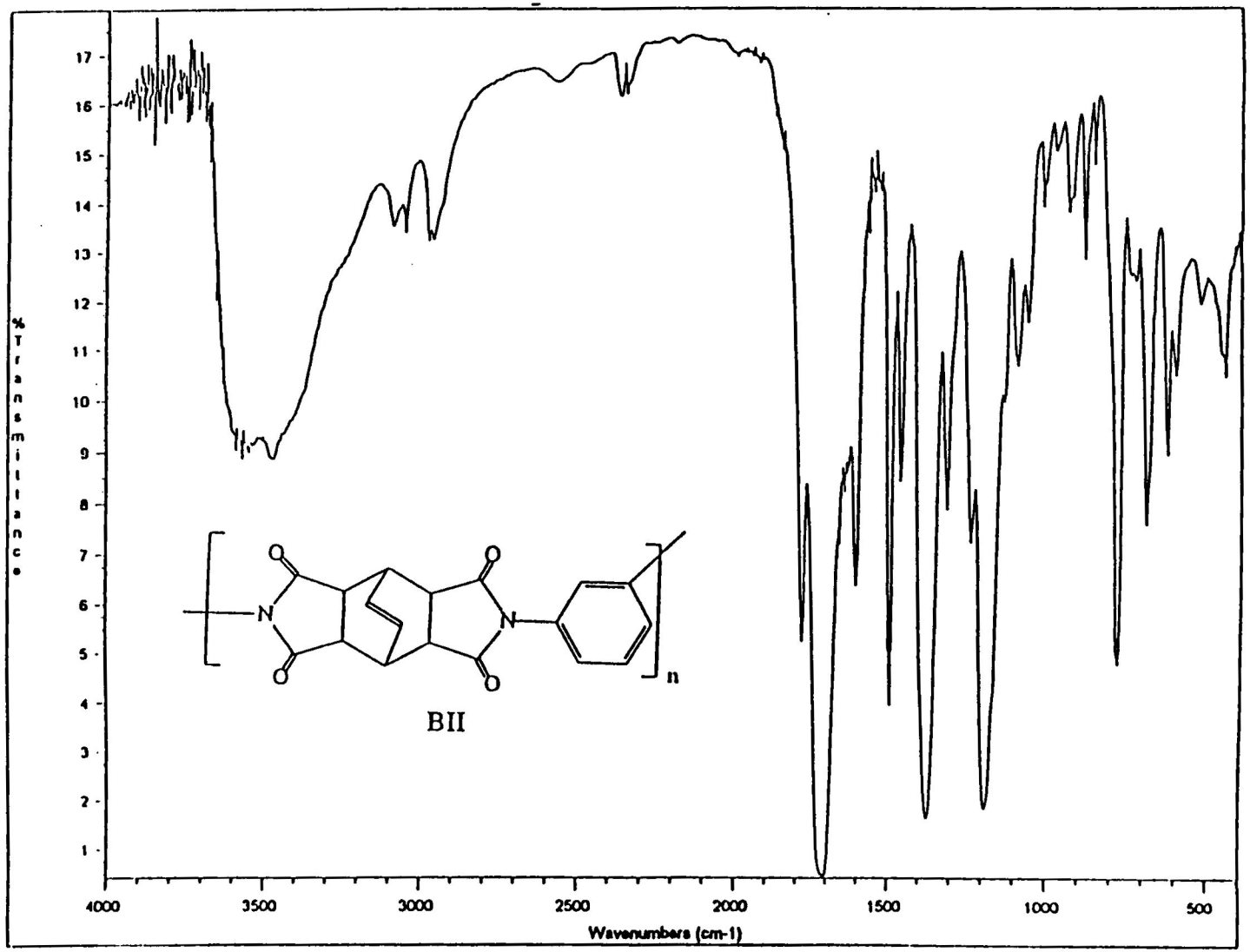

BII

Figure 21. Infrared spectrum of 1,3-phenylenediamine containing polyimide BII

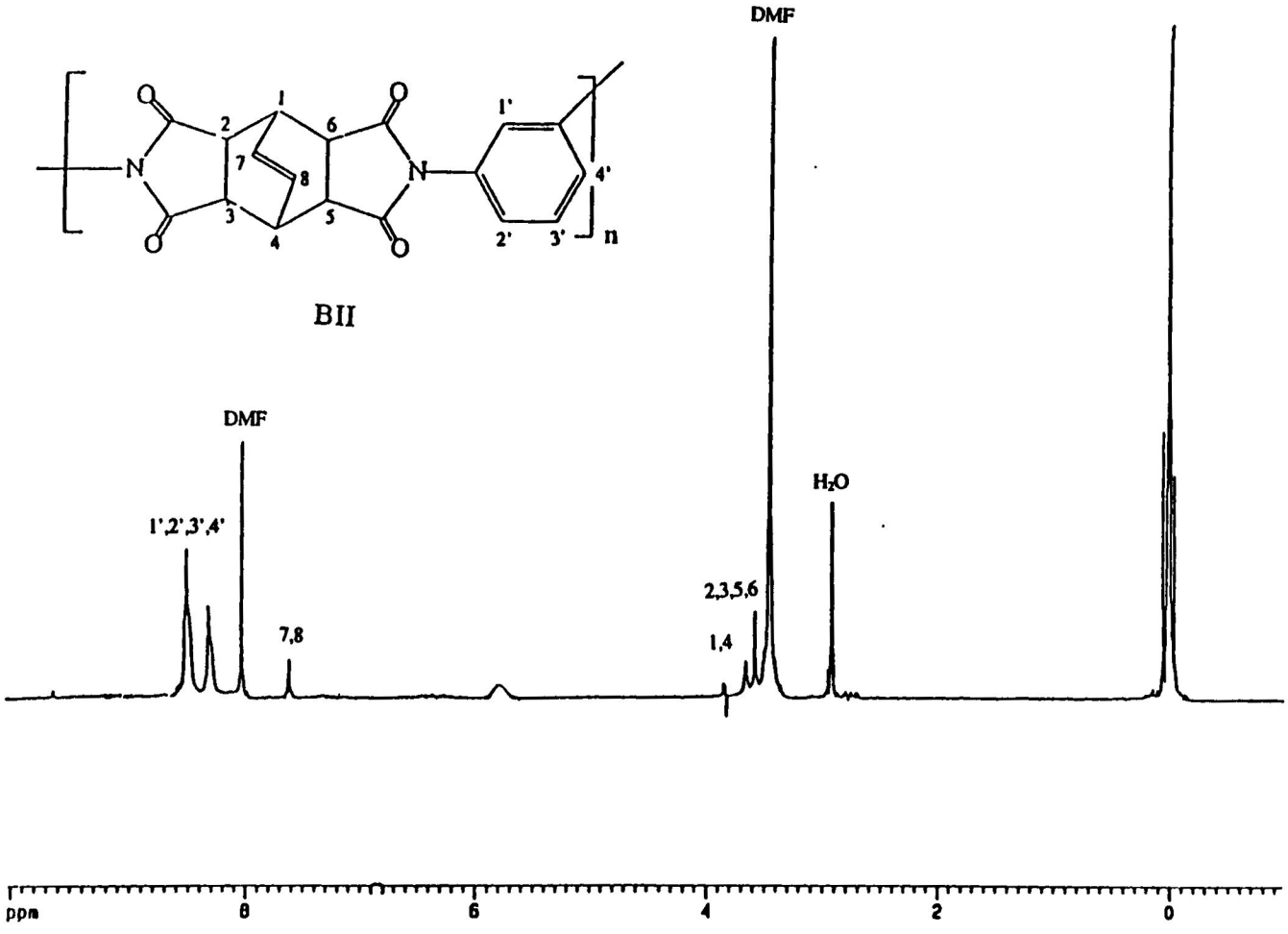

BII

Figure 22. ^{1}H NMR spectrum of 1,3-phenylenediamine containing polyimide BII in N,N-dimethylformamide-d_7

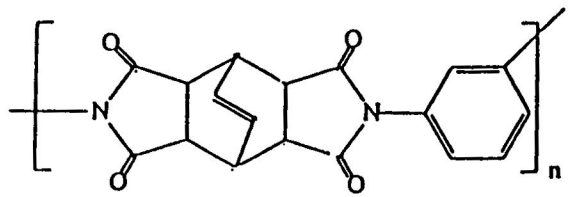

BII

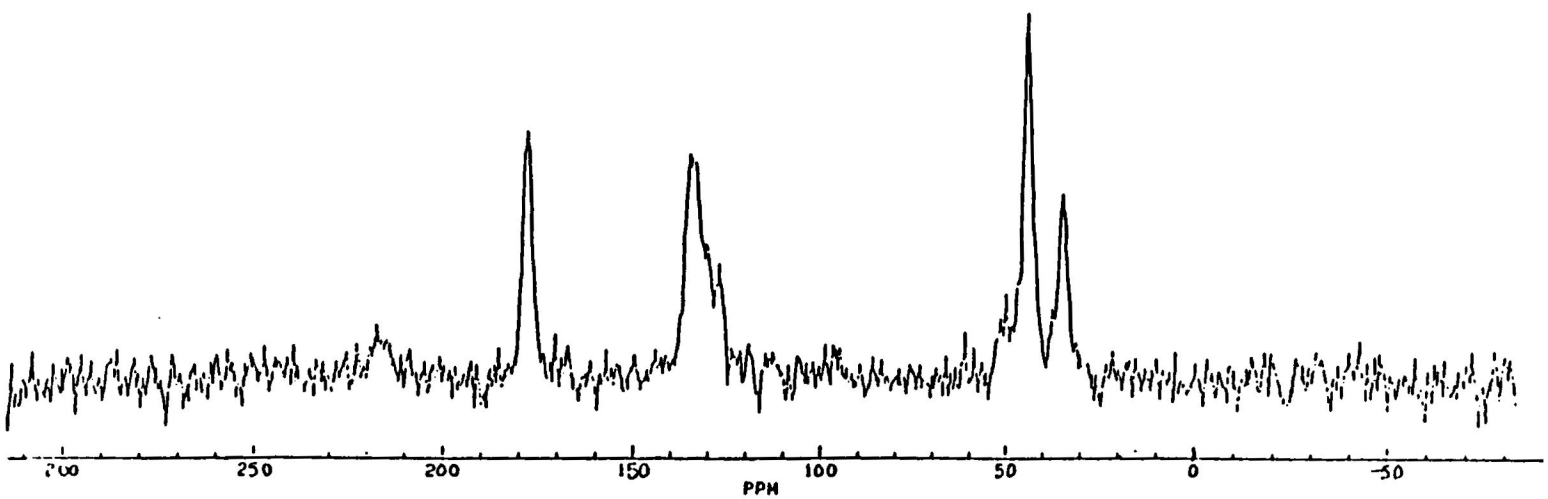

Figure 23. Solid state ^{13}C NMR spectrum of 1,3-phenylenediamine containing polyimide BII

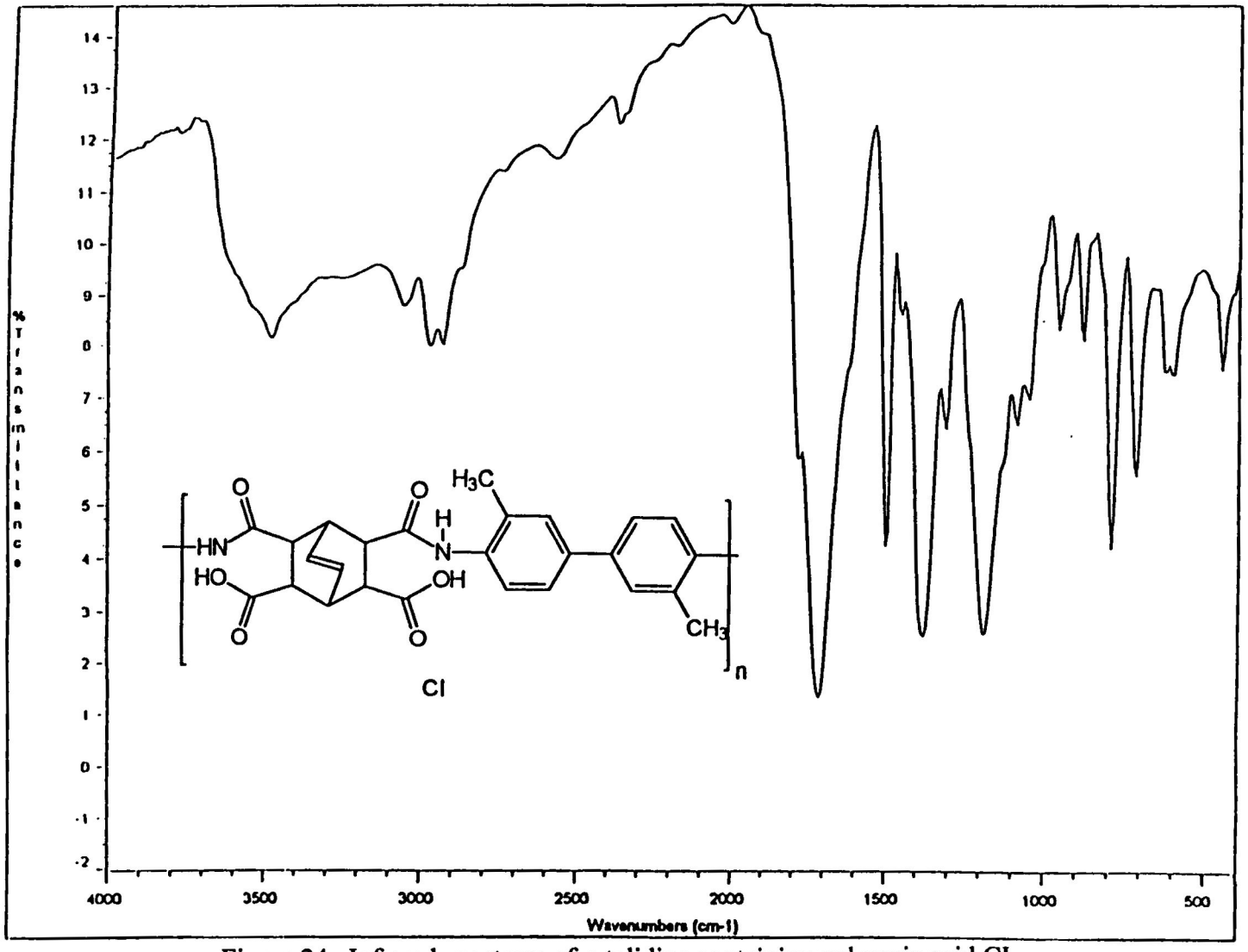

Figure 24. Infrared spectrum of *o*-tolidine containing polyamic acid CI

observed at 1716 and 1700 cm^{-1}, respectively. The carbon-carbon double bond (C=C) bridge head stretch of the bicyclic ring system is observed at 1611 cm^{-1}. The absorption at 1492 and 1374 cm^{-1} correspond to the amide N-C=O and imide carbon-nitrogen (C-N) stretching, respectively. The infrared absorption peak assignments for *o*-tolidine containing polyamic acid CI are summarized in Table 2.

Due to the intractability of the polymer, solution NMR was not performed. The solid state carbon-13 NMR spectrum of polyamic acid CI, shows a chemical shift at δ 18.3 ppm corresponding to the methyl carbon atoms. The chemical shifts from δ 30.0 to δ 50.0 ppm correspond to the bridge head and tertiary carbons of the bicyclic ring system, respectively. The chemical shifts from δ 120.0 to δ 135.0 ppm correspond to the bridge and the unsubstituted carbon atoms of the aromatic ring system. The substituted carbon of the aromatic ring is observed at δ 139.0 ppm. The peaks from δ 170.0 to δ 182.0 ppm correspond to the carbonyl of the imide, amide, and carboxylic, respectively. The solid state carbon-13 NMR spectrum of polyamic acid CI is presented in Figure 25.

The infrared spectrum of *o*-tolidine containing polyimide CII shows a medium band from 3618 to 3414 cm^{-1} corresponding to the overlapped N-H and O-H stretching. This is characteristic of incomplete ring closure. The sharp peaks from 3045 to 2927 cm^{-1} correspond to the C-H stretch of the bicyclic ring, the aromatic ring, and the methyl groups of the polymer. Characteristic symmetrical and unsymmetrical imide carbonyls (C=O) appear at 1788 and 1722 cm^{-1}, respectively. The absorption bands at 1710 and 1700 cm^{-1} correspond to the carboxylic and amide carbonyl (C=O) stretches, respectively. The absorption at approximately 1600 corresponds to the carbon-carbon double bond

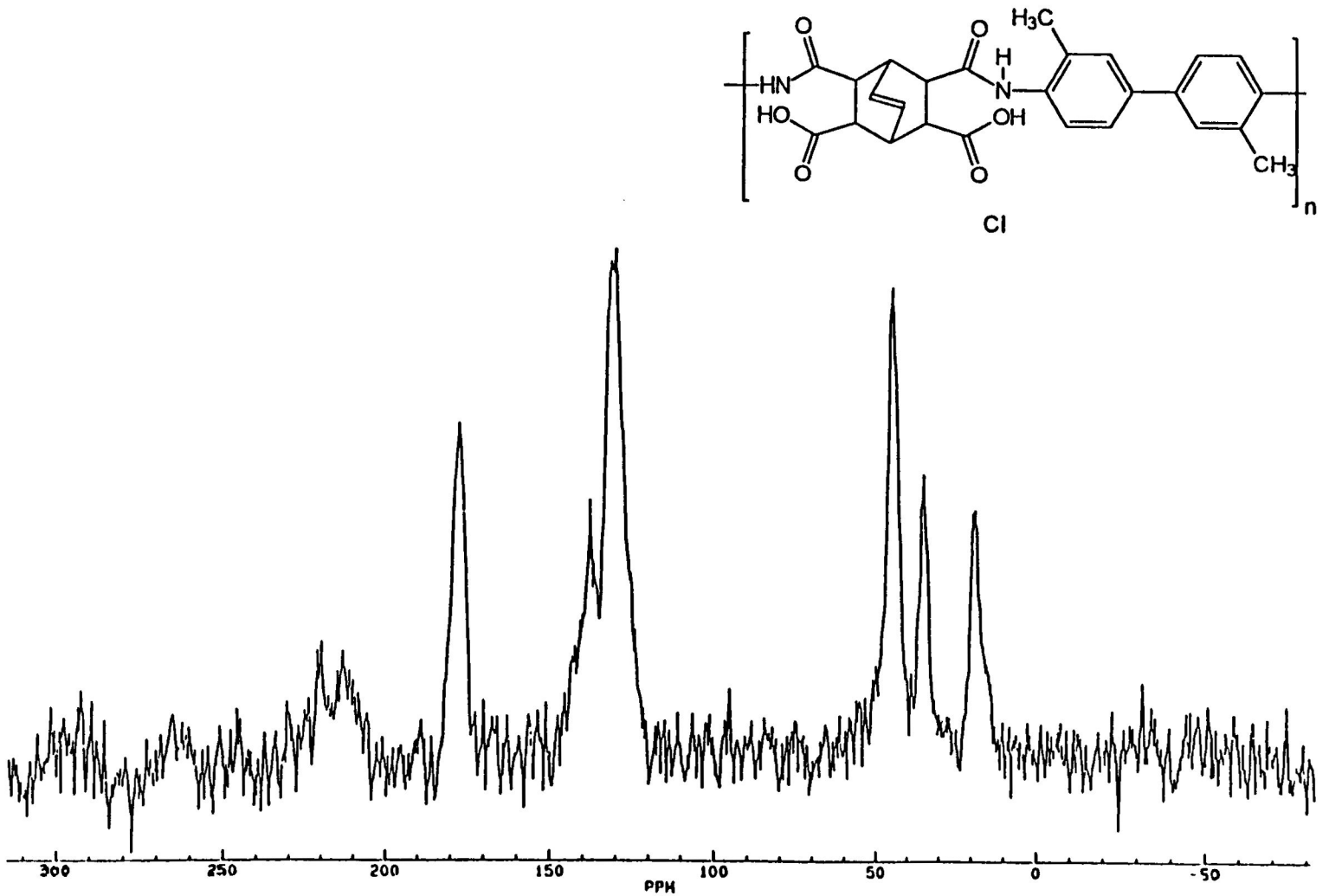

Figure 25. Solid state ^{13}C NMR spectrum of *o*-tolidine containing polyamic acid CI

(C=C) of the bicyclic ring system; the band at 1499 cm^{-1} corresponds to the amide N-C=O stretch. Evidence of imide structure is the absorption at 1374 cm^{-1} corresponding to the imide carbon-nitrogen (C-N) stretch, Figure 26. Infrared absorption peaks of *o*-tolidine containing polyimide CII are summarized in Table 3.

Due to the intractability of the polymer, solution NMR spectroscopy was not performed. The solid state carbon-13 NMR spectrum of *o*-tolidine containing polyimide CII is presented in Figure 27. The spectrum shows a chemical shift at δ 19.4 ppm corresponding to the methyl carbon atoms. The chemical shift at δ 34.6 corresponds to the bridge head carbons of the bicyclic ring, while the chemical shift at δ 44.3 ppm corresponds to the tertiary carbon atoms of the bicyclic ring. The peaks from δ 120.0 to δ 149.0 ppm correspond to the overlapping of the unsubstituted and substituted carbons of the aromatic ring and the carbons of the double bond in the bicyclic ring system. The chemical shift from δ 170.2 to δ 176.7 ppm corresponds to the carbon of the imide, carboxylic and amide carbonyl.

The infrared spectrum of 2,2'-bis(trifluoromethyl)benzidine containing polyamic acid DI is presented in Figure 28. The spectrum shows a broad band from 3499 to 2933 cm^{-1} corresponding to the N-H, and O-H stretching. A weak absorption at 1872 cm^{-1} corresponds to the carbonyl (C=O) stretching of some unreactive anhydride, at this stage of the polymerization. The symmetrical and unsymmetrical imide carbonyl (C=O) functional groups absorbs at 1788 and 1729 cm^{-1}, respectively. The peak at 1620 cm^{-1} corresponds to the carbon-carbon double bond (C=C) of the bridge in the bicyclic ring system. The absorption at 1499 corresponds to the amide N-C=O stretch; and the peak at

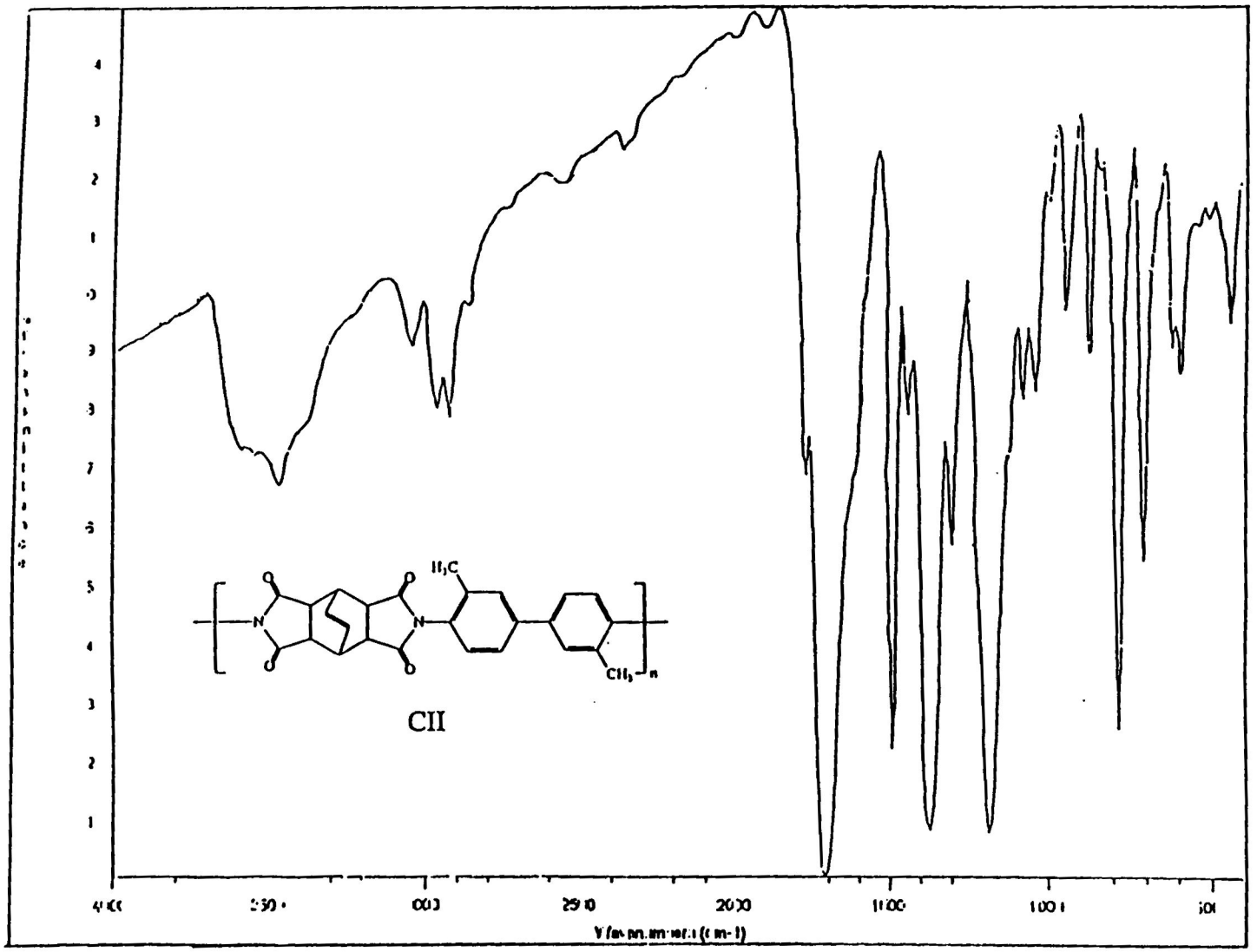

Figure 26. Infrared spectrum of *o*-tolidine containing polyimide CII

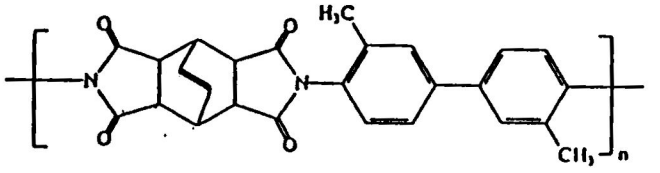

CII

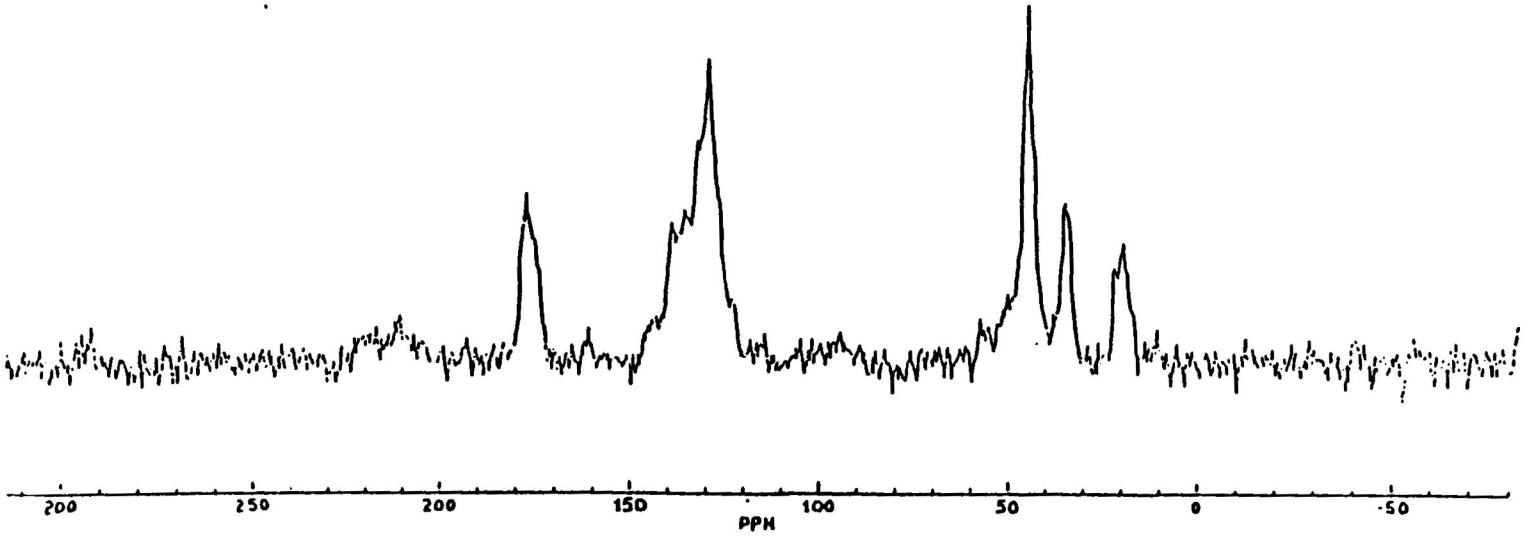

Figure 27. Solid state ^{13}C NMR spectrum of *o*-tolidine containing polyimide CII

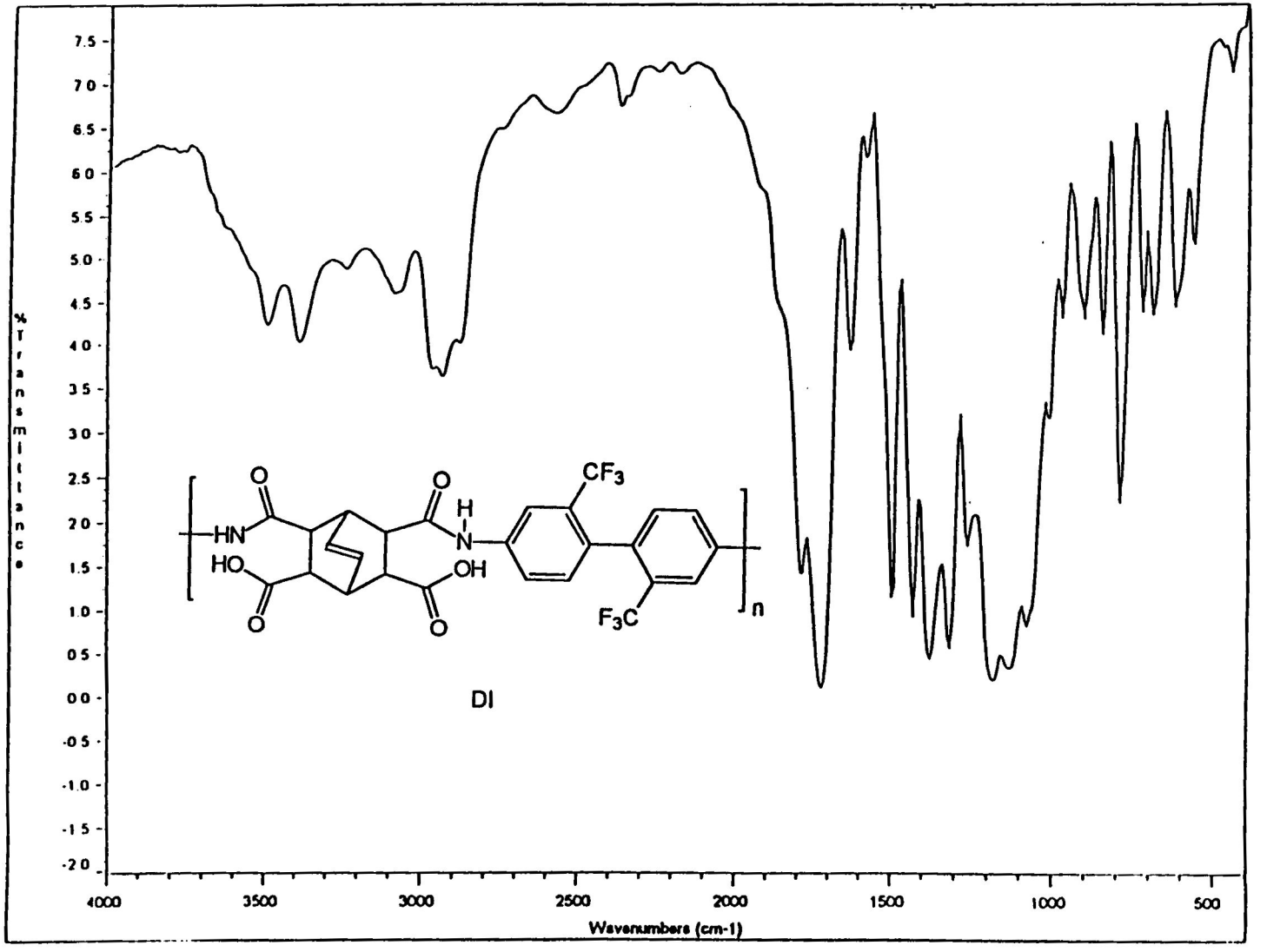

Figure 28. Infrared spectrum of 2,2'-bis(trifluoromethyl)benzidine containing polyamic acid DI

1374 cm^{-1} corresponds to the imide carbon-nitrogen (C-N) stretch. The broad absorption band observed from 1000 to 1200 cm^{-1} correspond to the trifluoromethyl group (CF_3) stretching. Infrared absorption peaks of 2,2'-bis(trifluoromethyl)benzidine containing polyamic acid DI are sumarized in Table 2.

The proton NMR of 2,2'-bis(trifluoromethyl)benzidine containing polyamic acid DI shows a chemical shift at δ 3.5 corresponding to the protons of the tertiary carbons of the bicyclic ring system (H-2, 3, 5, 6); and the chemical shift at δ 3.6 ppm corresponds to the bridge head protons (H-1, 4). The chemical shift at δ 5.7 corresponds to the N-H protons (H-9); the chemical shift at δ 6.4 corresponds to the protons of the bridge in the bicyclic ring system (H-7, 8), and the chemical shifts from δ 7.6 to δ 7.8 ppm correspond to the aromatic protons (H-1', 2', 3'), Figure 29.

The carbon-13 spectrum of 2,2'-bis(trifluoromethyl)benzidine containing polyamic acid DI is presented in Figure 30. The spectrum shows a chemical shift from δ 29.9 to δ 48.2 ppm corresponding to the bridge head carbons and the tertiary carbons of the bicyclic ring system. The peaks observed from δ 100.0 to δ 150.0 ppm correspond to the overlapping of the unsusbstituted, substituted, trifluoromethyl carbon atoms of the aromatic ring system, and the bridge carbons of the bicyclo ring system. The chemical shifts from δ 165.0 to δ 180.0 ppm correspond to the carbons of the imide, amide, and carboxylic carbonyls.

The infrared spectrum of 2,2'-bis(trifluoromethyl)benzidine containing polyimide DII is presented in Figure 31. The spectrum shows a medium absorption band from 3670 to 3447 cm^{-1} corresponding to the O-H stretch due to moisture. Symmetrical and

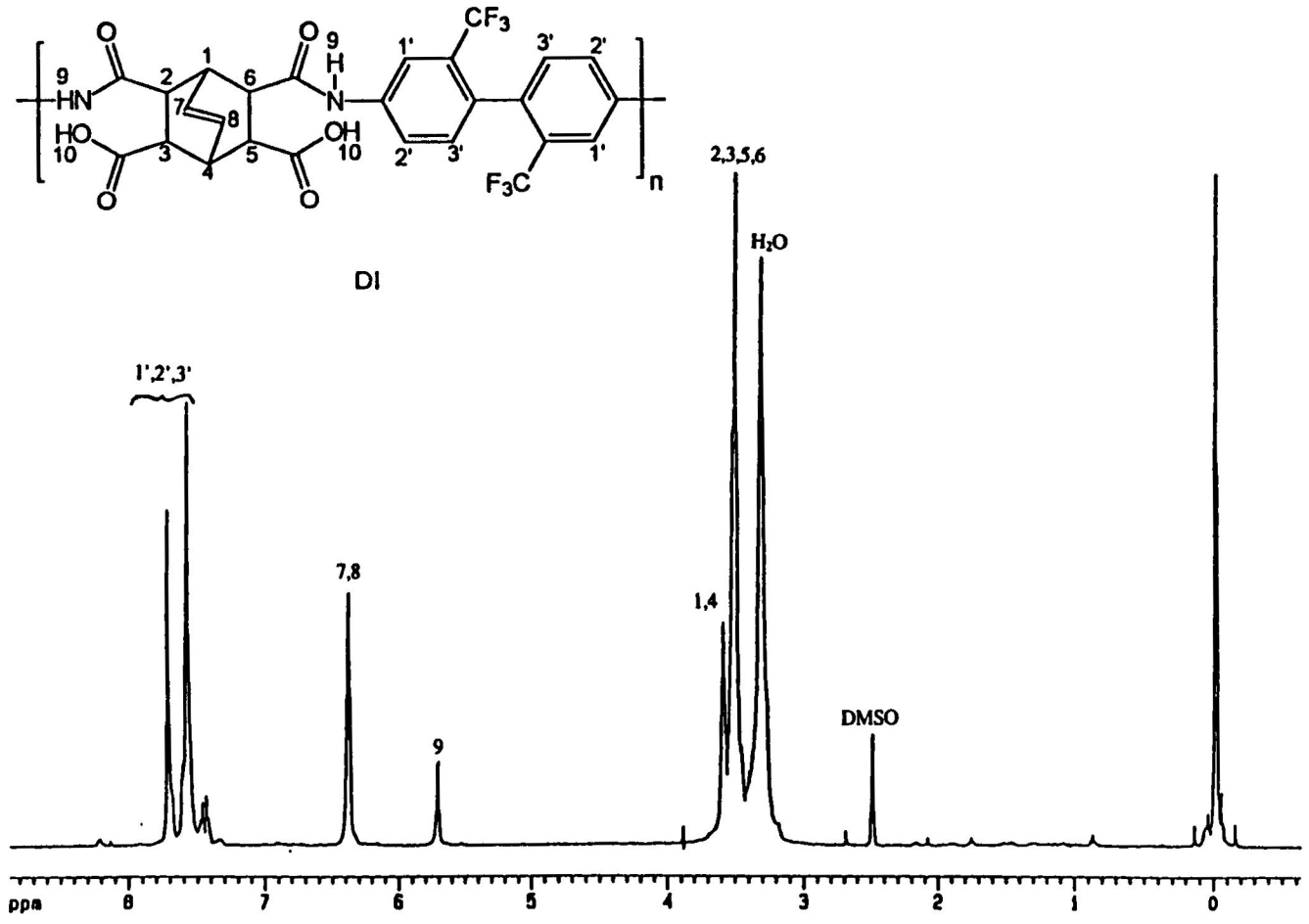

Figure 29. ^{1}H NMR spectrum of 2,2'-bis(trifluoromethyl)benzidine containing polyamic acid DI in dimethylsulfoxide-d_6

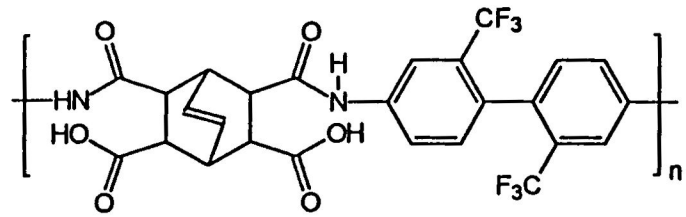

DI

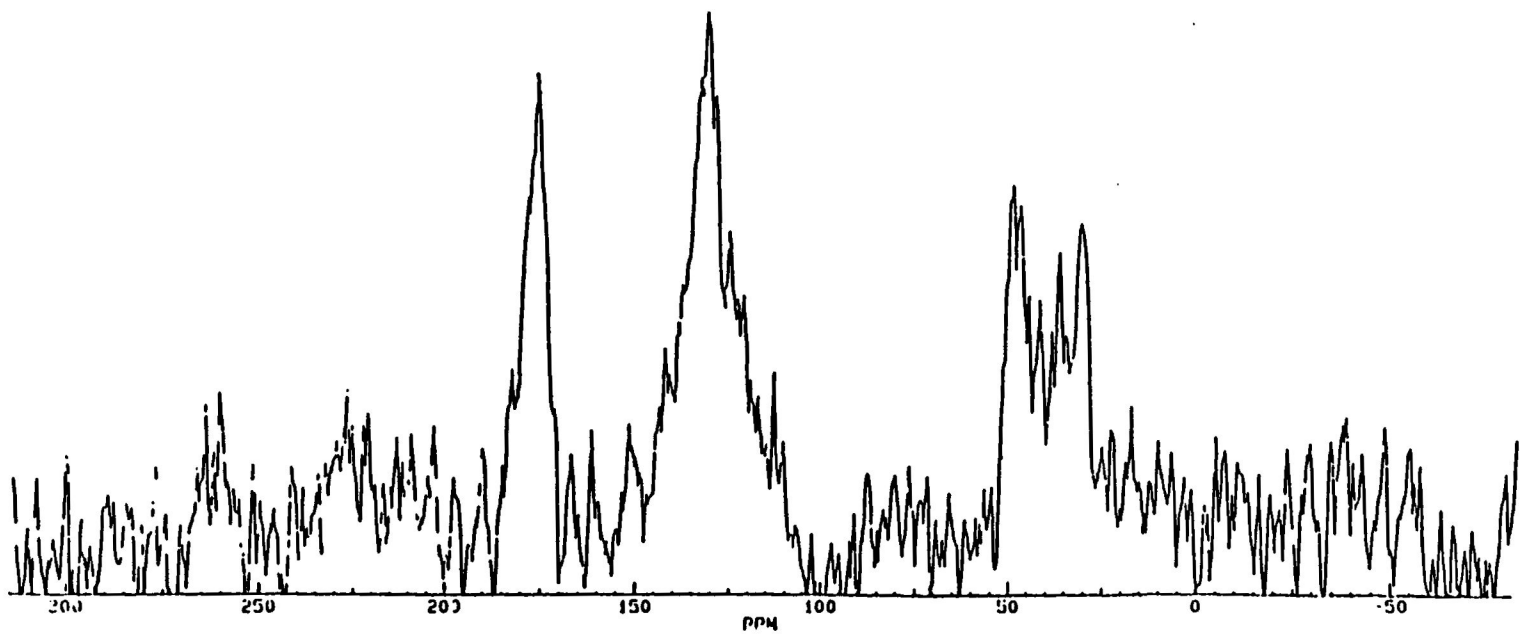

Figure 30. Solid state ^{13}C NMR spectrum of 2,2'-bis(trifluoromethyl)benzidine containing polyamic acid DI

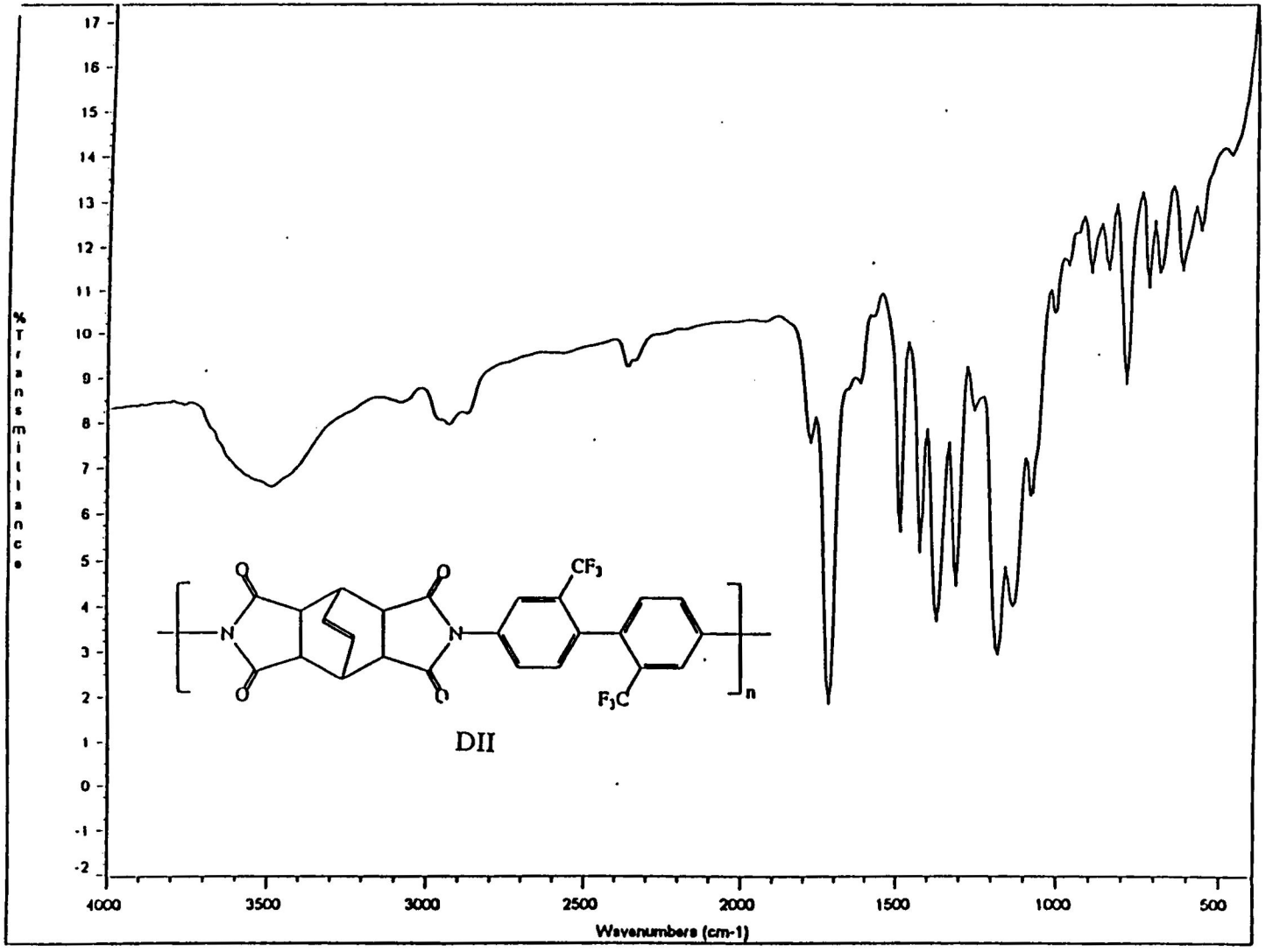

Figure 31. Infrared spectrum of 2,2'-bis(trifluoromethyl)benzidine containing polyimide DII

unsymmetrical imide carbonyl (C=O) stretching are observed at 1782 and 1729 cm^{-1}, respectively. The absorption at 1617 corresponds to the carbon-carbon double bond (C=C) of the bicyclic ring system; the absorption at 1512 corresponds to the amide N-C=O stretch, and the peak at 1374 cm^{-1} corresponds to the imide carbon-nitrogen (C-N) stretch. The trifluoromethyl functional group (CF_3) absorbs from 1100 to 1200 cm^{-1}. Infrared absorption peaks of 2,2'-bis(trifluoromethyl)benzidine containing polyimide DII are summarized in Table 3.

The proton NMR spectrum of 2,2'-bis(trifluoromethyl)benzidine containing polyimide DII is presented in Figure 32. The spectrum shows a chemical shift at δ 3.5 corresponding to the protons of the tertiary carbons in the bicyclic ring system (H-2, 3, 5, 6); a chemical shift at δ 3.6 corresponds to the bridge head protons (H-1, 4); the peak at δ 6.4 corresponds to the bridge protons of the bicyclic ring system (H-7, 8); and the chemical shifts from δ 7.5 to δ 7.8 ppm correspond to the aromatic protons (H-1', 2', 3').

The carbon-13 spectrum of 2,2'-bis(trifluoromethyl)benzidine containing polyimide DII shows a chemical shift at approximately δ 30.0 corresponding to the bridge head carbon atoms of the bicyclic ring system; the peaks from δ 125.6 to δ 136.6 ppm correspond to the overlapping of the aromatic carbon atoms, the carbons of the bridge of the bicyclic ring, and the carbons of the trifluoromethyl groups. The chemical shift at δ 177.3 ppm corresponds to the carbon of the imide carbonyl, Figure 33.

The infrared spectrum of 2,2'-bis(trifluoromethyl)benzidine containing polyamic acid EI shows a broad absorption band from 3624 to 2637 cm^{-1} corresponding to the overlapping of N-H, O-H, and C-H stretch. The absorption at 1788 corresponds to the

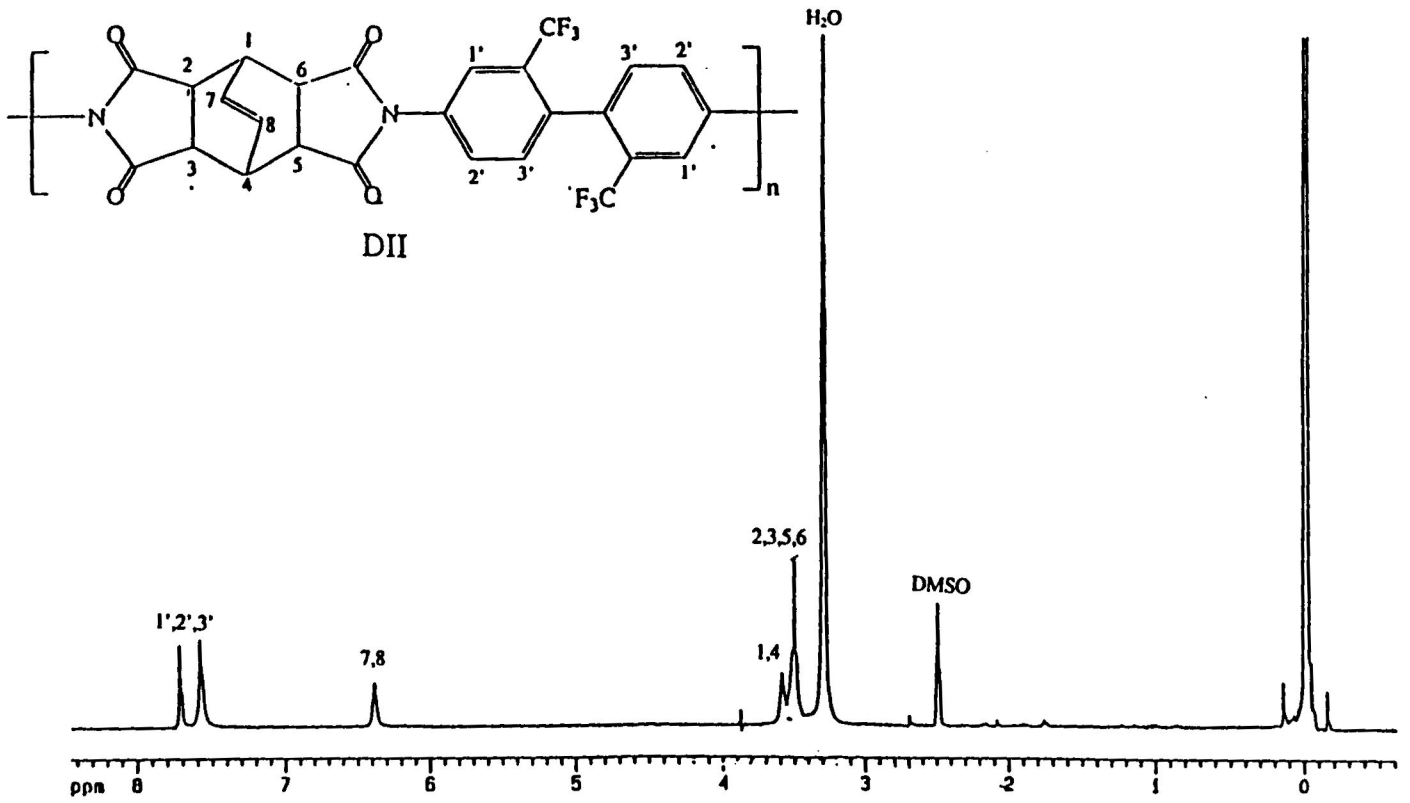

Figure 32. ^{1}H NMR spectrum of 2,2'-bis(trifluoromethyl)benzidine containing polyimide DII in dimethylsulfoxide-d_6

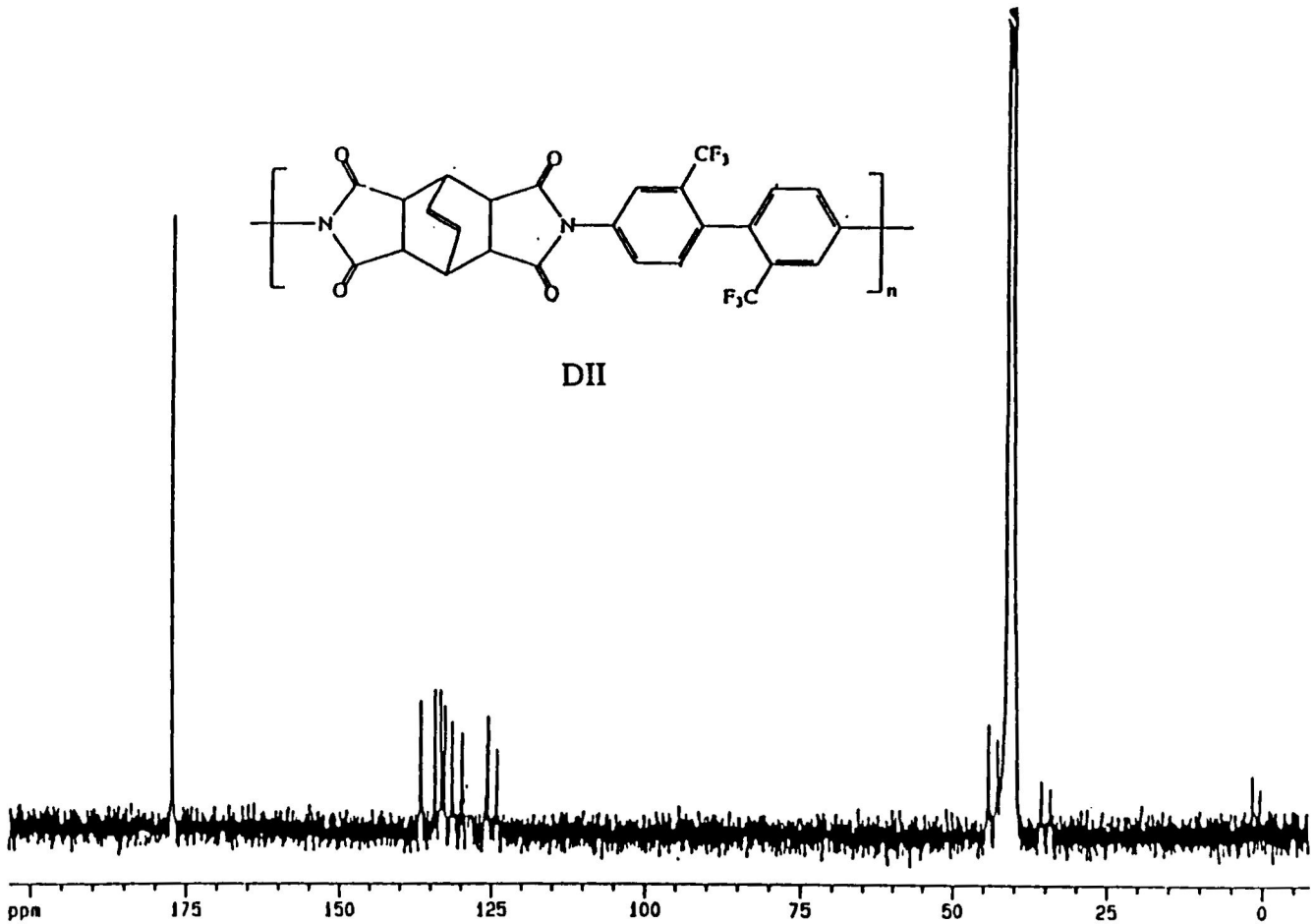

Figure 33. ^{13}C NMR spectrum of 2,2'-bis(trifluoromethyl)benzidine containing polyimide DII in dimethylsulfoxide-d_6

symmetrical imide carbonyl (C=O); the band at 1729 cm^{-1} corresponds to the unsymmetrical imide carbonyl (C=O). An overlapped absorption bands of the amide and carboxylic carbonyls (C=O) are observed from 1710 to 1690 cm^{-1}. The carbon-carbon double bond (C=C) shows an absorption at 1604; the peak at 1512 corresponds to the amide N-C=O stretch; the absorption at 1374 corresponds to the imide carbon-nitrogen (C-N) stretch; and the broad band from 1100 to 1200 cm^{-1} corresponds to the trifluoromethyl group (CF_3) stretch, Figure 34. The infrared absorption peaks of 2,2'-bis(trifluoromethyl) benzidine containing polyamic acid EI are summarized in Table 2.

The proton NMR spectrum of 2,2'-bis(trifluoromethyl)benzidine containing polyamic acid EI indicates a chemical shift at δ 5.8 ppm corresponding to the polyamic acid N-H proton (H-3). The chemical shifts from δ 7.8 to δ 8.6 ppm correspond to the unsubstituted aromatic protons (H-1 to 3'). The polyamic acid O-H proton (H-4) shows a chemical shift at δ 10.8 ppm, Figure 35.

The carbon-13 NMR spectrum of 2,2'-bis(trifluoromethyl)benzidine containing polyamic acid EI shows a broad chemical shift from δ 112.0 to δ 140.0 ppm corresponding to the overlapping of the aromatic and trifluoromethyl carbon atoms. The chemical shifts from δ 160.0 to δ 170.0 ppm correspond to the overlapping of the imide, amide and carboxylic carbon atoms, Figure 36.

The infrared spectrum of 2,2'-bis(trifluoromethyl)benzidine containing polyimide EII is presented in Figure 37. The spectrum shows a broad band from 3592 to 2631 cm^{-1} which corresponds to the N-H, O-H, and C-H overlapped stretch. This is evidence of incomplete ring closure. The absorption peak at 1782 corresponds to the symmetrical

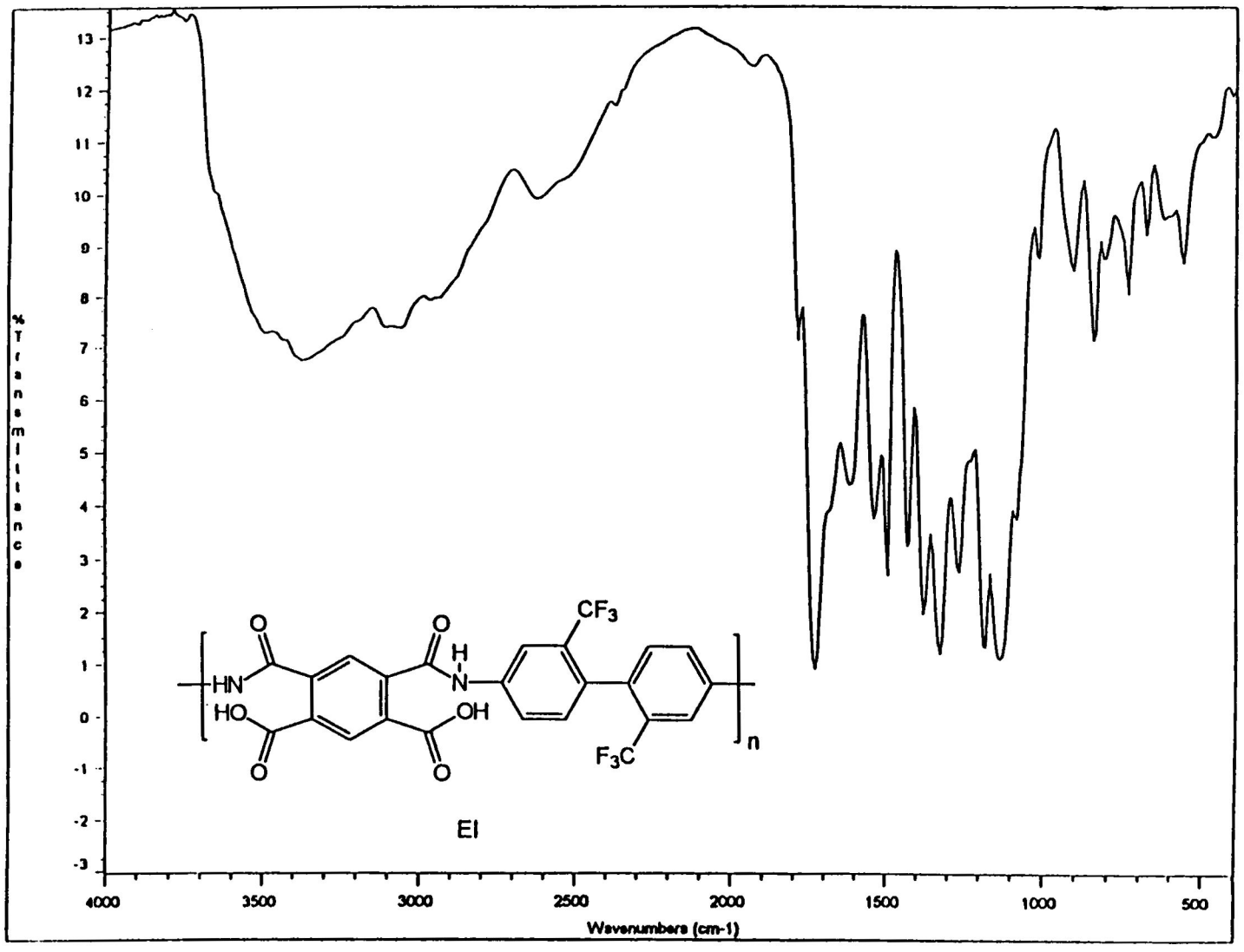

Figure 34. Infrared spectrum of 2,2'-bis(trifluoromethyl)benzidine containing polyamic acid EI

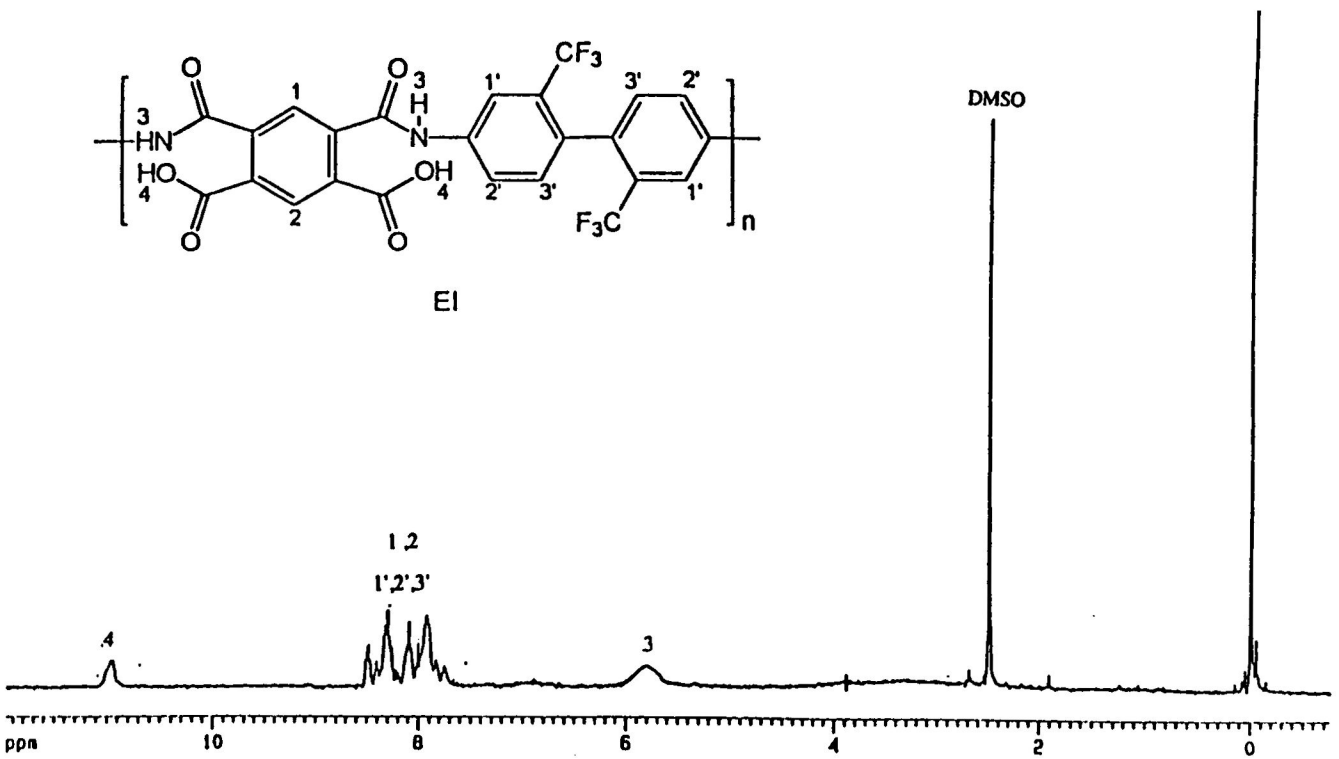

Figure 35. ^{1}H NMR spectrum of 2,2'-bis(trifluoromethyl)benzidine containing polyamic acid EI in dimethylsulfoxide-d_6

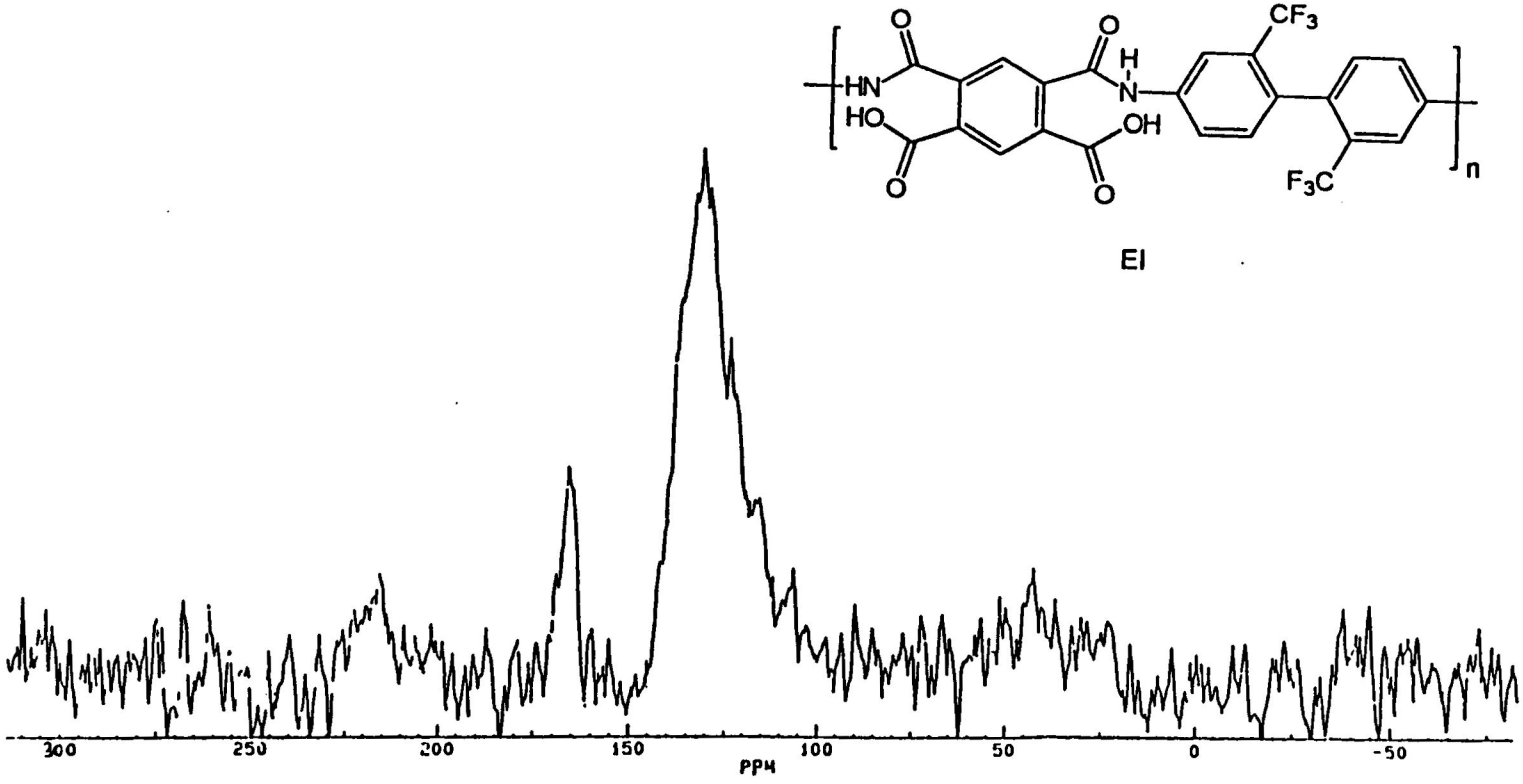

Figure 36. Solid state ^{13}C NMR spectrum of 2,2'-bis(trifluoromethyl)benzidine containing polyamic acid EI

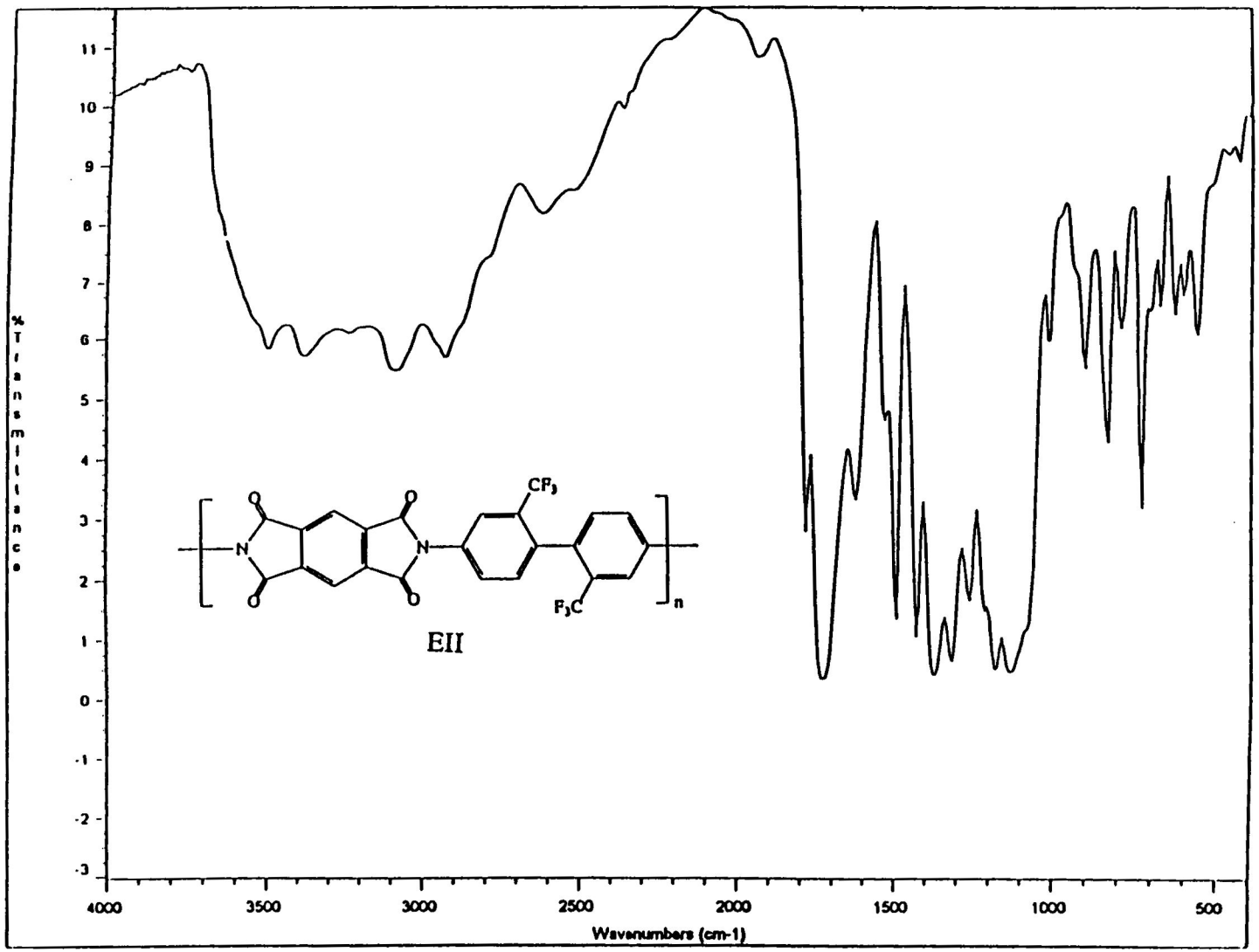

Figure 37. Infrared spectrum of 2,2'-bis(trifluoromethyl)benzidine containing polyimide EII

imide carbonyl; the peak at 1729 corresponds to the unsymmetrical imide carbonyl (C=O) stretch; the absorption at 1710 and 1700 correspond to the carboxylic and amide carbonyl (C=O) stretch, respectively; the absorption band at 1600 cm^{-1} corresponds to the carbon-carbon double bond (C=C) of the bicyclic ring system. The sharp absorption band at 1492 corresponds to the amide N-C=O stretch; and at 1374 cm^{-1} corresponds to the imide carbon-nitrogen (C-N) stretch. The trifluoromethyl group (CF_3) absorbs from 1100 to 1200 cm^{-1}. Infrared absorption peaks of 2,2'-bis(trifluoromethyl)benzidine containing polyimide EII are presented in Table 3.

The proton NMR spectrum of 2,2'-bis(trifluoromethyl)benzidine containing polyimide EII is presented in Figure 38. The spectrum shows a chemical shift at δ 5.9 corresponding to the N-H protons of the amic acid and a shift at δ 10.9 ppm is indicative of the amic acid O-H proton due to incomplete ring closure. The chemical shifts from δ 7.3 to δ 8.5 ppm (H-1 to 3') correspond to the protons of the aromatic system.

The carbon-13 NMR spectrum of 2,2'-bis(trifluoromethyl)benzidine containing polyimide EII is presented in Figure 39. The spectrum shows a chemical shift from δ 112.0 to δ 140.0 ppm corresponding to the overlapped aromatic and trifluoromethyl carbon atoms. The chemical shifts from δ 165.4 to δ 170.0 ppm correspond to the overlapped imide, amide and carboxylic carbon atoms.

Thermal Characterization

The differential scanning calorimetry (DSC) curves of 1,4-phenylenediamine containing polyamic acid AI under argon and in air are presented in Figure 40. Under

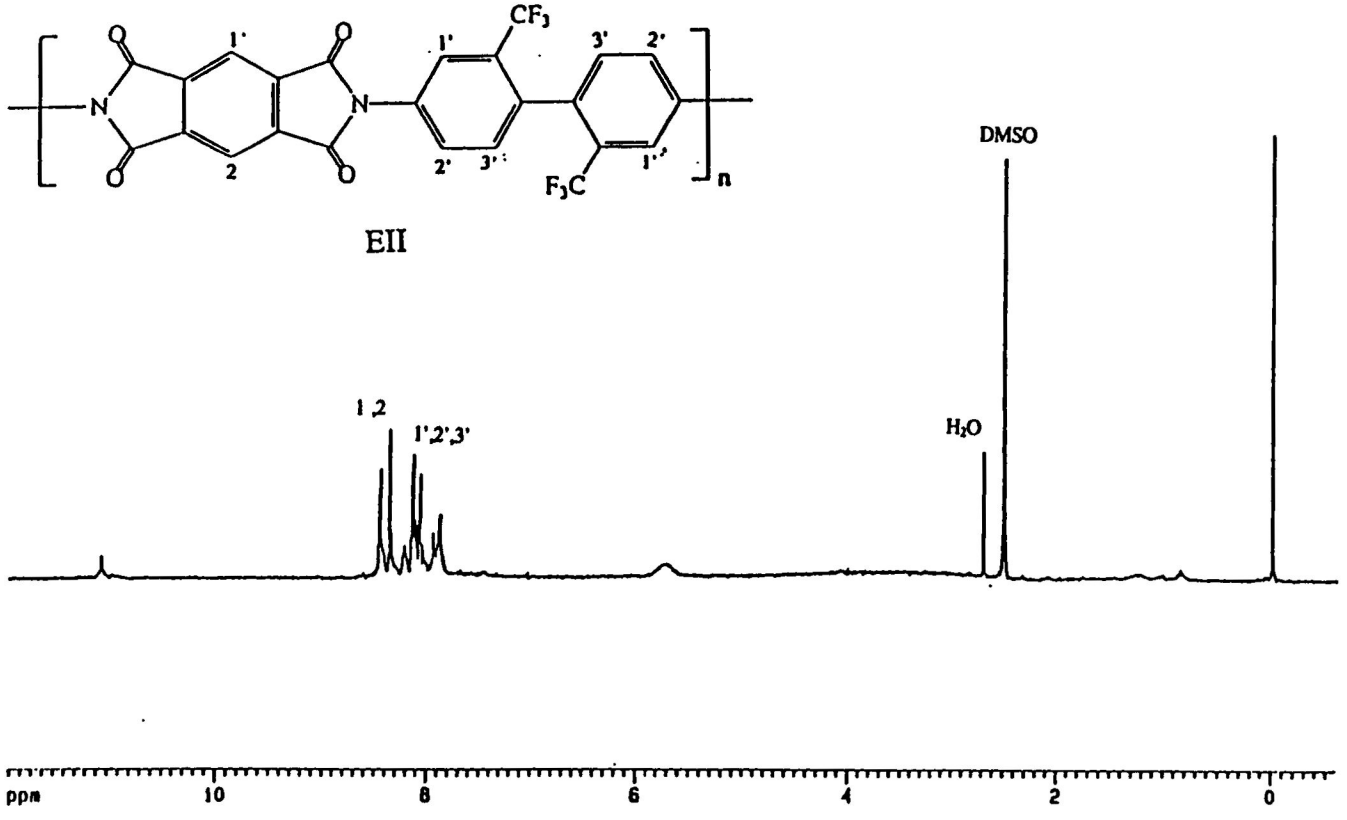

Figure 38. ^{1}H NMR spectrum of 2,2'-bis(trifluoromethyl)benzidine containing polyimide EII in dimethylsulfoxide-d_6

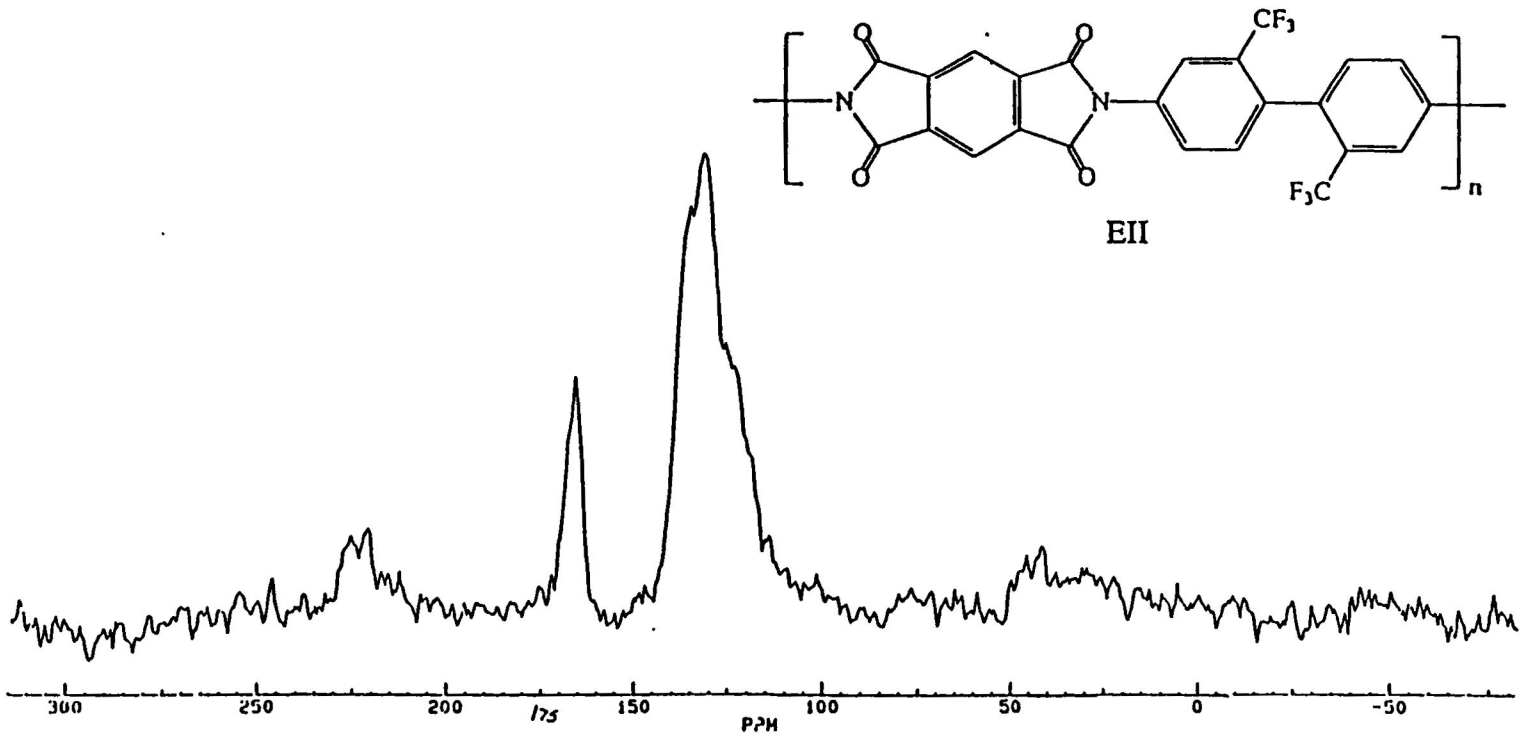

Figure 39. Solid state ^{13}C NMR spectrum of 2,2'-bis(trifluoromethyl)benzidine containing polyimide EII

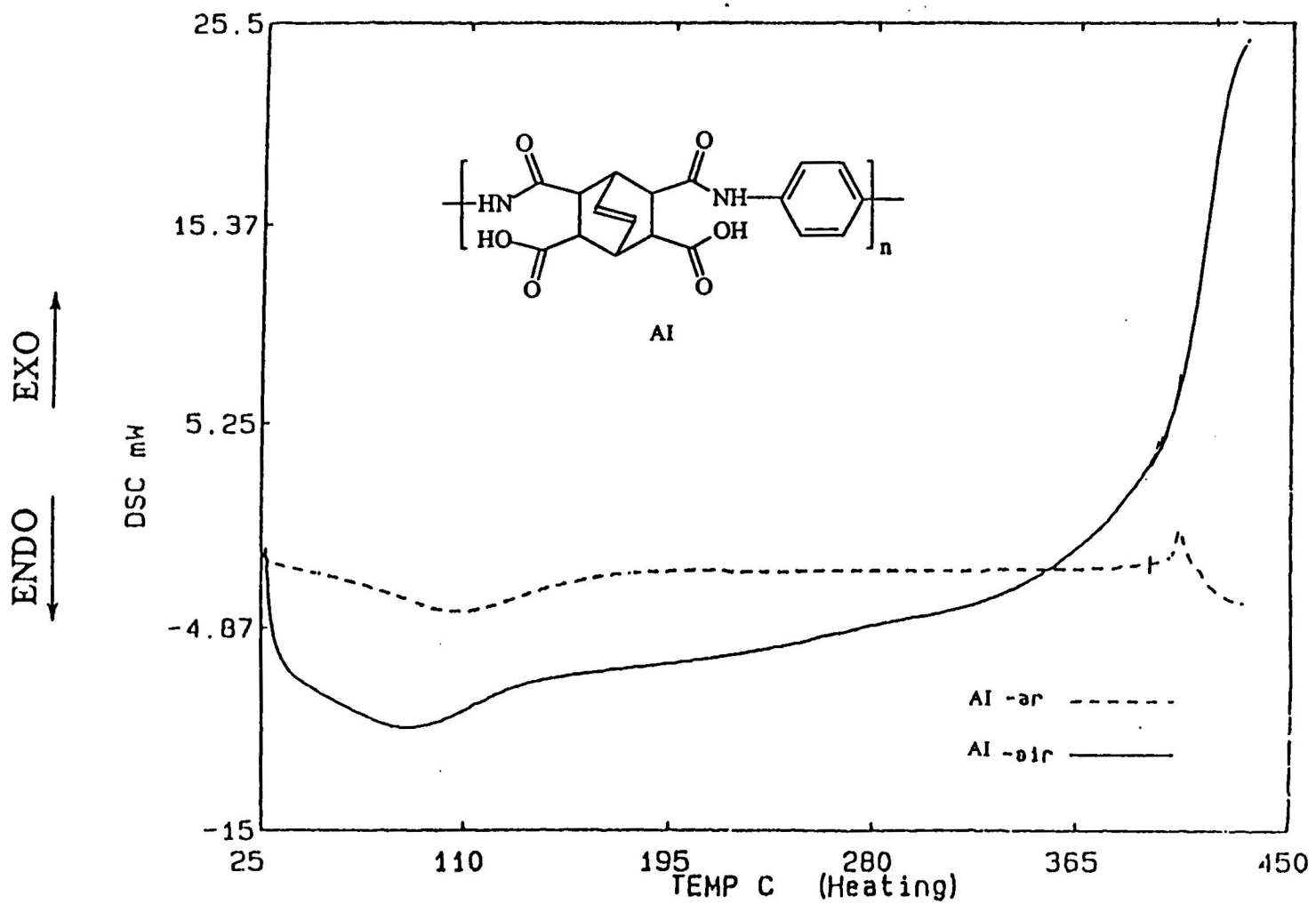

Figure 40. DSC curves of 1,4-phenylenediamine containing polyamic acid AI under argon and in air

argon atmosphere, the DSC curve of 1,4-phenylenediamine containing polyamic acid AI indicates a sharp exotherm at 407 °C corresponding to the decomposition temperature. No glass transition temperature (Tg) was observed. In air, thermooxidative decomposition temperature begins at 350 °C. No melting or crystalline properties were observed under the hot stage optical polarizing microscope up to 300 °C.

The thermogravimetric analysis (TGA) curves of 1,4-phenylenediamine containing polyamic acid AI under argon and in air are presented in Figure 41. Under argon atmosphere, an onset of decomposition occurs at 408 °C with a weight loss of approximately 32 % at ca. 428 °C. 1,4-Phenylenediamine containing polyamic acid AI exhibits a decomposition temperature at 397 °C in air. These results indicate that 1,4-phenylenediamine containing polyamic acid AI decomposed faster in air than under argon atmosphere.

The differential scanning calorimetry (DSC) curves of 1,4-phenylenediamine containing polyimide AII under argon and air are presented in Figure 42. Under argon atmosphere, an exotherm is observed at 421 °C due to decomposition. In air, an onset of decomposition was observed at 400 °C, no melting transitions were observed. A glass transition temperature (Tg) was not observed under argon or in air. The polyimide decomposed faster in air than under argon due to thermooxidative decomposition. No melting transitions were observed under hot stage optical polarizing microscope up to 300 °C.

The thermogravimetric analysis (TGA) curves of 1,4-phenylenediamine containing polyimide AII under argon and air are presented in Figure 43. Under argon, an onset of

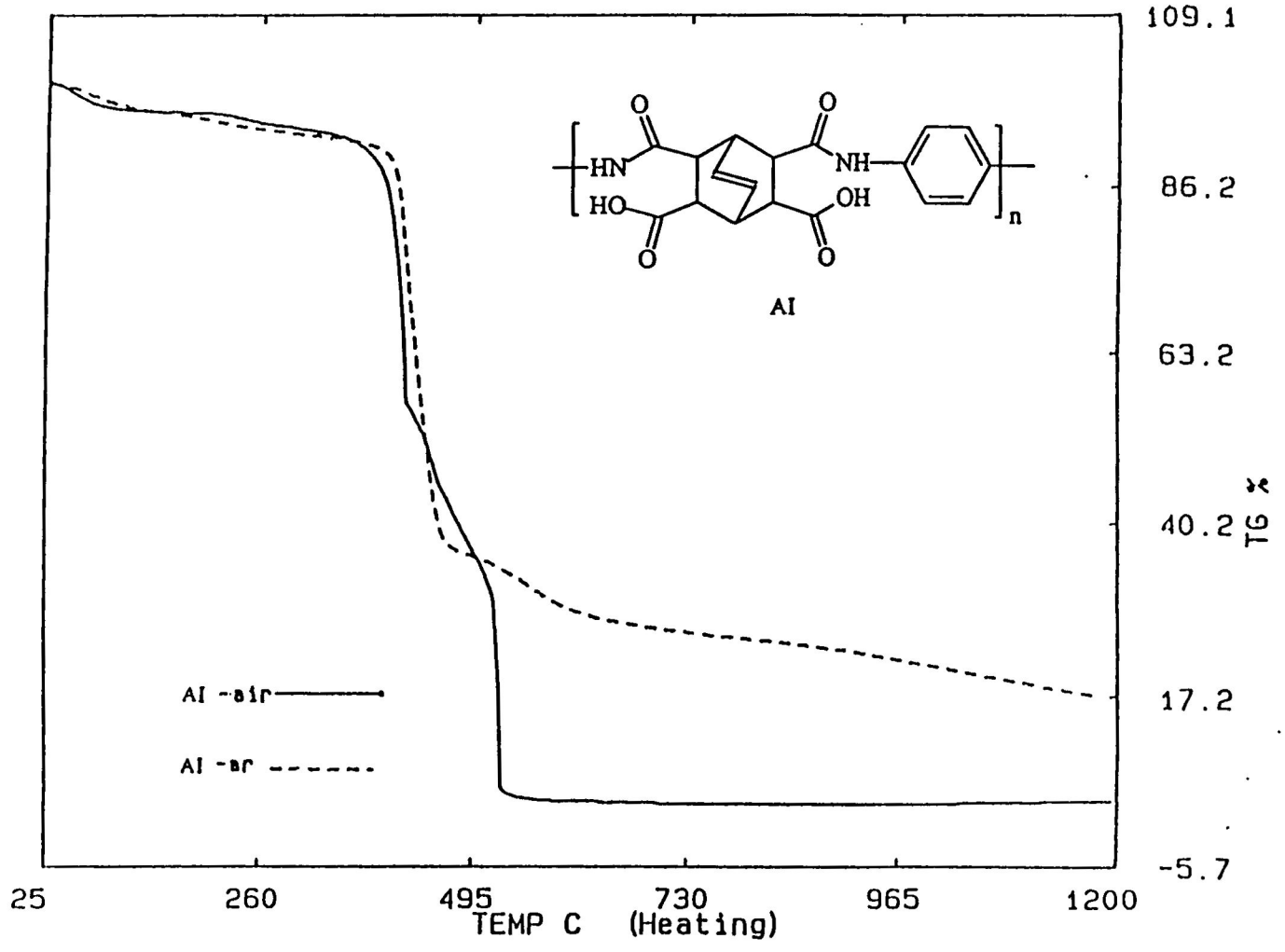

Figure 41. TGA curves of 1,4-phenylenediamine containing polyamic acid AI under argon and in air

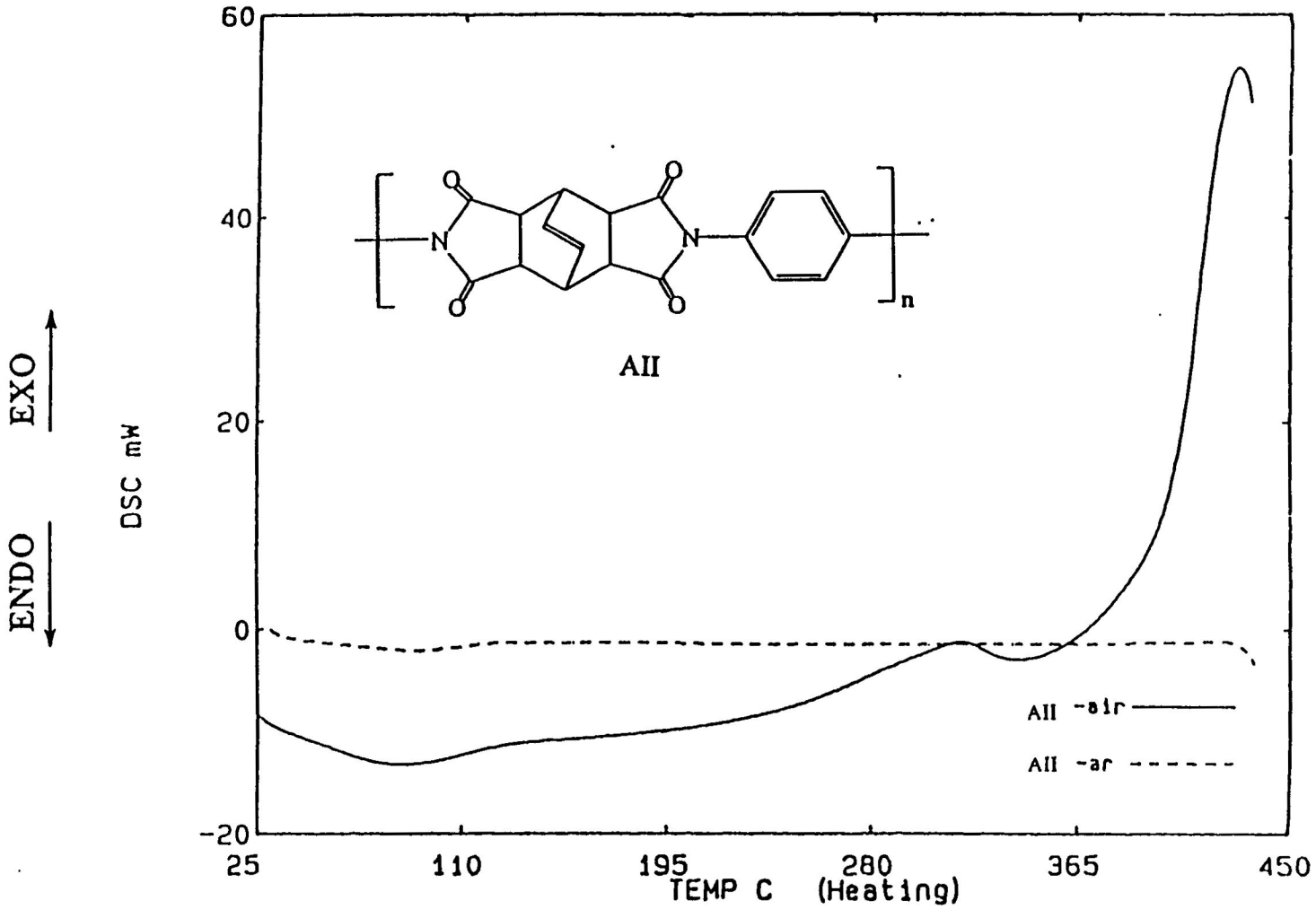

Figure 42. DSC curves of 1,4-phenylenediamine containing polyimide AII under argon and in air

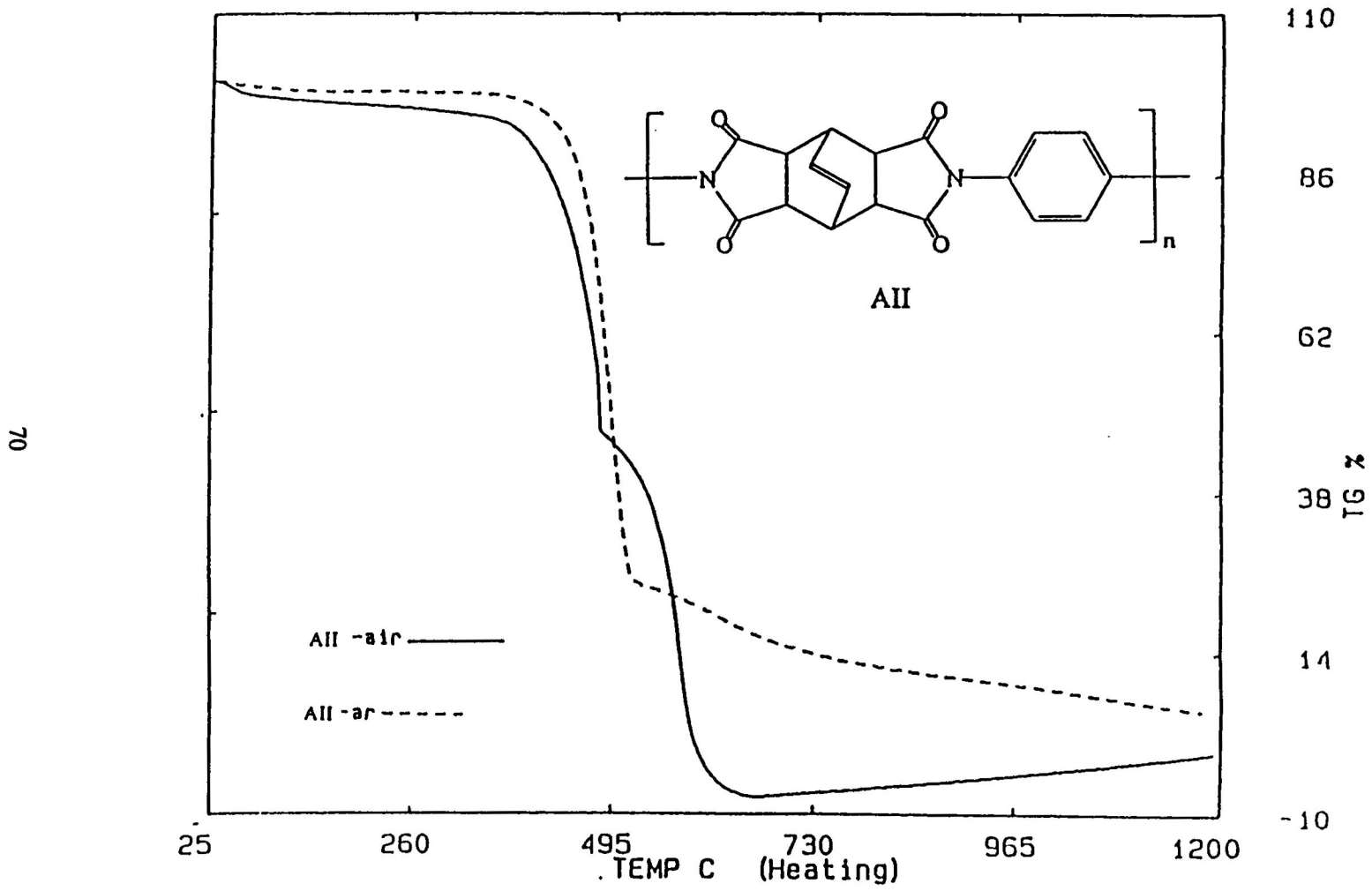

Figure 43. TGA curves of 1,4-phenylenediamine containing polyimide AII under argon and in air

decomposition is observed at 460 °C with a weight loss of approximately 40 % at ca. 485 °C. Polyimide AII shows an onset of decomposition at 422 °C in air.

The differential scanning calorimetry (DSC) curves of 1,3-phenylenediamine containing polyamic acid BI under argon and in air are presented in Figure 44. Under argon atmosphere, the DSC curve shows a decomposition temperature at 409 °C. In air, an onset of decomposition was observed at 400 °C, and no melting transitions were observed. Hot stage optical polarizing microscope shows no melting temperature up to 300 °C.

The thermogravimetric analysis curves of 1,3-phenylenediamine containing polyamic acid BI under argon and in air are presented in Figure 45. Under argon atmosphere, the TGA curve indicates an onset of decomposition at 401 °C with a weight loss of approximately 32 % at ca. 420 °C. In air, polyamic acid BI was stable up to 400 °C.

The differential scanning calorimetry curves of polyimide BII under argon and in air atmospheres are presented in Figure 46. Under argon atmosphere, a decomposition temperature is observed at 415 °C, no glass transition temperature was observed. In air, polyimide BII was stable up to 390 °C followed with a fast thermooxidative decomposition. Softening and glass transition temperatures (Tg) were not observed. Hot stage optical polarizing microscope shows no melting transitions up to 300 °C.

The thermogravimetric analysis (TGA) curves of 1,3-phenylenediamine containing polyimide BII under argon and in air are presented in Figure 47. An onset of

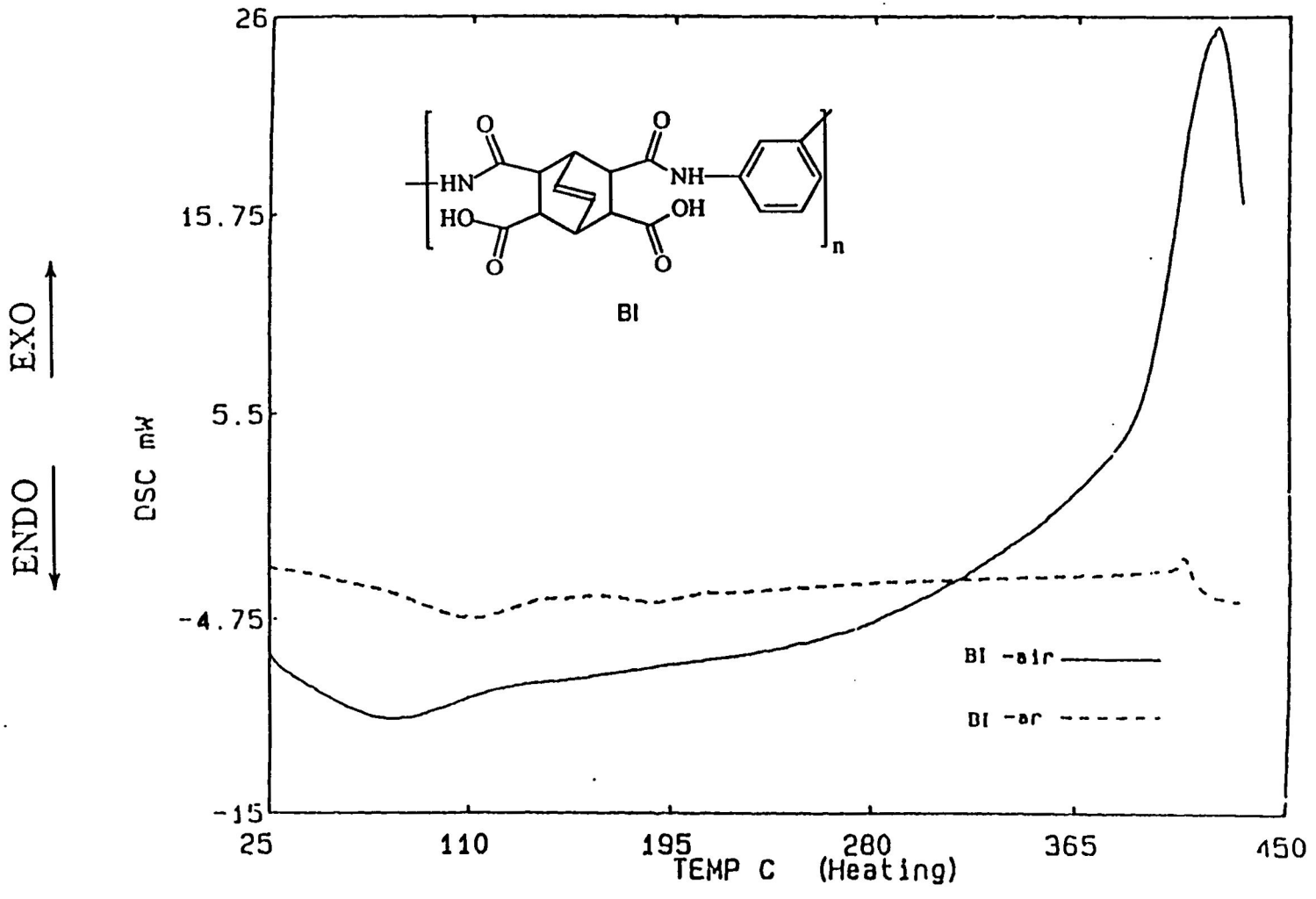

Figure 44. DSC curves of 1,3-phenylenediamine containing polyamic acid BI under argon and in air

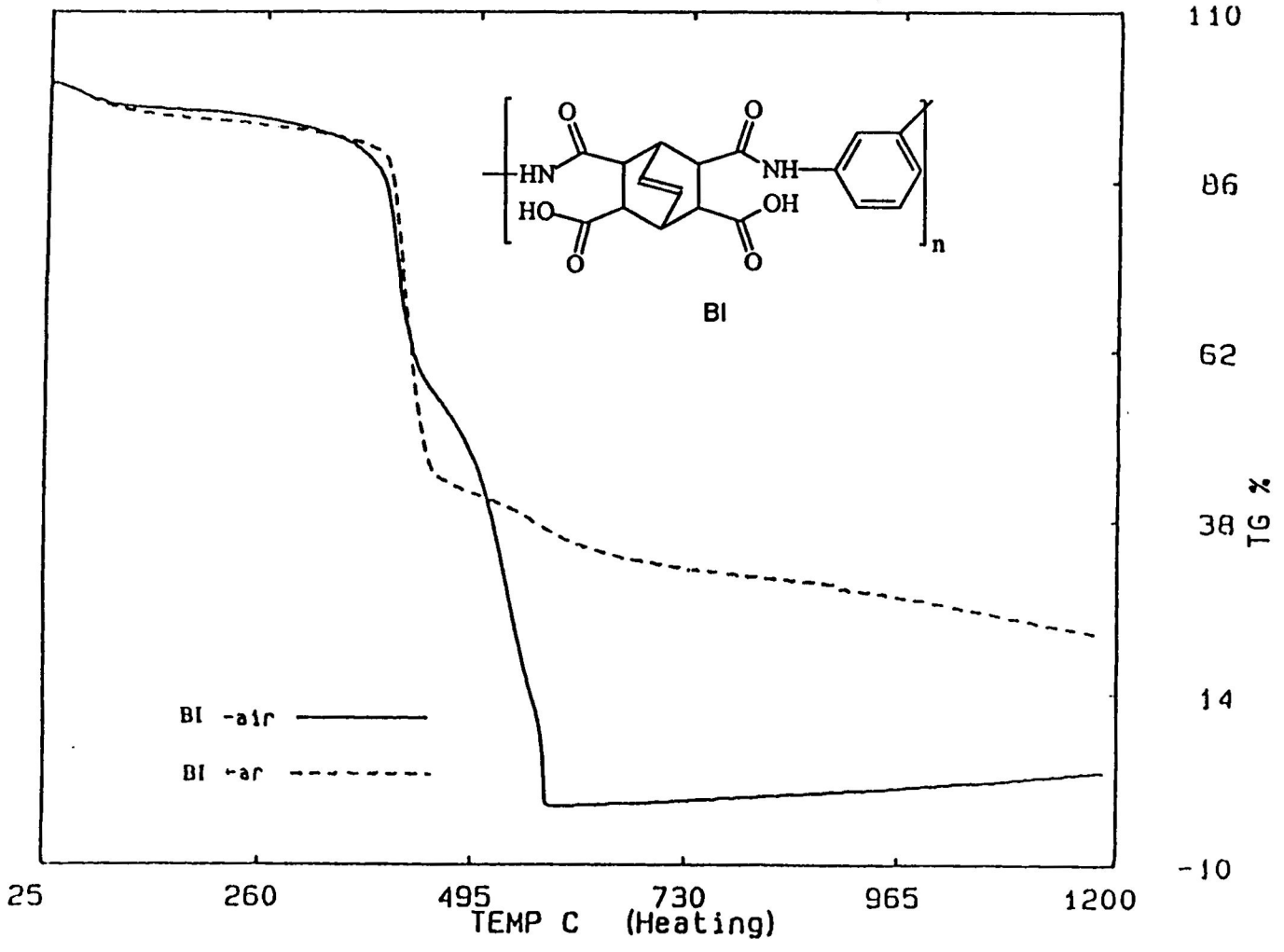

Figure 45. TGA curves of 1,3-phenylenediamine containing polyamic acid BI under argon and in air

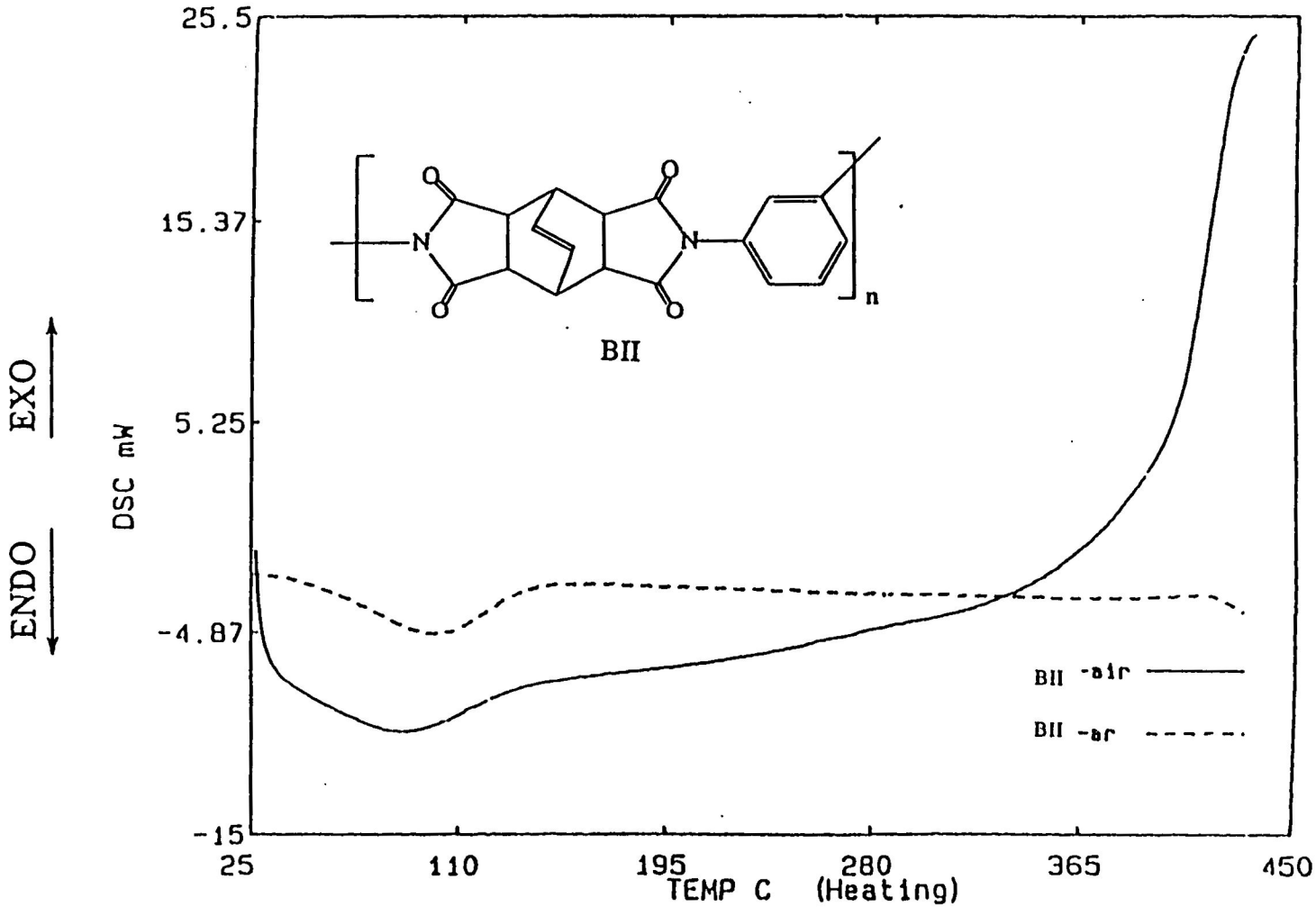

Figure 46. DSC curves of 1,3-phenylenediamine containing polyimide BII under argon and in air

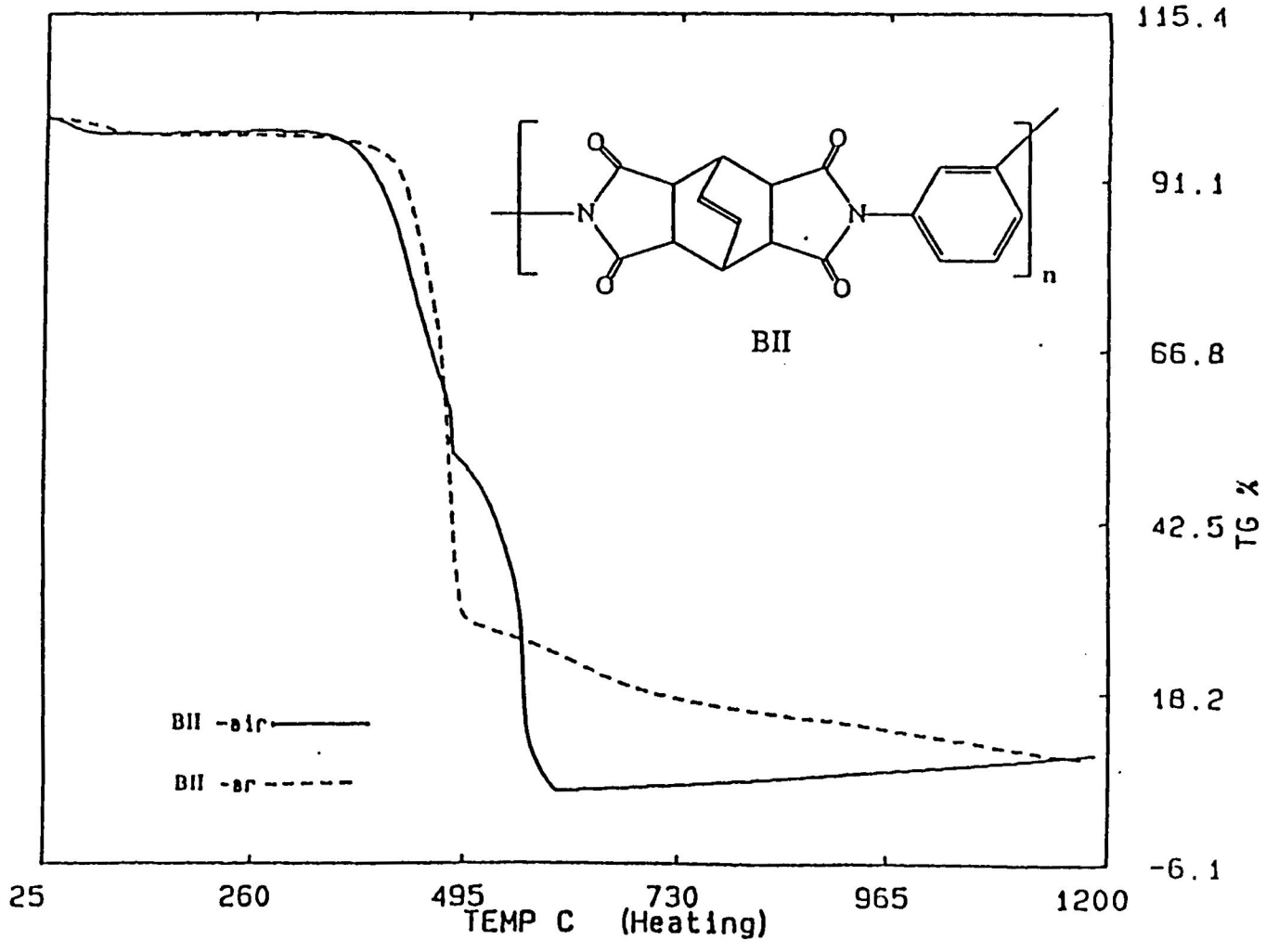

Figure 47. TGA curves of 1,3-phenylenediamine containing polyimide BII under argon and in air

decomposition at 456 °C with a weight loss of approximately 40 % at ca. 470 °C, is observed under argon. In air, polyimide BII was stable up to 393 °C.

The differential scanning calorimetry (DSC) curves of *o*-tolidine containing polyamic acid CI under argon and in air are presented in Figure 48. The DSC curve of *o*-tolidine containing polyamic acid CI indicates no decomposition temperature up to 420 °C, under argon atmosphere. Glass transition temperature (Tg) and crystalline melting temperature (Tc) were not observed, under argon and in air. The polyamic acid CI indicates no decomposition temperature up to 420 °C, in air. Hot stage optical polarizing microscope shows no melting transitions up to 300 °C.

The thermogravimetric analysis (TGA) curves of *o*-tolidine containing polyamic acid CI under argon and air atmospheres are presented in Figure 49. Under argon atmosphere, the TGA curve of polyamic acid CI shows an onset of decomposition at 386 °C with a weight loss of approximately 40 % at ca. 479 °C. In air, onset of decomposition occurs at 373 °C.

The differential scanning calorimetry (DSC) curves of *o*-tolidine containing polyimide CII under argon and air in are presented in Figure 50. Under argon atmosphere, no decomposition temperature was observed up to 420 °C. No glass transition temperature (Tg), melting temperature (Tm) and crystalline melting temperature (Tc) were observed. In air, the DSC curve of *o*-tolidine containing polyimide CII shows no decomposition up to 420 °C. Neither a softening temperature nor a glass transition temperature were observed. Hot stage optical microscope shows no melting transitions up to 300 °C.

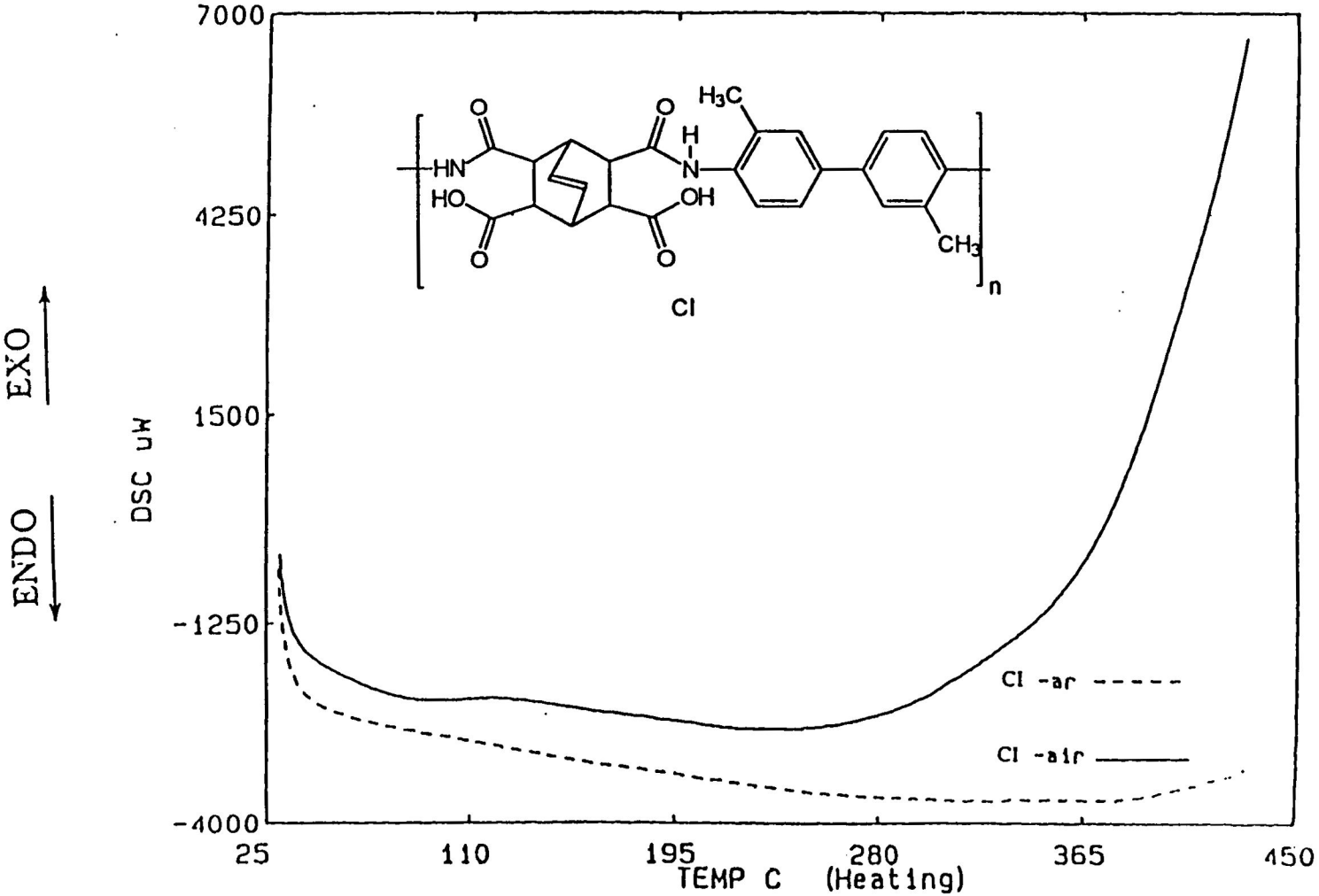

Figure 48. DSC curves of *o*-tolidine containing polyamic acid CI under argon and in air

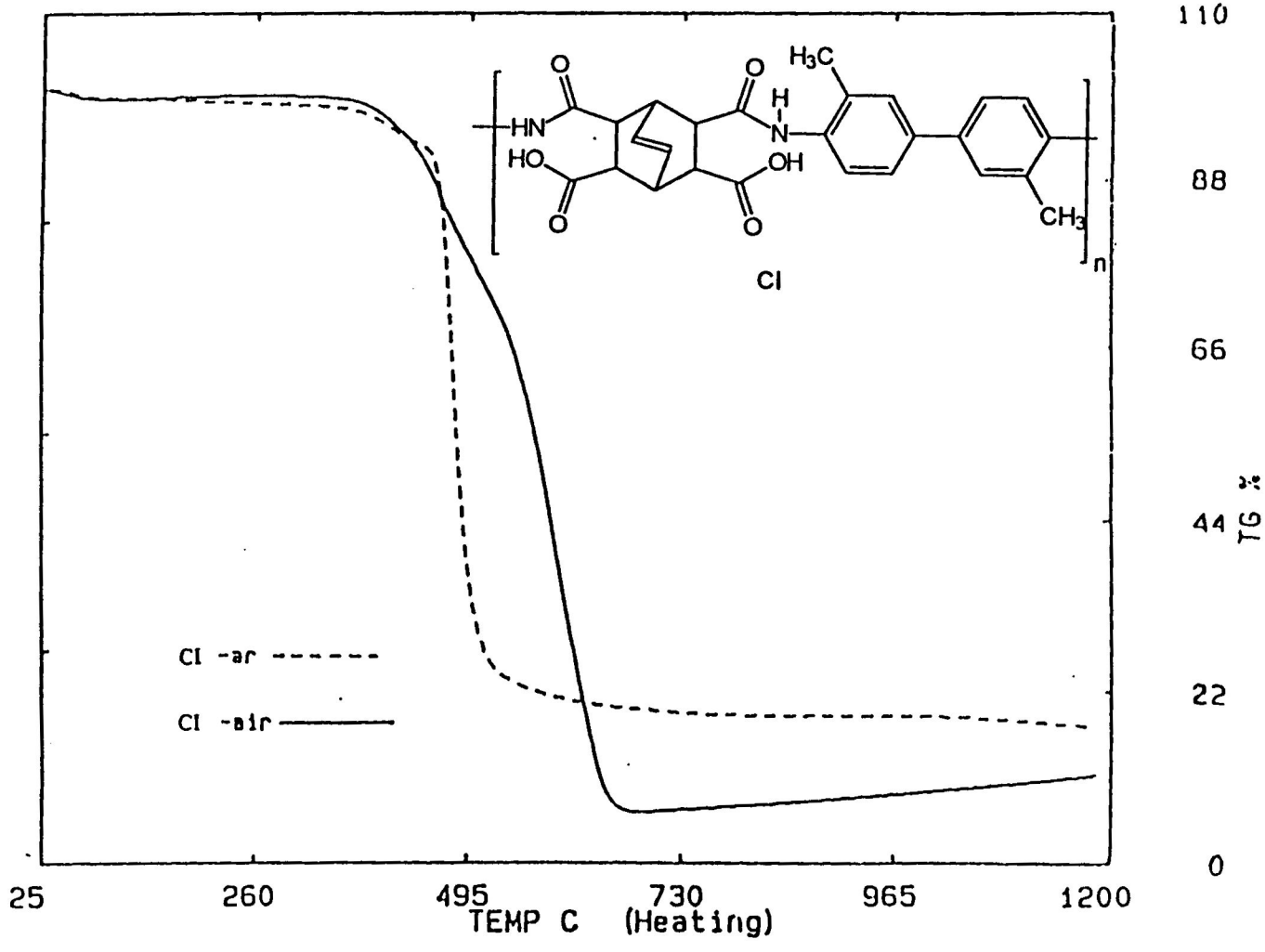

Figure 49. TGA curves of *o*-tolidine containing polyamic acid CI under argon and in air

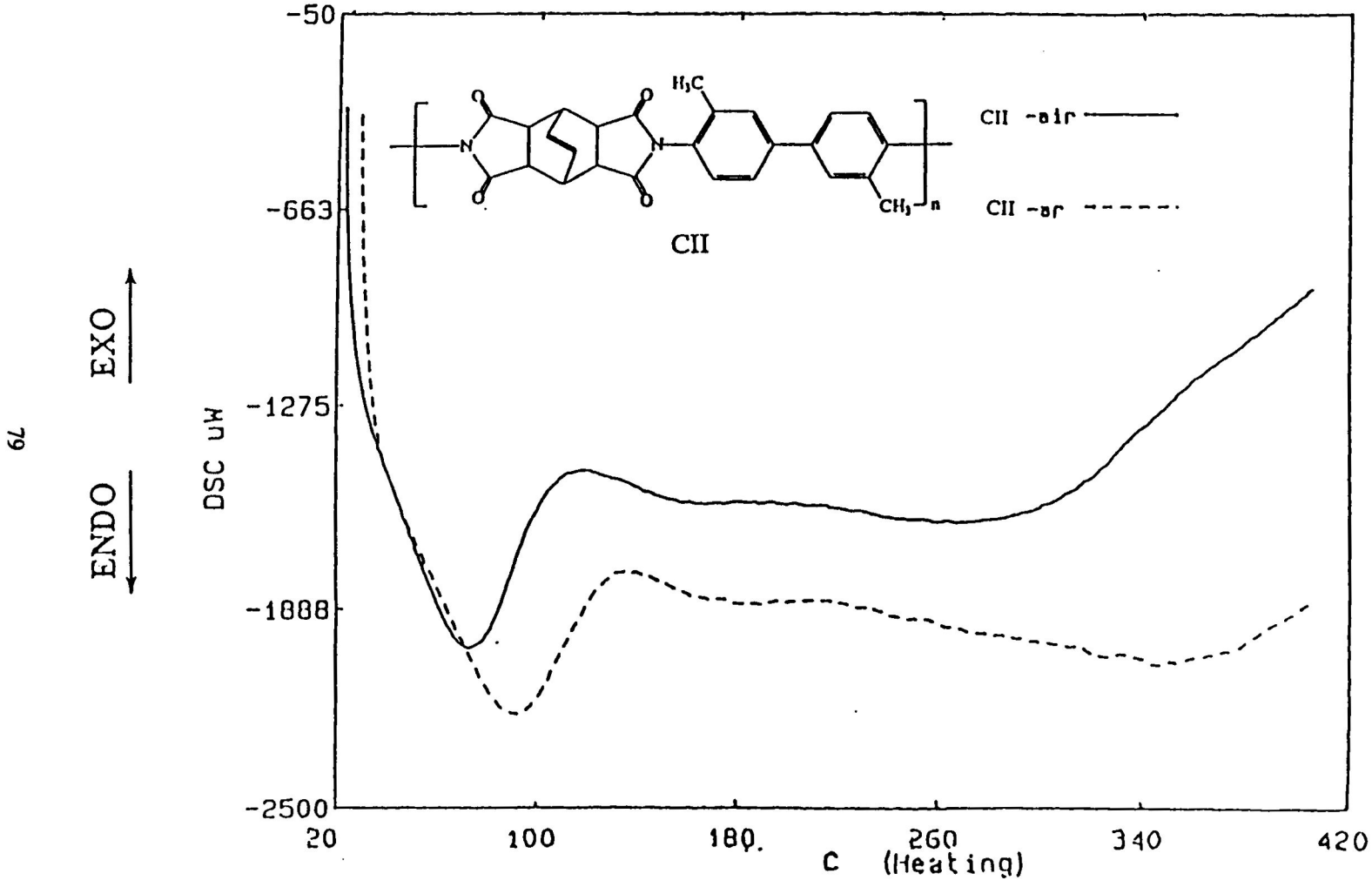

Figure 50. DSC curves of *o*-tolidine containing polyimide CII under argon and in air

The thermogravimetric analysis (TGA) curves of *o*-tolidine containing polyimide CII under argon and in air are presented in Figure 51. Under argon atmosphere, an onset of decomposition temperature at 424 °C. Polyimide CII is stable up to 410 °C, in air.

The differential scanning calorimetry (DSC) curves of 2,2'-bis(trifluoromethyl) benzidine containing polyamic acid DI under argon and in air are presented in Figure 52. Under argon atmosphere, the DSC curve of 2,2'-bis(trifluoromethyl)benzidine containing polyamic acid DI indicates a glass transition temperature at 203 °C, and a recrystallization temperature at 400 °C. The DSC curve of polyamic acid DI, in air shows a glass transition temperature at 201 °C and a recrystallization temperature at 400 °C. No melting transitions were observed on the hot stage optical polarizing microscope up to 300 °C.

The thermogravimetric analysis (TGA) curves of 2,2'-bis(trifluoromethyl)benzidine containing polyamic acid DI under argon and in air are presented in Figure 53. Under argon atmosphere, the TGA curve of polyamic acid DI indicates an onset of decomposition at 414 °C with a weight loss of approximately 40 % at ca. 436 °C. In air, the polyamic acid DI shows an onset of decomposition at 390 °C with a weight loss of approximately 6 % at ca. 516 °C.

The differential scanning calorimetry (DSC) curves of polyimide DII under argon and in air are presented in Figure 54. Under argon, a melting transition temperature is observed at 386 °C. In air, the DSC curve of polyimide DII shows a glass transition temperature (Tg) at 231, a broad recrystallization temperature exotherm at 279, and a melting temperature at 324 °C. Optical polarizing microscope of the film of polyimide

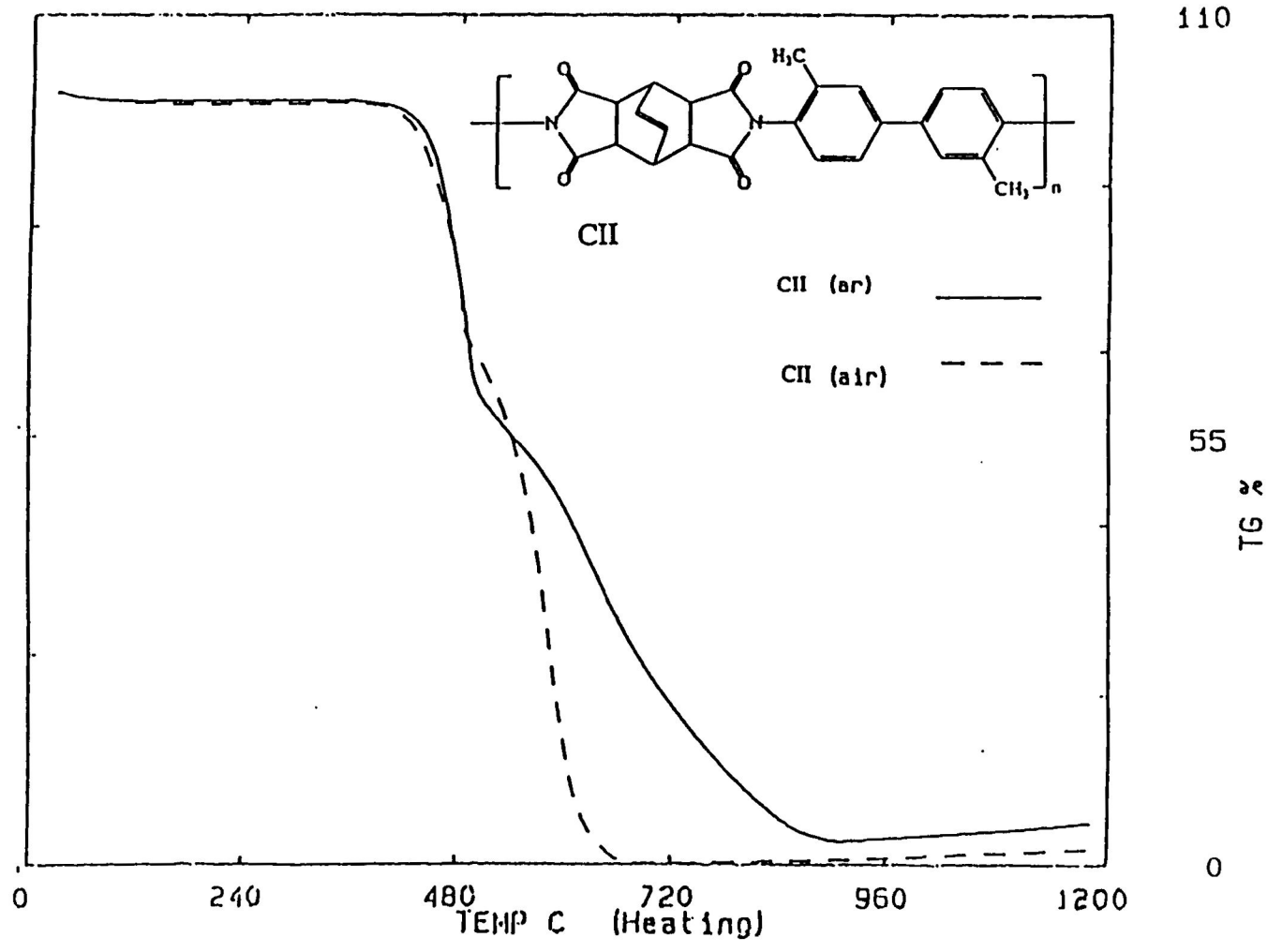

Figure 51. TGA curves of *o*-tolidine containing polyimide CII under argon and in air

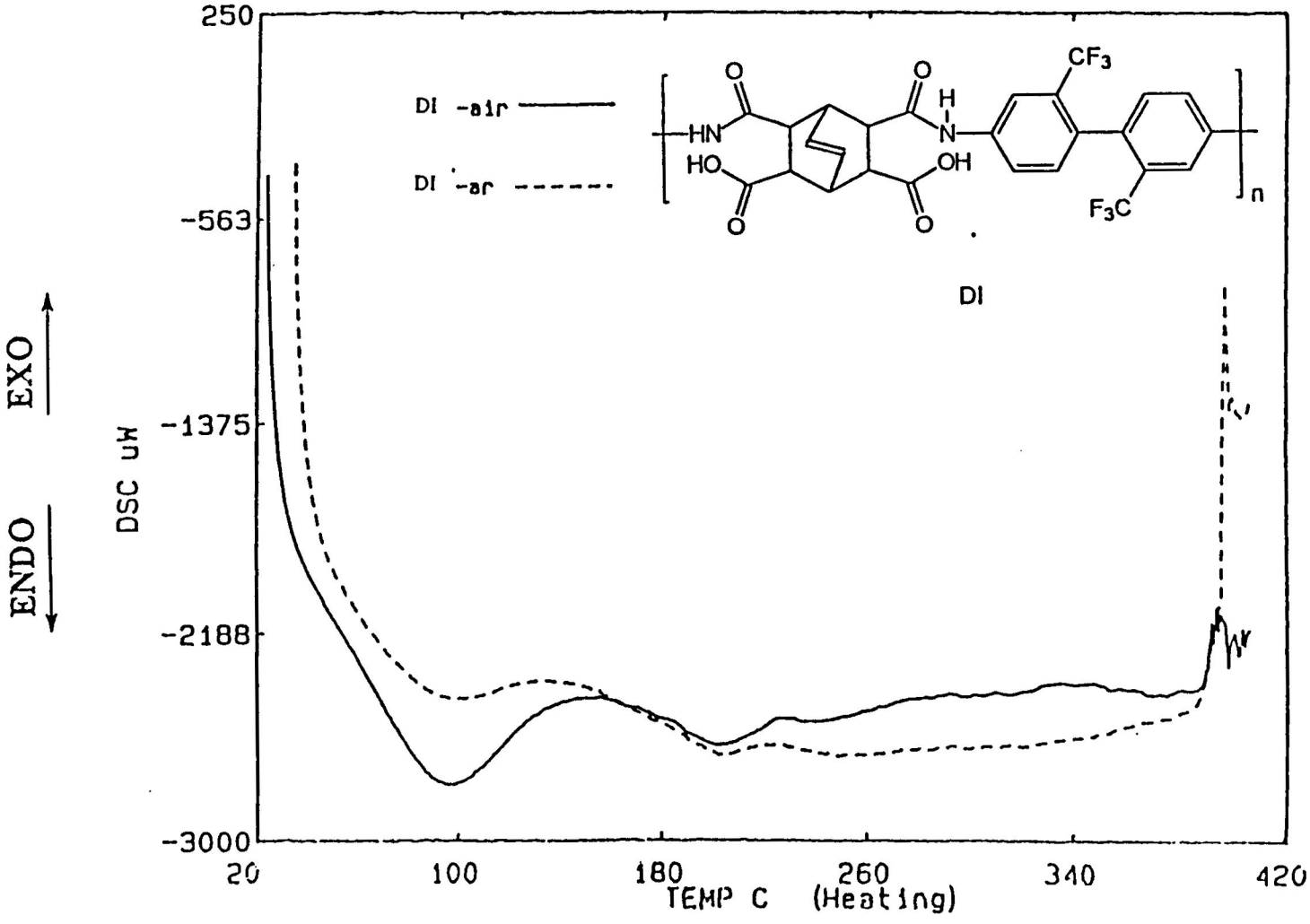

Figure 52. DSC curves of 2,2'-bis(trifluoromethyl)benzidine containing polyamic acid DI under argon and in air

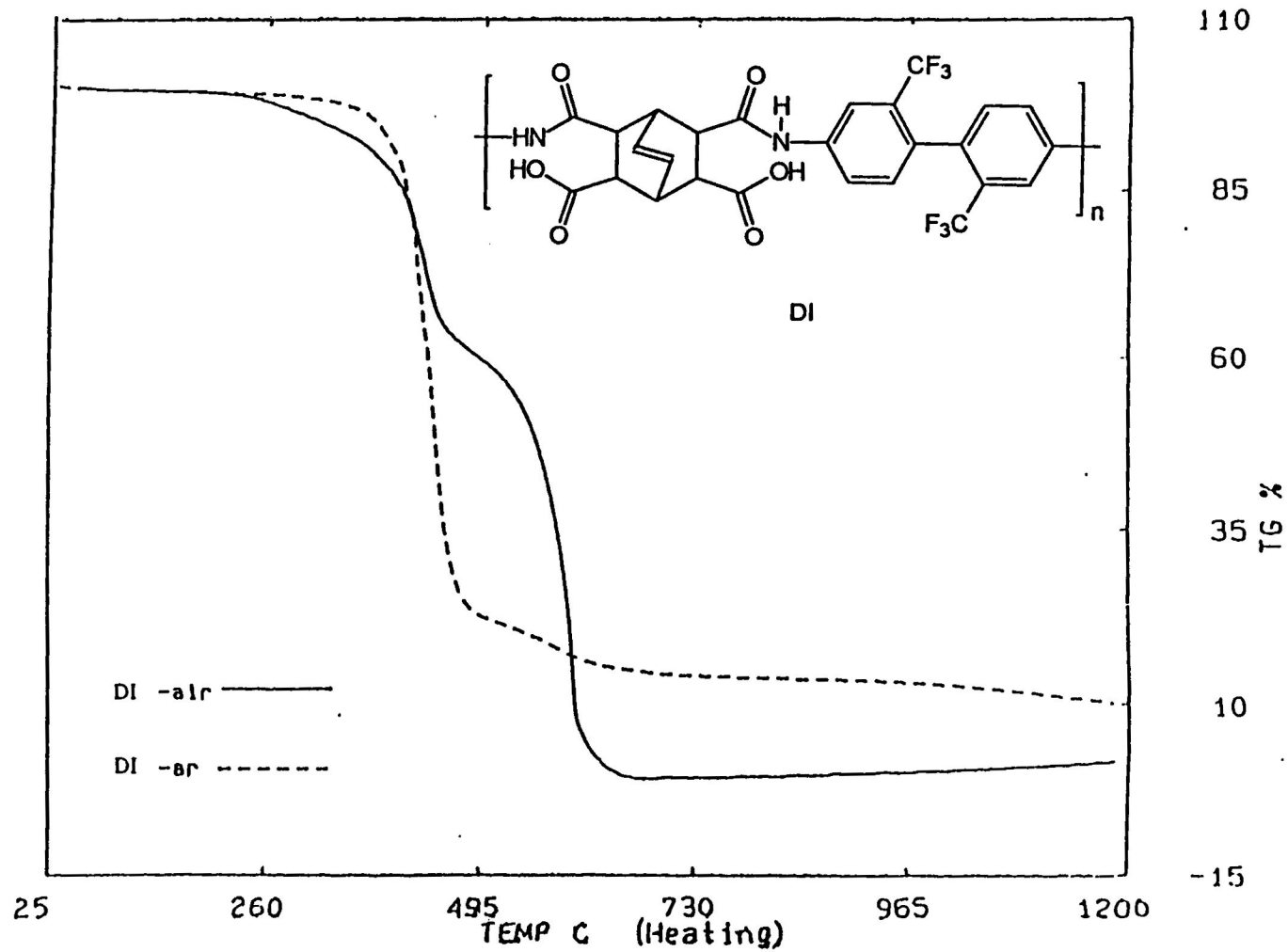

Figure 53. TGA curves of 2,2'-bis(trifluoromethyl)benzidine containing polyamic acid DI under argon and in air

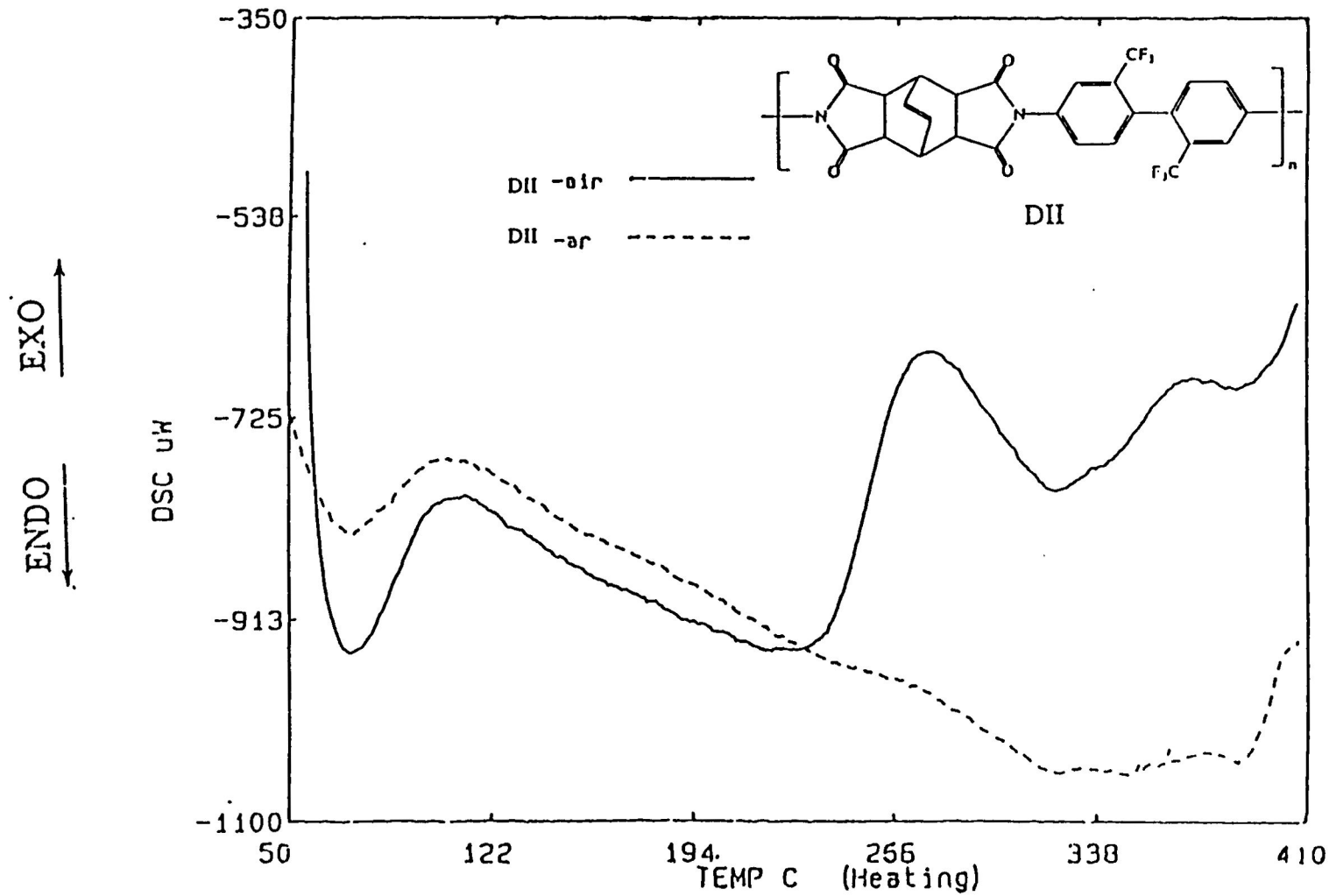

Figure 54. DSC curves of 2,2'-bis(trifluoromethyl)benzidine containing polyimide DII under argon and in air

DII, cast from NMP, shows the formation of blue and yellow birefringence phase at room temperature, Figure 55.

The thermogravimetric analysis (TGA) curves of polyimide DII under argon and in air are presented in Figure 56. Under argon, an onset of decomposition is observed at 414 °C with a weight loss of approximately 32 % at ca. 425 °C. In air, the onset of decomposition temperature occurs at 418 °C with a weight loss of approximately 40 % at ca. 500 °C.

The differential scanning calorimetry (DSC) curves of 2,2'-bis(trifluoromethyl)benzidine containing polyamic acid EI under argon and in air, are presented in Figure 57. Under argon atmosphere, polyamic acid EI shows a glass transition temperature (Tg) endotherm at 233 and a recrystallization temperature at 401 °C. In air, the DSC curve indicates a glass transition temperature at 234, and a recrystallization temperature at 400 °C. Hot stage optical polarizing microscope shows the formation of blue and yellow birefringence fluid after the evaporization of NMP solvent.

The thermogravimetric analysis (TGA) curves of polyamic acid, EI, under argon and in air are presented in Figures 58. Under argon atmosphere, polyamic acid EI shows a decomposition temperature at 602 °C. In air, the TGA curve of polyamic acid EI shows a decomposition temperature at 581 °C.

The differential scanning calorimetry (DSC) curves of polyimide EII under argon and in air are presented in Figure 59. Under argon atmosphere, a glass transition temperature is observed at 184 °C. No melting transitions were observed. In air, a glass

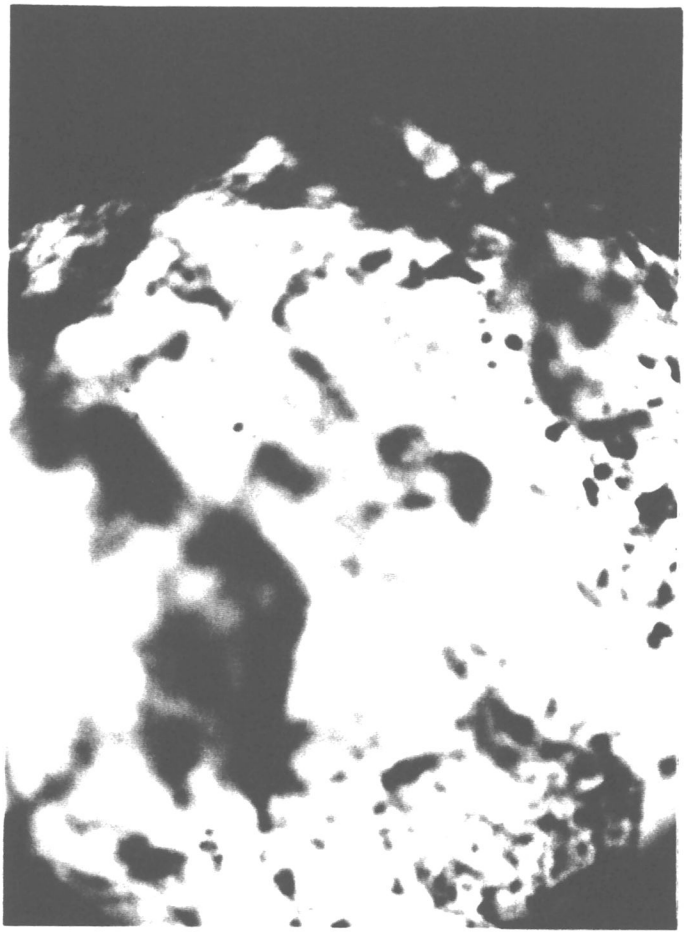

Figure 55. Optical polarizing micrograph of film DII cast from NMP

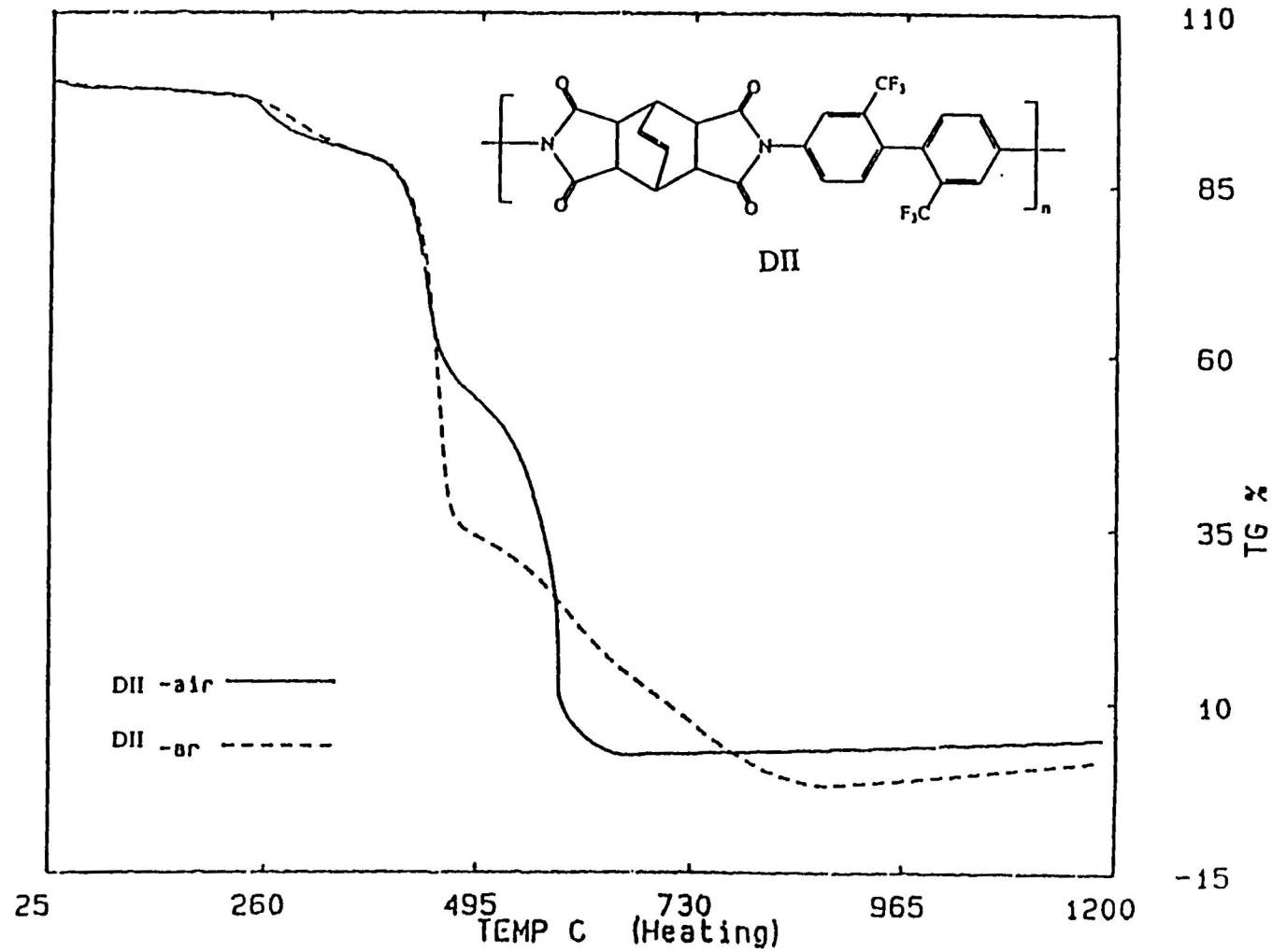

Figure 56. TGA curves of 2,2'-bis(trifluoromethyl)benzidine containing polyimide DII under argon and in air

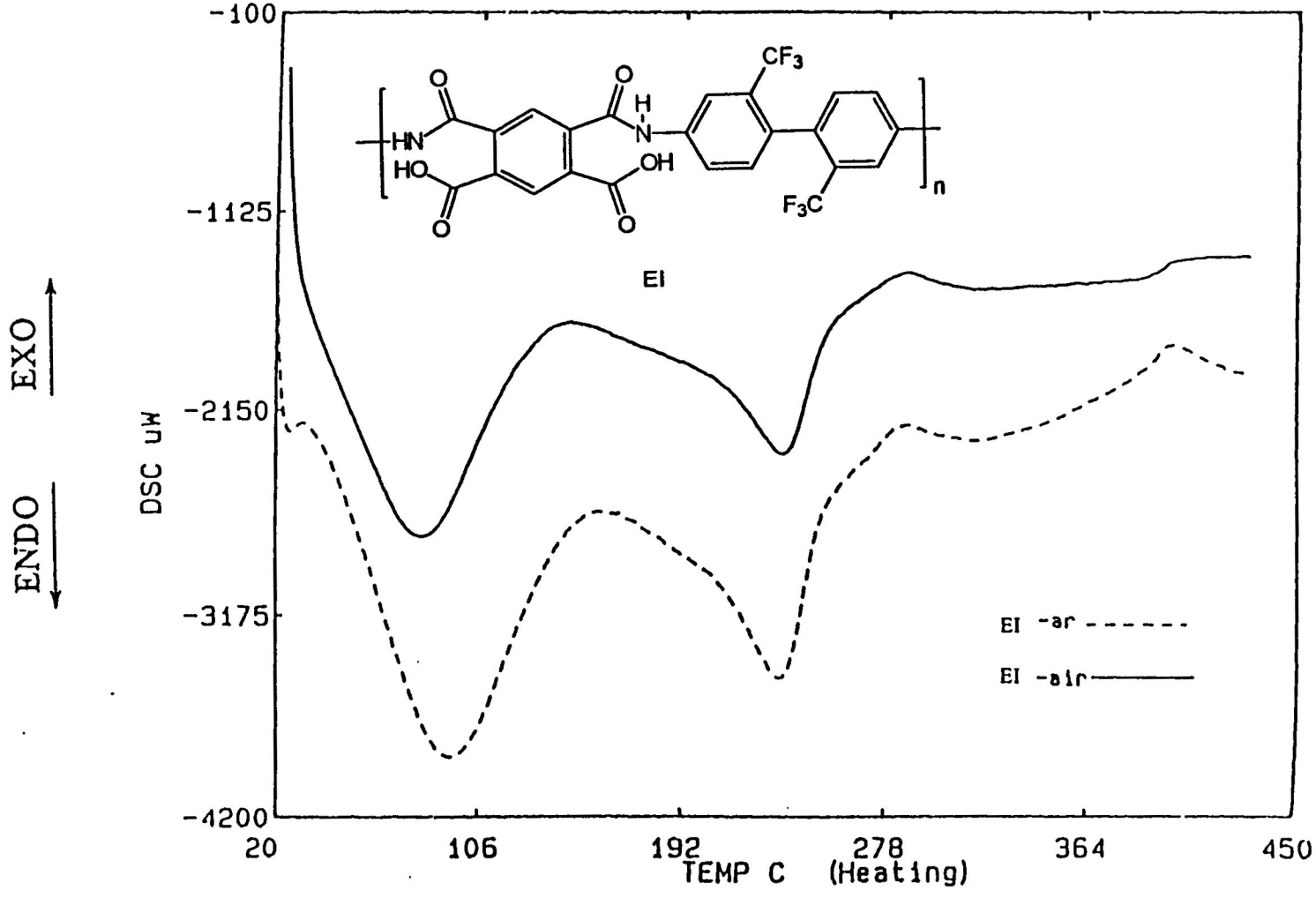

Figure 57. DSC curves of 2,2'-bis(trifluoromethyl)benzidine containing polyamic acid EI under argon and in air

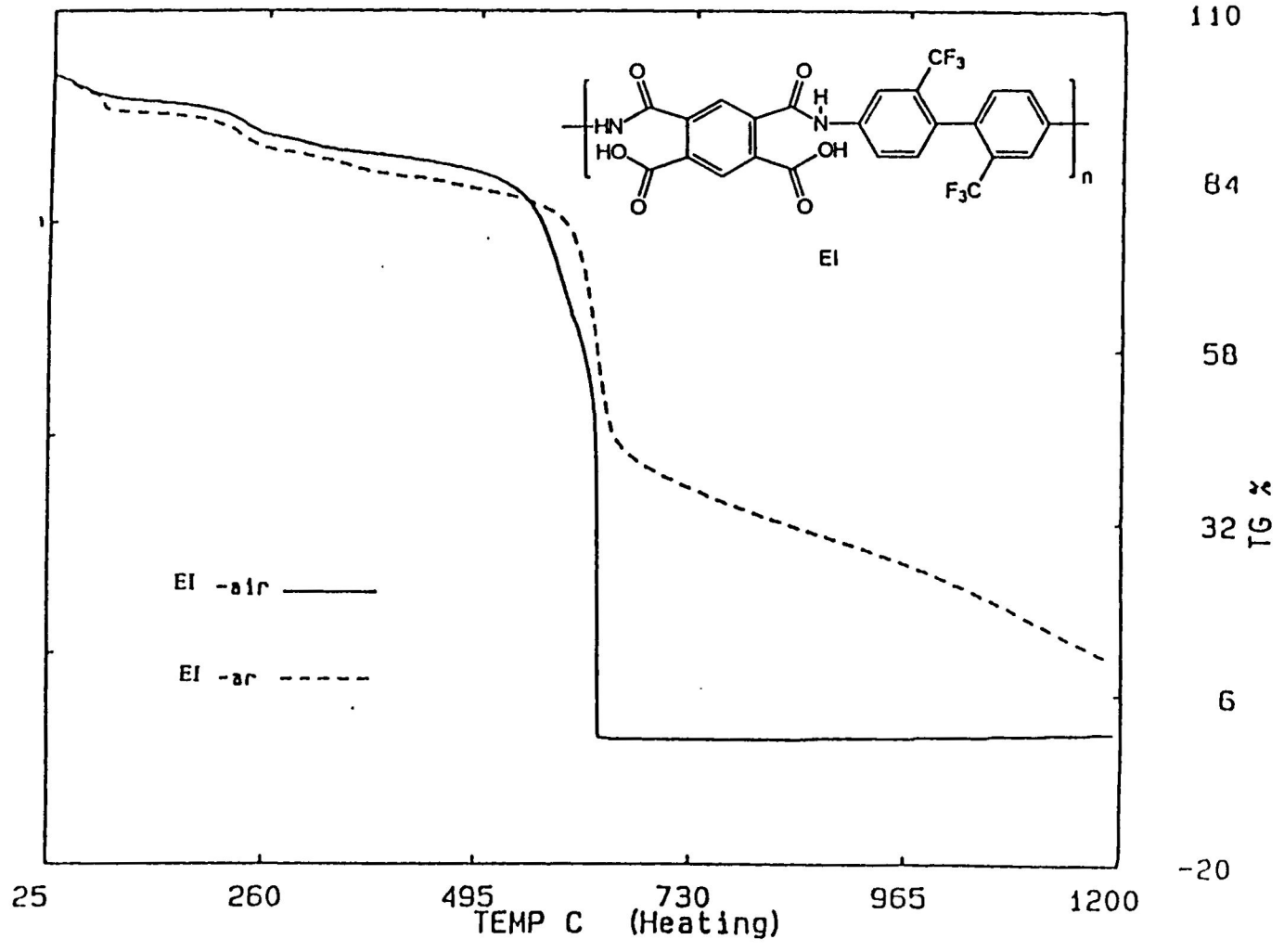

Figure 58. TGA curves of 2,2'-bis(trifluoromethyl)benzidine containing polyamic acid EI under argon and in air

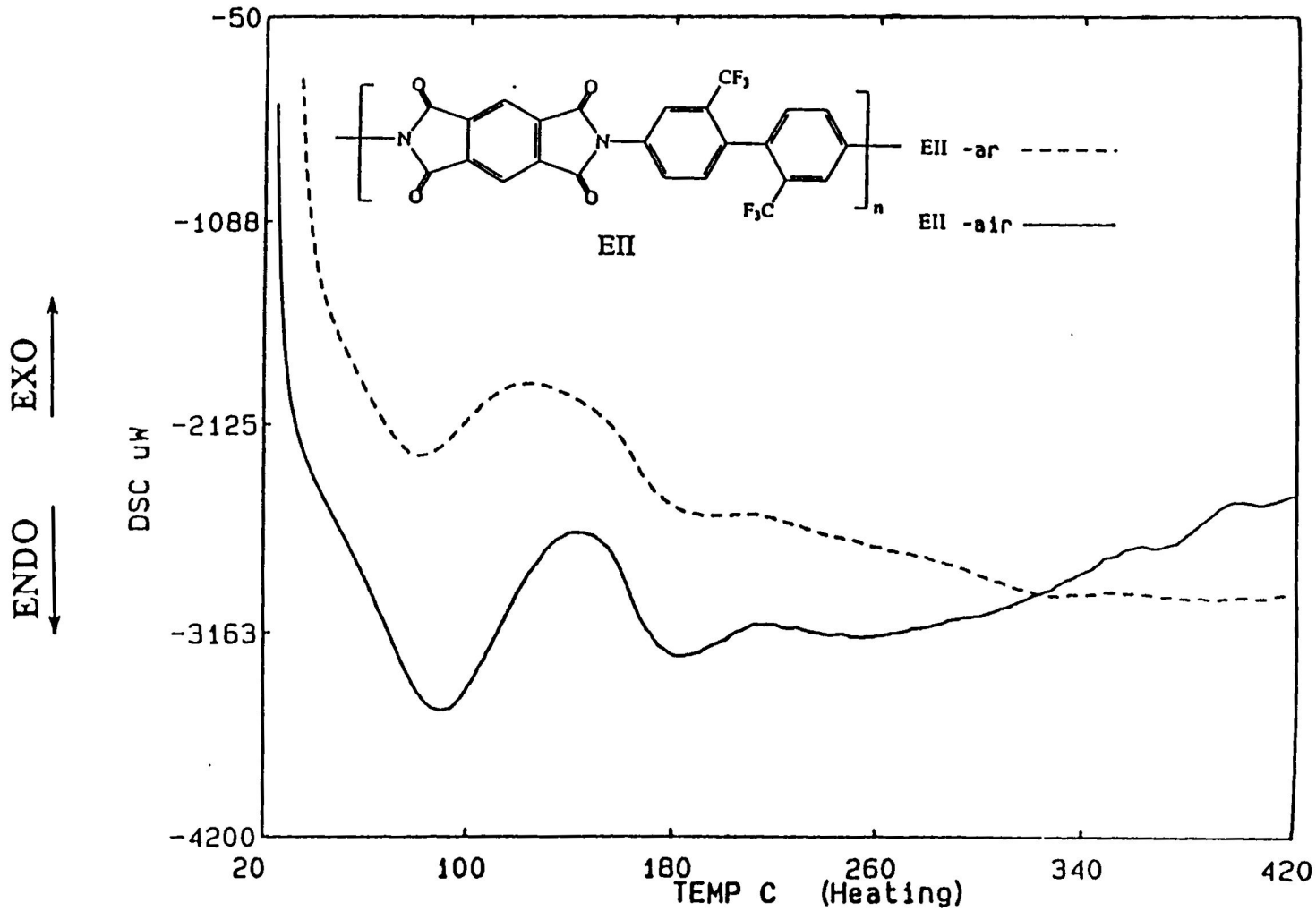

Figure 59. DSC curves of 2,2'-bis(trifluoromethyl)benzidine containing polyimide EII under argon and in air

transition temperature (Tg) is observed at 184 °C. Hot stage optical microscopy shows the formation of blue and yellow birefringence fluid after the evaporization of the NMP solvent.

The thermogravimetric analysis (TGA) curves of polyimide EII under argon and air atmospheres are presented in Figure 60. An onset of decomposition is observed at 363 °C under argon atmosphere. The onset of decomposition, in air for polyimide EII was observed at 393 °C.

Solution Properties

Table 4 summarizes the solubility properties of the polyamic acids and polyimides at room temperature and their inherent viscosities at 30 °C.

Table 4. Solubility properties and Inherent viscosity measurements of the polyamic acids and the polyimides

Polymer	Inherent viscosity dL/g	Solubility							
		NMP	DMAc	DMF	DMSO	H_2SO_4	MSA	TMU	Acetone
AI	0.2[a]	+-	-	+-	+	+	+	-	-
AII	0.3[a]	+-	+-	-	+-	+	+	+-	-
BI	0.3[a]	+-	-	+	+	+	+	-	-
BII	0.4[a]	-	+-	-	+-	+	+	+-	-
CI	0.3[a]	-	-	-	-	+	+-	-	-
CII	0.4[a]	-	-	-	-	+	+	-	-
DI	0.2[b]	+	+	+	+	+	+	+	+
DII	0.8[b]	+	+	+	+	+	+	+	+
EI	0.5[b]	+	+	+	+	+	+	+	+
EII	0.7[b]	+-	+-	+-	+-	+	+	+-	+-

[a]viscosities measured in concentrated sulfuric acid; [b]viscosities measured in dimethyl sulfoxide (DMSO); (+), soluble; (+-), partially soluble; (-), insoluble; NMP, 1-methyl-2-pyrrolidinone; DMAc, dimethylacetamide; DMF, dimethylformamide; MSA, methane sulfonic acid; TMU, tetramethylurea

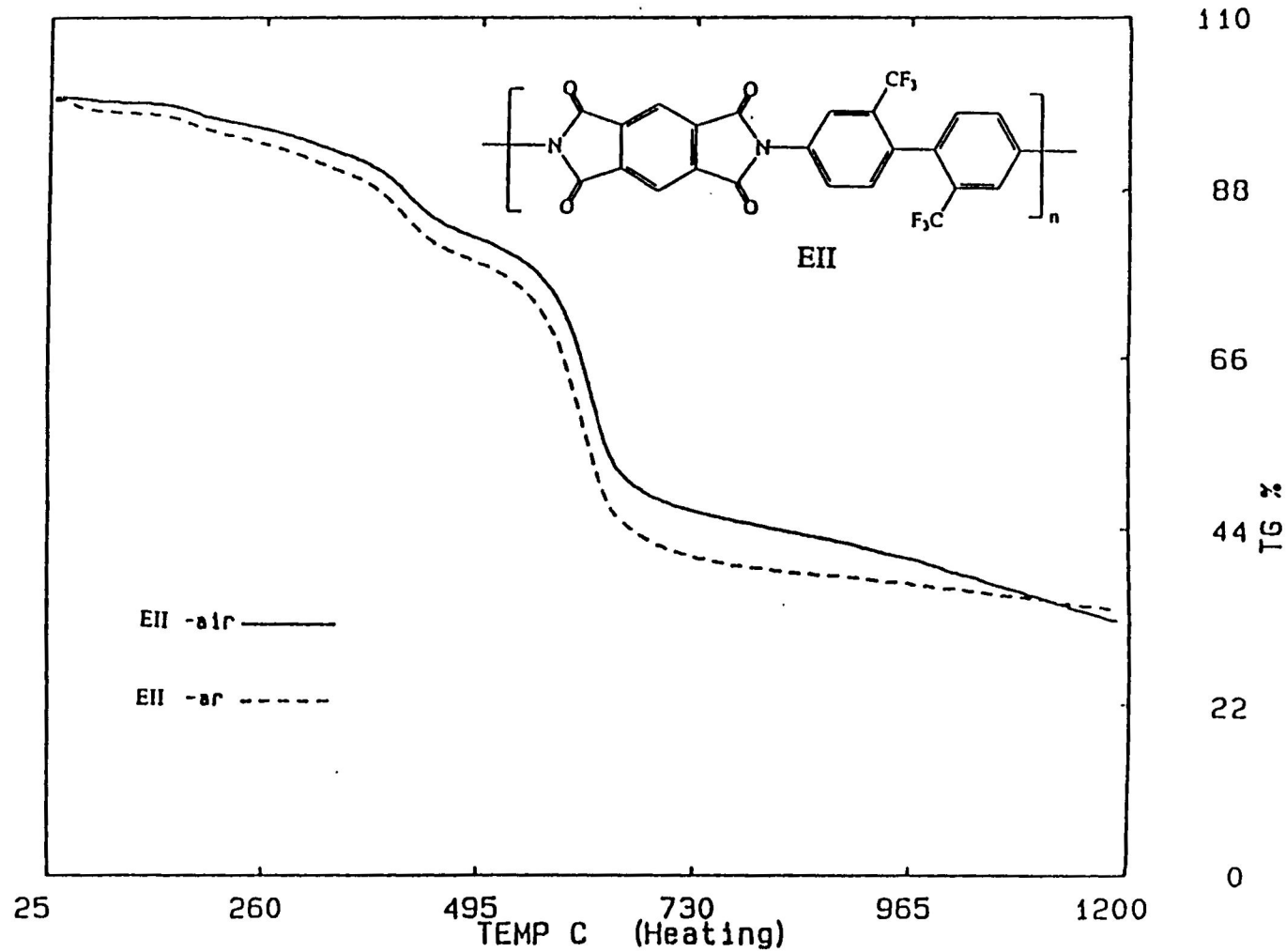

Figure 60. TGA curves of 2,2'-bis(trifluoromethyl)benzidine containing polyimide EII under argon and in air

The solubility data shows that 1,4-phenylenediamine and 1,3-phenylenediamine containing polyamic acids, AI, BI, and the corresponding polyimides, AII, BII, were generally soluble in corrosive solvents such as concentrated sulfuric acid and methane sulfonic acid (MSA). Polyamic acids DI and EI, and polyimide DII were soluble in all the solvents that were tested. Polyimide EII was partially soluble in all the solvents that were tested. The decreased solubility of EI is attributed to the presence of 1,2,4,5-benzene tetracarboxylic acid dianhydride, increasing the aromatic character of the polymer. Polyamic acids DI and EI, and polyimide DII were soluble in all the solvents that were tested due to the flexibility of the polymer backbone resulting from the non-coplanar character of the diamine used. Also, the electron-withdrawing properties of the trifluoromethyl group reduced the intractability of these polymers.

Low inherent viscosities observed suggest low molecular weights. The slight difference in inherent viscosities of polyamic acids AI, BI, and CI versus the corresponding polyimides AII, BII, and CII indicated that no significant changes in the degree of polymerization occurred in the thermal conversion from polyamic acids to the polyimides. Higher inherent viscosities were observed for polyimides DII and EII derived from 2,2'-bis(trifluoromethyl)benzidine suggesting higher molecular weights.

Polymer Morphology

The X-ray scattering pattern for the polyamic acids and the polyimides are presented in Appendix I. The morphology of the polyamic acids and the corresponding polyimides are summarized on Table 5.

Table 5. Morphological data of the polyamic acids and the polyimides

Polymer	Morphology
AI	Amorphous
AII	Semi-crystalline
BI	Amorphous
BII	Semi-crystalline
CI	Amorphous
CII	Semi-crystalline
DI	Amorphous
DII	Crystalline
EI	Amorphous
EII	Amorphous

X-ray results shows that the polyamic acids are amorphous. Polyimide EII, also has an amorphous morphology. Polyimides AII, BII and CII are semi-crystalline. The X-ray scattering graphs of these polymers exhibit well defined peaks at low angles which is indicative of semi-crystalline polymers. (This is due to diffused diffraction, indicating some order in the polymer.) Polyimide DII exhibits crystalline morphology indicated by the intense and sharp peaks up to 90°. This indicates an ordered arrangement of the polymer molecules.

CONCLUSION

Novel polyimides containing the bicyclo[2.2.2]oct-7-ene moiety together with unsubstituted phenyl and substituted biphenyl moieties were developed. A reduction in the symmetry and a reduction in the π-electron density of the polymer backbones are two important factors in improving solubility for the systems.

Polyimides derived from unsubstituted phenyl moieties and bicyclo[2.2.2]oct-7-ene ring system exhibited enhance solubility compared to wholly rigid aromatic polyimides while maintaining high thermal stability. Polyimides containing 2,2'-disubstituted biphenyl moieties with trifluoromethyl groups (CF_3) exhibited enhanced solubility over those derived from 3,3' disubstituted biphenyl moieties with methyl (CH_3) groups. Thermal and thermooxidative stability was higher for polyimides derived from disubstituted biphenyl moieties (CF_3 or CH_3) and bicyclic ring systems. Besides their excellent solution and thermal properties, the polyimides were generally white and can be easily cast into films or spun into fibers.

High molecular weight polyimides were obtained in systems derived from bicyclo[2.2.2]oct-7-ene ring system and trifluoromethyl substituted biphenyl moieties as indicated by inherent viscosity measurements.

Polymers with biphenyl moieties substituted in the 2,2' positions with trifluoromethyl groups (CF_3) exhibited higher crystalline order than polymers substituted in the 3,3' positions with methyl groups (CH_3).

A logical extension of this work will be to study the conversion of the bicyclo[2.2.2]oct-7-ene ring system to the more stable aromatic polyimide via pyrolysis, monitored by thermogravimetric-mass spectrometer (TG-MS). Also, the fabrication of films and fibers can be accomplished using the precursor polyimide containing the bicyclo[2.2.2]oct-7-ene ring system followed by conversion to the more stable polyimide to give films and fibers with high performance properties.

The use of bicyclo[2.2.2]oct-7-ene ring system can be applied to other polymeric systems to prepare high performance polymers with improved processability.

APPENDIX I

1.1. X-ray scattering pattern of 1,4-phenylenediamine containing polyamic acid AI

1.2. X-ray scattering pattern of 1,4-phenylenediamine containing polyimide AII

1.3. X-ray scattering pattern of 1,3-phenylenediamine containing polyamic acid BI

1.4. X-ray scattering pattern of 1,3-phenylenediamine containing polyimide BII

1.5. X-ray scattering pattern of *o*-tolidine containing polyamic acid CI

1.6. X-ray scattering pattern of *o*-tolidine containing polyimide CII

1.7. X-ray scattering pattern of 2,2'-bis(trifluoromethyl)benzidine containing polyamic acid DI

1.8. X-ray scattering pattern of 2,2'-bis(trifluoromethyl)benzidine containing polyimide DII

1.9. X-ray scattering pattern of 2,2'-bis(trifluoromethyl)benzidine containing polyamic acid EI

1.10. X-ray scattering pattern of 2,2'-bis(trifluoromethyl)benzidine containing polyimide EII

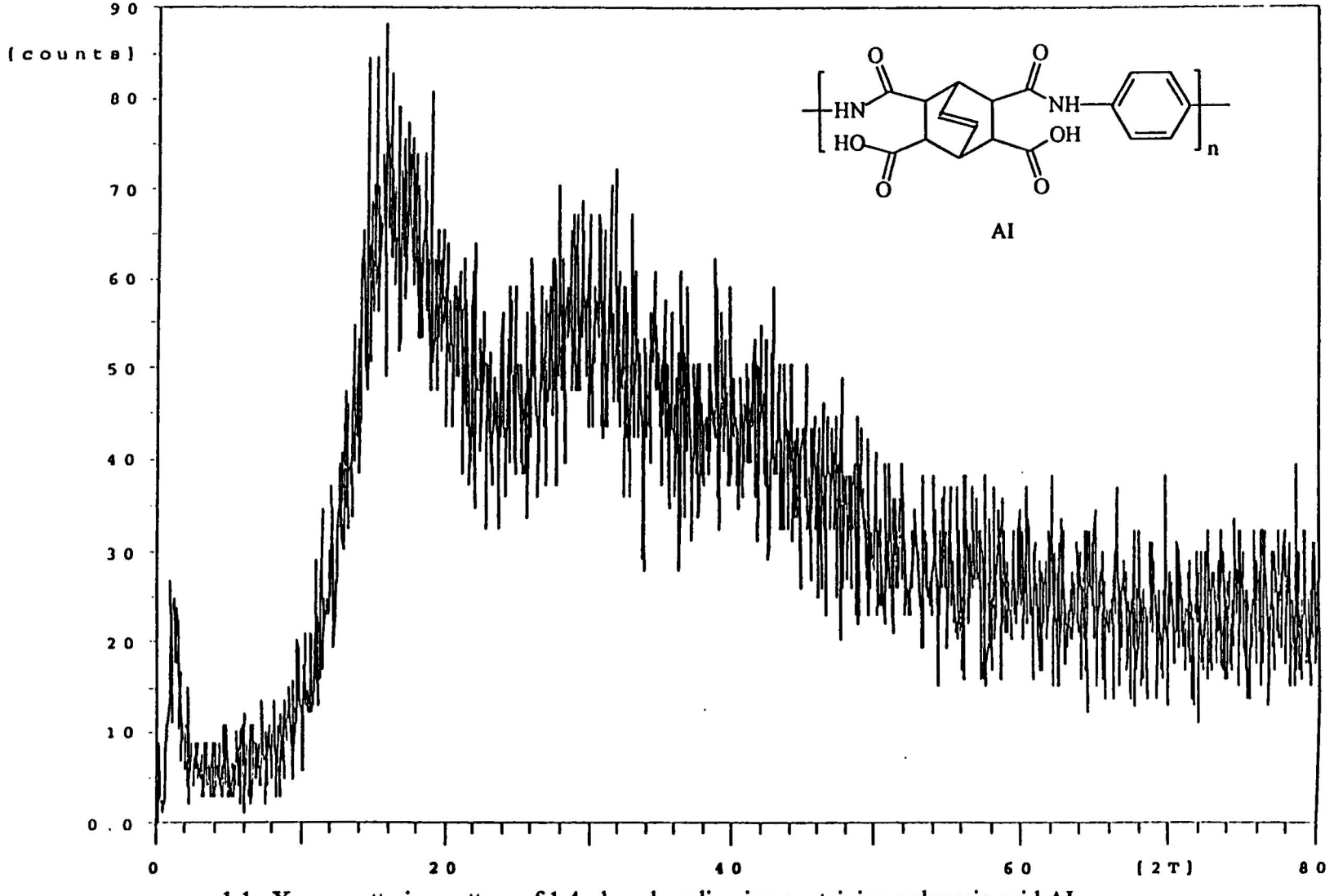

AI

1.1. X-ray scattering pattern of 1,4-phenylenediamine containing polyamic acid AI

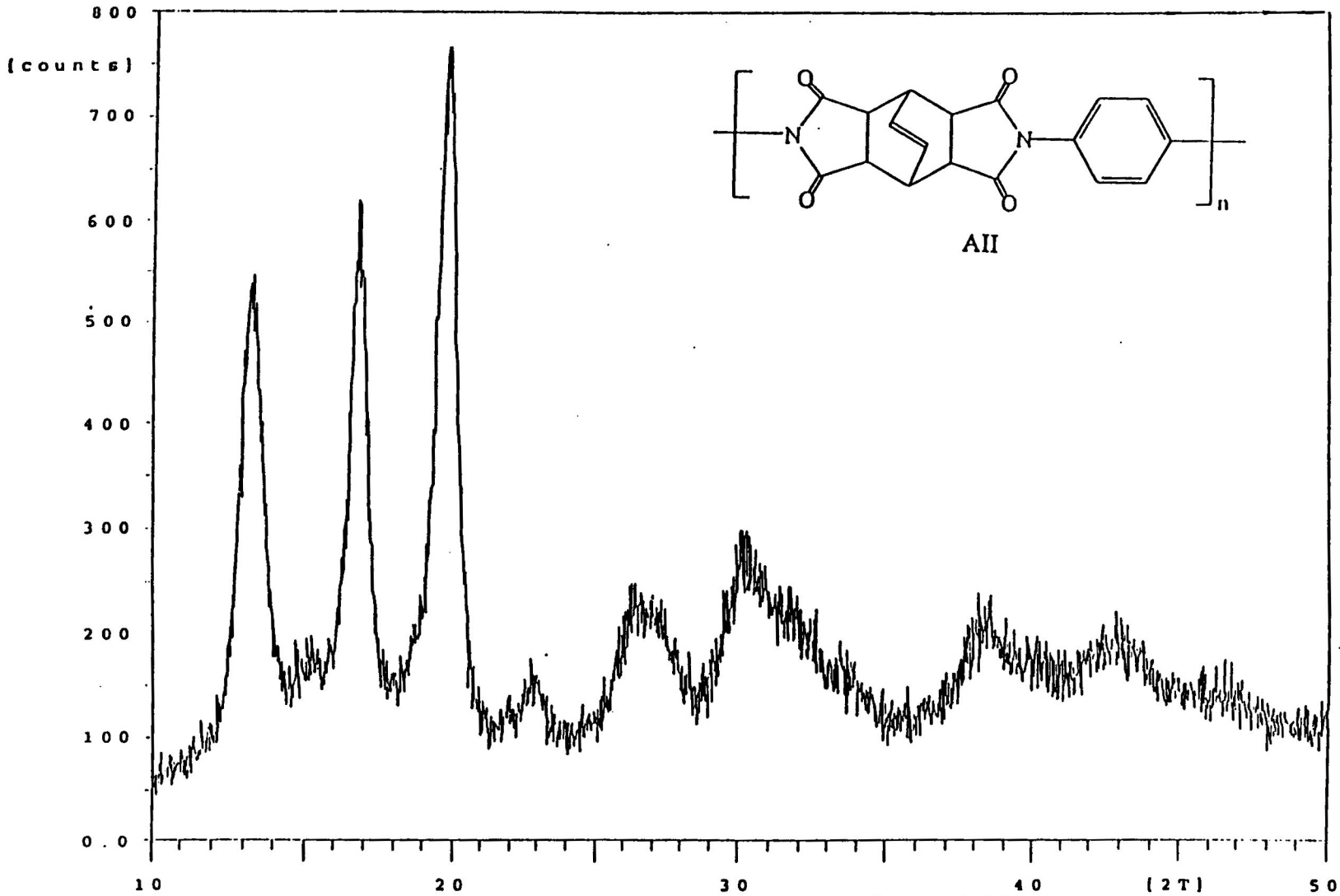

AII

1.2. X-ray scattering pattern of 1,4-phenylenediamine containing polyimide AII

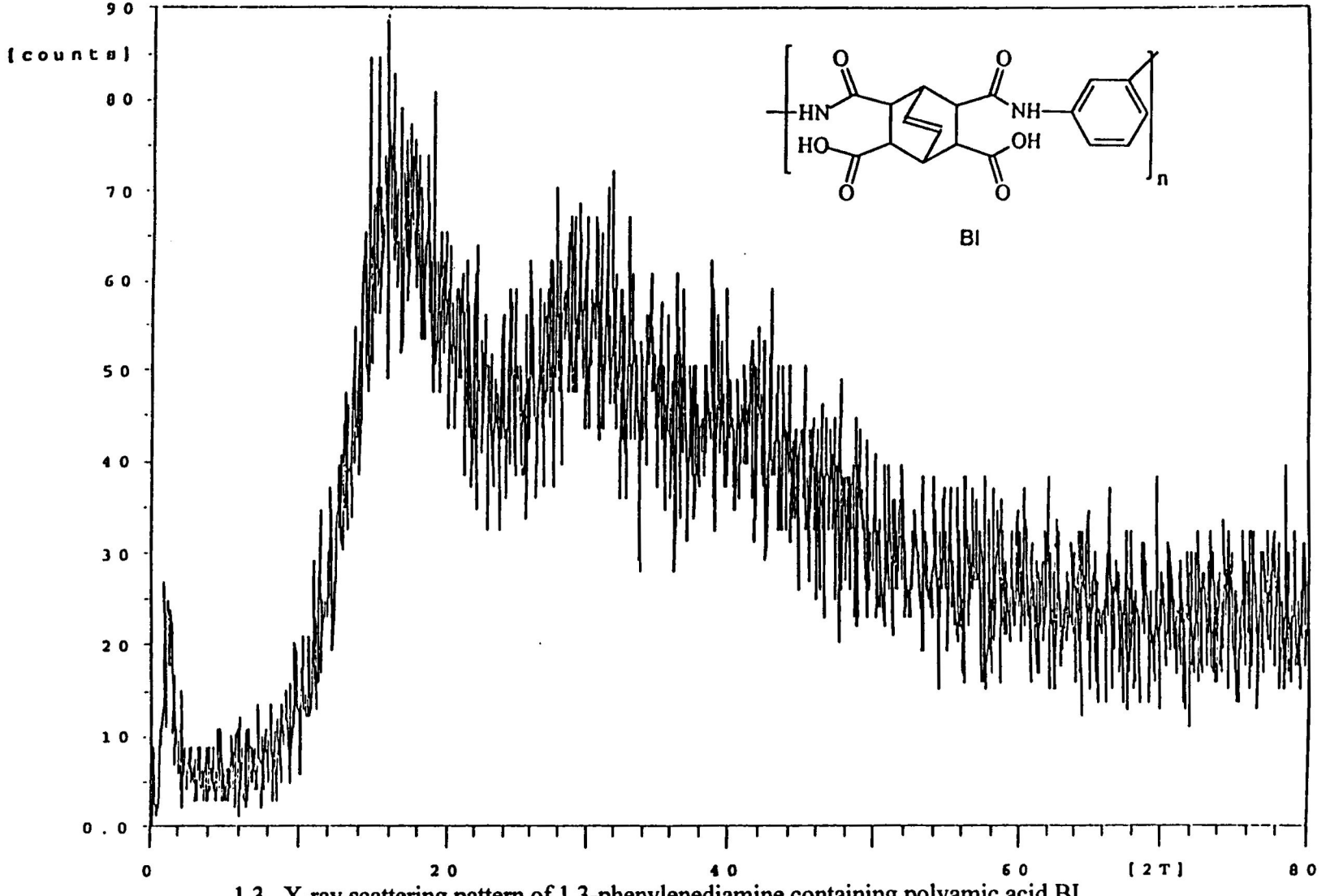

1.3. X-ray scattering pattern of 1,3-phenylenediamine containing polyamic acid BI

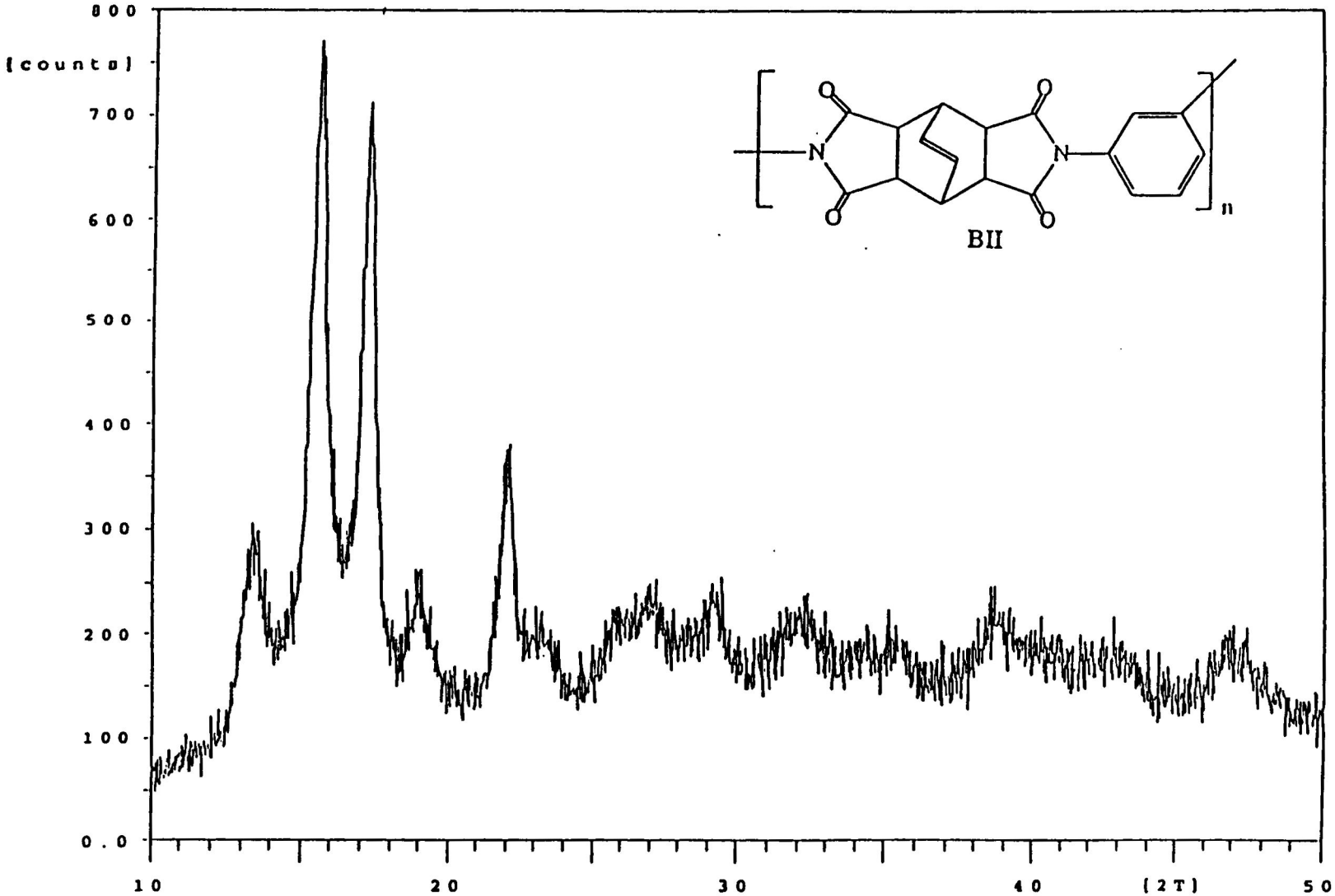

BII

1.4. X-ray scattering pattern of 1,3-phenylenediamine containing polyimide BII

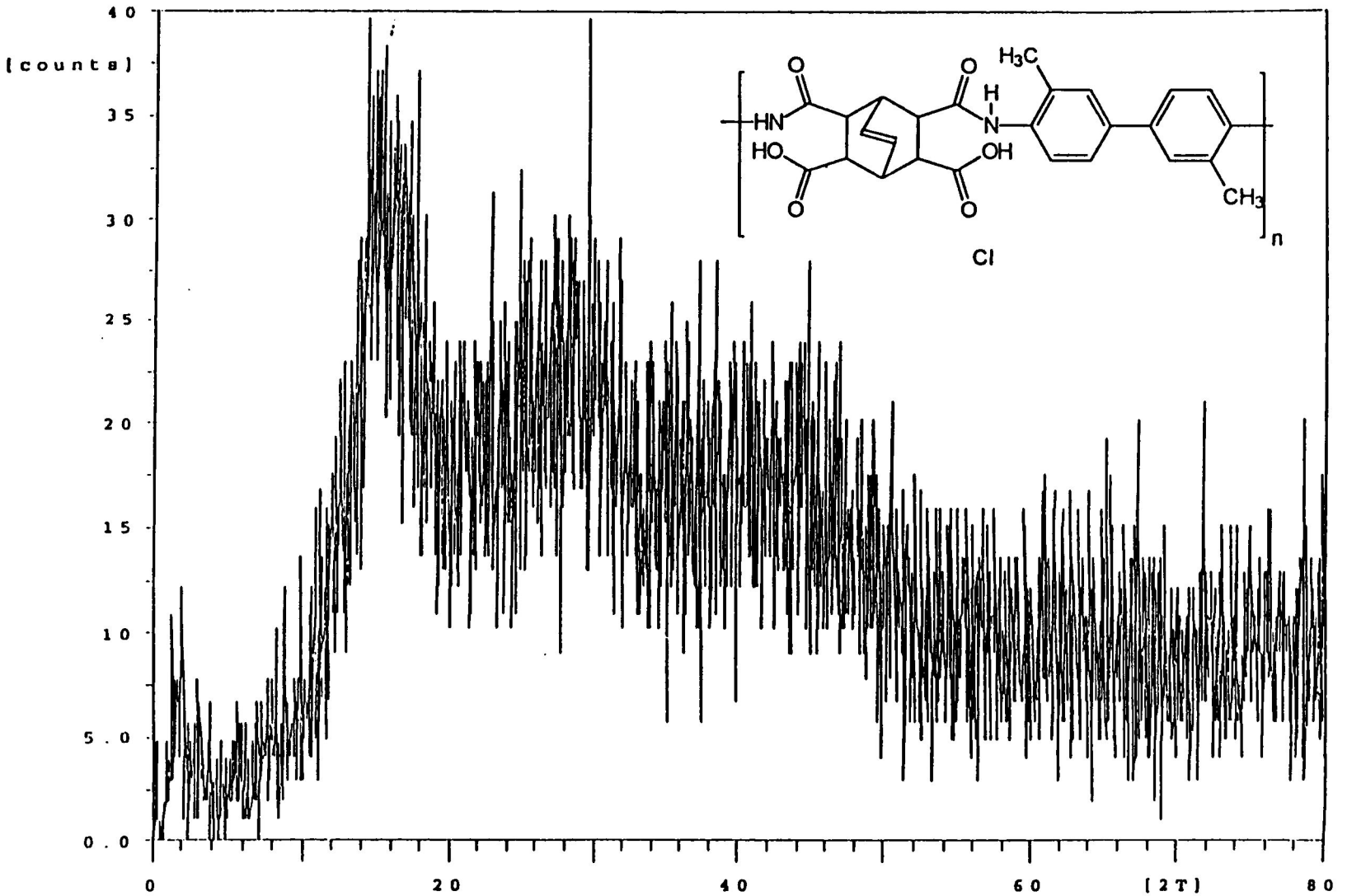

1.5. X-ray scattering pattern of *o*-tolidine containing polyamic acid CI

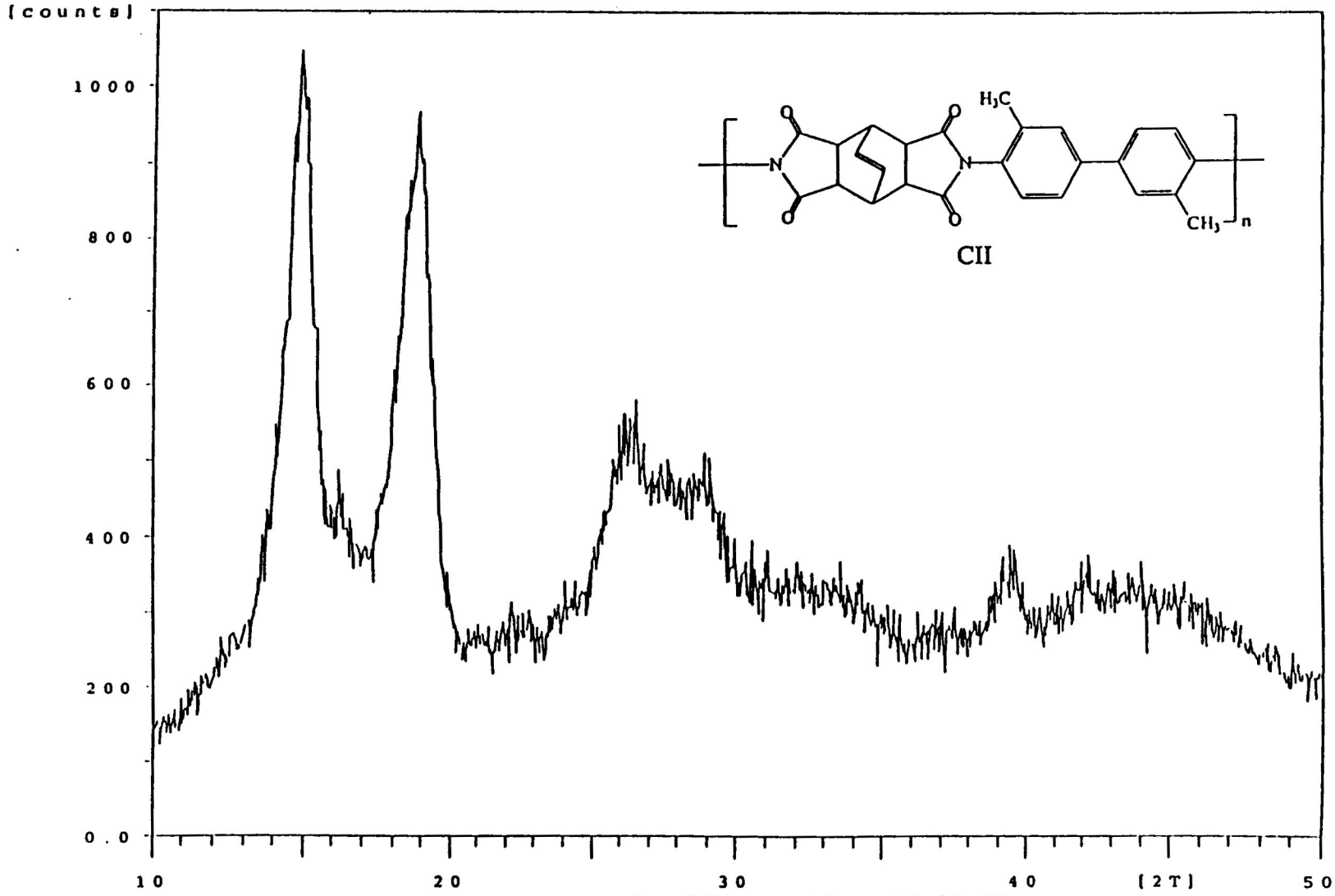

1.6. X-ray scattering pattern of *o*-tolidine containing polyimide CII

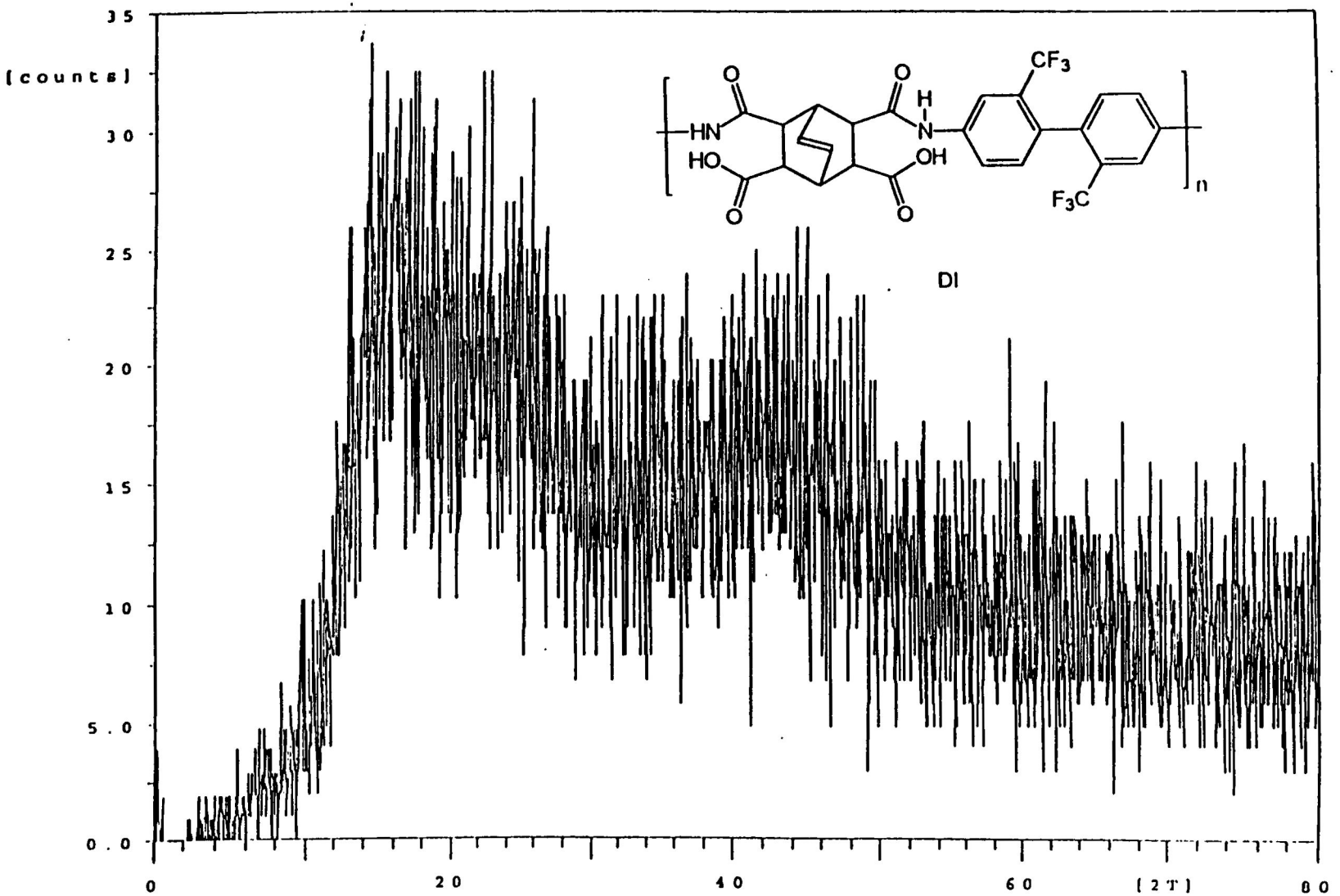

1.7. X-ray scattering pattern of 2,2'-bis(trifluoromethyl)benzidine containing polyamic acid DI

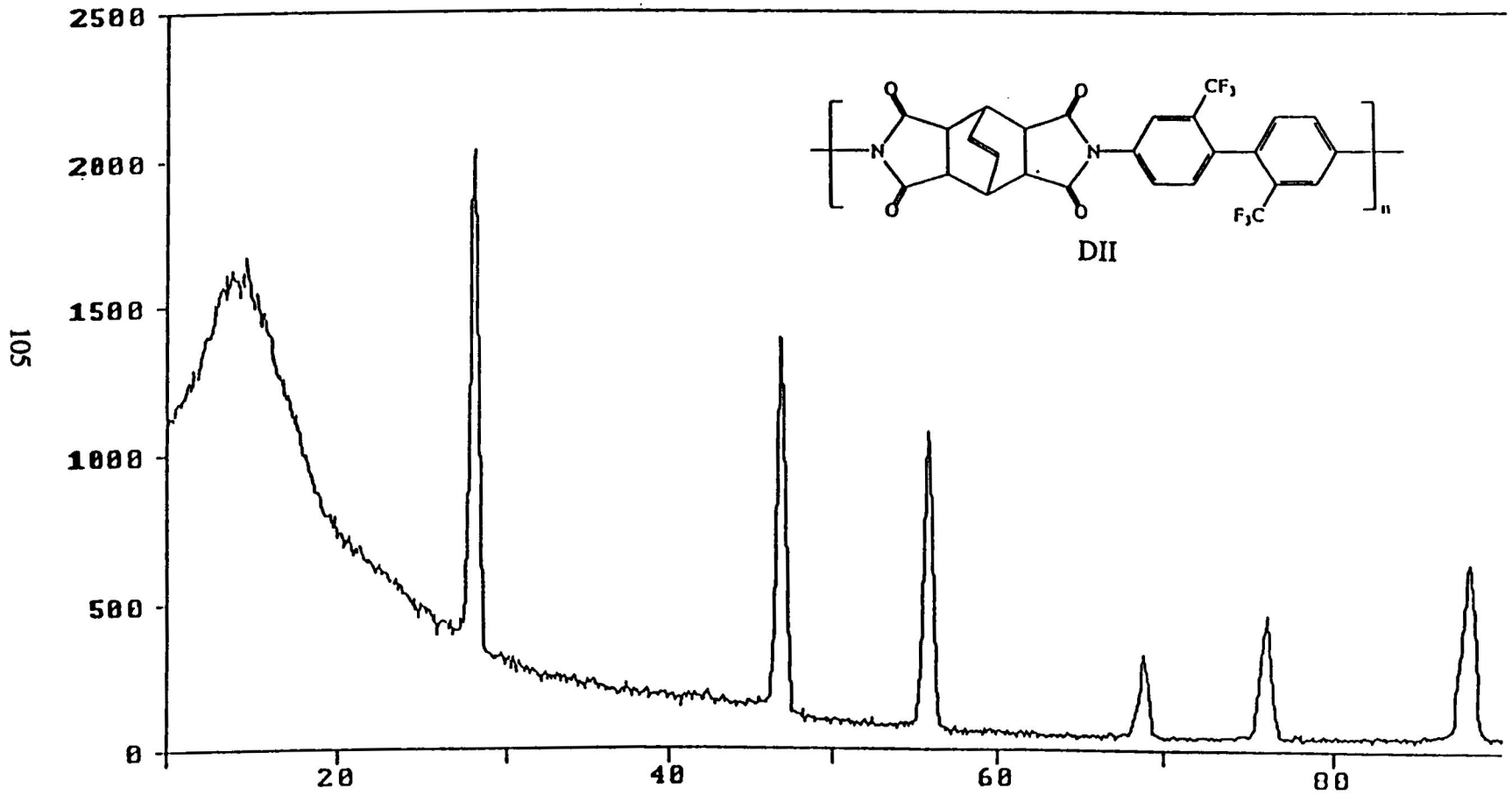

DII

1.8. X-ray scattering pattern of 2,2'-bis(trifluoromethyl)benzidine containing polyimide DII

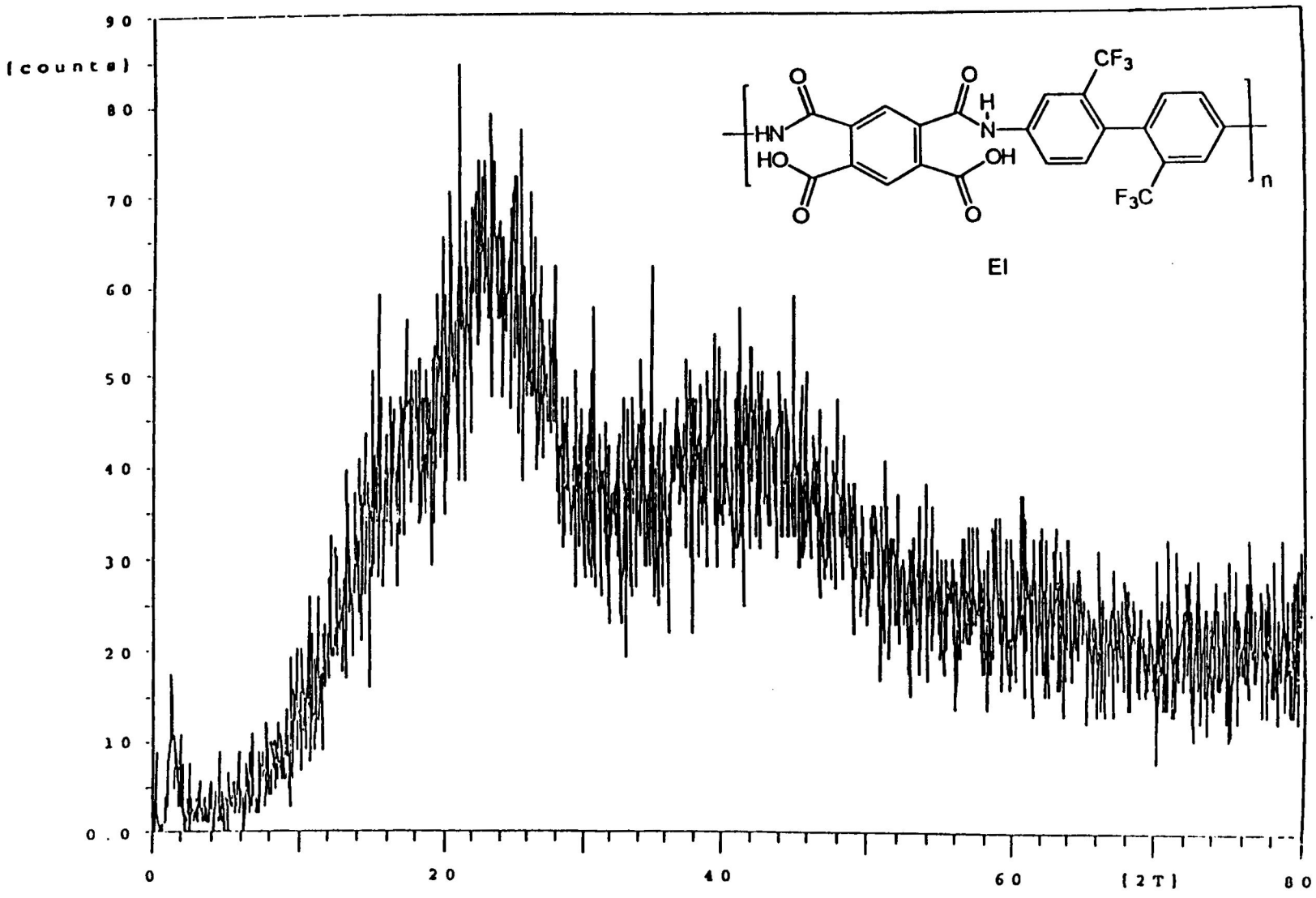

1.9. X-ray scattering pattern of 2,2'-bis(trifluoromethyl)benzidine containing polyamic acid EI

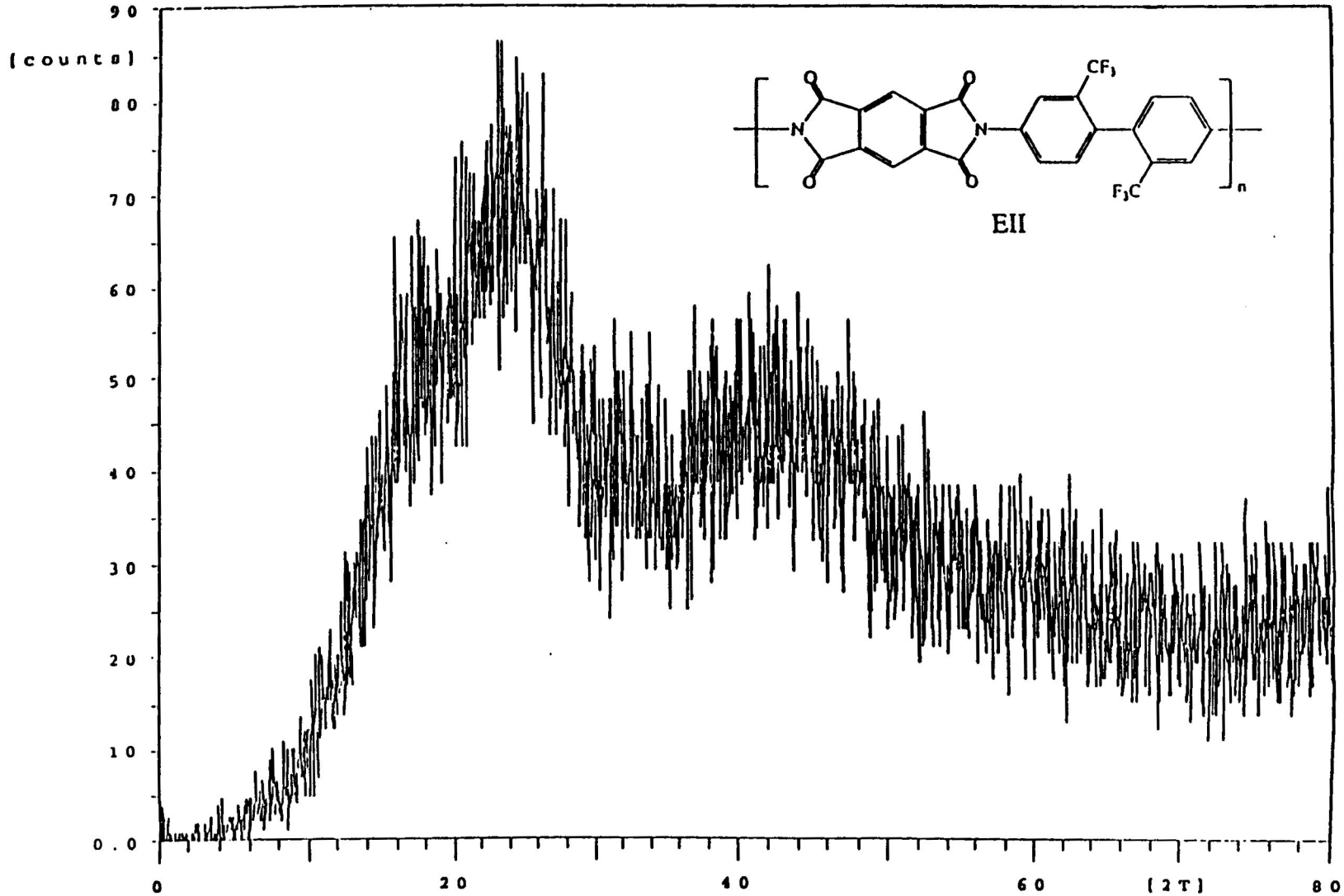

EII

1.10. X-ray scattering pattern of 2,2'-bis(trifluoromethyl)benzidine containing polyimide EII

REFERENCES

1. Stevens, M.P., *Polymer Chemistry an Introduction*, (Oxford University Press), New York, 10 (1990).
2. Allcock, H. R.; Lampe, F. W., *Contemporary Polymer Chemistry*, 2nd edition, (Prentice-Hall, Inc.), 36 (1990).
3. Bogert, T.M., *J. Am. Chem. Soc.*, 30, 1140 (1908).
4. E. U. du Pont de Nemours & Co., *French Pat.*, 1, 239, 491 (1960).
5. Wilson, D.; Stenzerberger, H. D.; Hergenrother, P. M., *Polyimides*, (Blackie & Son Ltd.), New York, 227 (1990).
6. *ibid*, 282 (1990).
7. Frazer, A.H., *High temperature resistant polymers*, Wiley Interscience, New York (1968).
8. Sroog, C.E., *Macromol. Rev.*, 11, 161 (1976).
9. Colter, R. J.; Matzner, M., *Ring-Forming Polymerizations*, Part B2, (Academic Press), New York (1972).
10. Yoshio, I., *High Perform. Polym.*, 7, 337 (1995).
11. Stenzerberger, H. D.; Herzog, M.; Romer, W.; Scheiblich, R.; Reeres, N. J., *Br. Polym. J.*, 15, 2 (1983).
12. *ibid*, 114 (1990).
13. Stenzerberger, H. D., *Br. Polym. J.*, 20, 389 (1988).

14. Southcott, M.; Amone, M.; Senger, J.; Wang, A.; Polio, A.; Sheppard, C. H., *High Perform. Polym.*, 6, 1 (1994).

15. Serafini, T. T.; Delvigs, P.; Lightsey, G. R., *J. Appl. Polym. Sci.*, 16, 905 (1972).

16. Chang, G. E.; Jones, R. J., *Proc. 28th Natl. SAMPE Symposium*, 728 (1983).

17. Chuang, C. K; Vannucci, R. D; Ansari, I.; Lerny, L. L.; Scheiman, D. A., *J. of Polym. Sci., Part A, Polym. Chem. Ed.*, 32, 1341 (1994).

18. Becker, H. K.; Hans, W. S., *Macromolecules*, 25, 6784 (1992).

19. Harris, F. W.; Feld, W. A.; Lanier, C. H., *J. Appl. Polym. Sci.*, 26, 421 (1975).

20. Imai, Y.; Maldar, N. N.; Kakimoto, M., *J. Polym. Sci., Polym. Chem. Ed.*, 22, 2189 (1984).

21. Liou, G. S.; Marruyama, M.; Kakimoto, M.; Imai, Y., *J. Polym. Sci., Part A, Polym. Chem. Ed.*, 31, 2499 (1993).

22. Eashoo, M.; Wu, Z.; Zhang, A.; Shen, D.; Tse, C.; Harris, F. W.; Cheng, S. Z. D., *Macromol. Chem. Phys.*, 195, 2207 (1994).

23. Dewar, M. J. S.; Goldberg, R. S., *J. Am. Chem. Soc.*, 92, 1582 (1970).

24. Roberts, J. D.; Moreland, W. T., *J. Am. Chem. Soc.*, 25, 2167 (1953).

25. Polk, M.; Banks, H.; Harruna, I.; Nandu, M.; Onwumene, F.; Phingodhipakkiya, M.; Venkatasubramania, N., *Mol. Cryst. and Liq. Cryst.*, 157, 1 (1988).

26. Harruna, I. I.; Polk, M. B., *J. Polym. Sci., Part A, Polym. Chem. Ed.*, 28, 285 (1990).